

COMPRESSION ROLLING OF TIMBER

A THEORETICAL MODEL

AND EXPERIMENTAL VERIFICATION

A thesis
submitted in fulfilment
of the requirements for the Degree
of
Master of Engineering in Mechanical Engineering
in the University of Canterbury

By
Xixian Deng

University of Canterbury

September 1990

CONTENT

ABSTRACT

CHAPTER ONE: INTRODUCTION

- 1.1 IMPROVEMENT IN THE PROPERTIES OF TIMBER
- 1.2 THE DEFINITION AND ORIGIN OF COMPRESSION ROLLING
- 1.3 AIMS AND TASKS OF THE RESEARCH

CHAPTER TWO: LITERATURE REVIEW

- 2.1 LITERATURE ON COMPRESSION ROLLING PROCESS
- 2.2 LITERATURE CONCERNED WITH EFFECTS OF COMPRESSION ROLLING OF THE TIMBER BOARDS

CHAPTER THREE: ANALYSIS OF COMPRESSION ROLLING PROCESS

- 3.1 BASIC ASSUMPTIONS AND INFLUENCE FACTORS OF COMPRESSION ROLLING
- 3.2 SYMBOLS AND DEFINITIONS
- 3.3 MATHEMATICAL RELATIONS ON COMPRESSION ROLLING
- 3.4 THE DYNAMIC PROPERTIES OF COMPRESSION ROLLING OF TIMBER BOARD
 - 3.4.1 MECHANISM OF BITE AND FRICTION OF COMPRESSION ROLLING PROCESS
 - 3.4.2 THE SPEED OF COMPRESSION ROLLING
 - 3.4.3 LOAD AND TORQUE OF COMPRESSION ROLLING

CHAPTER FOUR: COMPRESSION ROLLING MACHINE

- 4.1 GENERAL FUNCTIONS AND FEATURES OF THE COMPRESSION ROLLING DEVICE
- 4.2 THE FUNCTIONS AND FEATURES OF THE HYDRAULIC POWER SYSTEM
- 4.3 SPECIFICATION

CHAPTER FIVE: THE APPLICATION OF INSTRUMENTATION AND MICROCOMPUTER FOR MEASUREMENTS AND DATA ACQUISITION

- 5.1 THE AIMS AND RANGE OF THE APPLICATION
- 5.2 MEASUREMENT OF TORQUE AND LOAD
 - 5.2.1 BASIC PRINCIPLE OF THE MEASUREMENT
 - 5.2.2 SIGNAL CONDITIONING CIRCUIT--THE WHEATSTONE BRIDGE FOR STRAIN GAUGES SIGNAL CONDITIONING
 - 5.2.3 RELATED MEASURING DEVICES
 - 5.2.4 CALIBRATION
- 5.3 MEASUREMENT OF SPEED
- 5.4 COMPUTER-AIDED EXPERIMENT
 - 5.4.1 THE PRINCIPLE OF ANALOG TO DIGITAL CONVERSION
 - 5.4.2 THE METHODS AND DEVICES INTERFACING TO THE COMPUTER
 - 5.4.3 COMPUTER PROGRAMME DESIGN FOR THE EXPERIMENT

CHAPTER SIX: EXPERIMENT PROCEDURE

- 6.1 MATERIAL
- 6.2 METHODS
 - 6.2.1 DIGITAL IDENTIFICATION SYSTEM
 - 6.2.2 COMPRESSION ROLLING TREATMENTS
 - 6.2.3 MEASUREMENT OF LOAD AND TORQUE DURING ROLLING

6.2.4 MEASUREMENT OF HARDNESS OF TIMBER BOARDS

6.3 METHODS AND PROCEDURE OF DATA PROCESSING

CHAPTER SEVEN: THE RESULTS OF THE EXPERIMENTS

7.1 THE MEASURING RESULTS OF COMPRESSION ROLLING OF
TIMBER BOARD

7.2 HARDNESS CHANGE DURING COMPRESSION ROLLING

7.3 RELATIONSHIP BETWEEN MECHANICAL PROPERTIES AND
TREATMENT CONDITIONS

CHAPTER EIGHT: DISCUSSION AND CONCLUSION

8.1 THE EVALUATION AND COMPARISON OF THE RESULTS

8.2 CONCLUSION

8.3 THE PROSPECTIVE RESEARCH FIELDS ON COMPRESSION
ROLLING

8.3.1 FROM CLEAR WOOD TO COMMERCIAL GRADE TIMBER BOARD

8.3.2 KNOT EFFECT AND STRENGTH BEHAVIOUR DURING
COMPRESSION

8.3.3 STUDIES ON THE POSSIBILITY OF IMPREGNATING TIMBER
USING THE VACUUM OCCURRING DURING THE
DECOMPRESSION PHASE

ACKNOWLEDGEMENT

APPENDIX

APPENDIX 1: PRINCIPLE OF THE RESISTANCE-TYPE STRAIN GAUGE

APPENDIX 2: THE SELECTION AND INSTALLATION OF THE STRAIN
GAUGES

A.2.1 THE CONSIDERATION OF SELECTION

A.2.2 SPECIFICATION

A.2.3 INSTALLATION

APPENDIX 3: REFERENCE ON HYDRAULIC SYSTEM

APPENDIX 4: THE RESULTS OF THE DATA ANALYSIS

REFERENCES

ABSTRACT

This research on compression rolling of timber boards concentrates on the following aspects:

1. Analysing the compression rolling process.
2. Developing the instrumentation and the computerized data acquisition to acquire the parameters of compression rolling.
3. Studying the effects of compression rolling on timber boards

A theoretical model approaches the results of the experiment on compression rolling of timber boards. The surface and properties of timber boards are not obviously changed if the compression level is less than 10%, but are changed to a small degree when the compression level is increased from 10% to 17%. There are splits and resin expellation on the surface of timber board when the compression level is more than 17%. The hardness on the surface of the timber boards is increased 4% at 15% compression level and 6.6% at 17% compression level.

This thesis includes eight chapters. Its main contents are Chapter 3 -- theoretical analysis, Chapter 5 -- application of instruments and the computer, Chapter 6 -- experiment procedure, Chapter 7 -- results and Chapter 8 -- discussions and conclusions.

CHAPTER ONE:

INTRODUCTION

1.1 IMPROVEMENT IN THE PROPERTIES OF TIMBER

Throughout recorded history, wood has been of enormous economic significance to the development and industrialization of nations. Gradually we have come to recognize that it is very important to improve the properties of wood and to use it more economically. Many scientists and workers are doing research in this field. This research is concentrated on improving the mechanical properties of wood, such as specific density, hardness, by compression rolling. There are opportunities for using the same technique to aid preservative treatments.

With regard to preservative treatments, numerous methods, biological, chemical and mechanical, have been evaluated. Although many of these processes have had positive results, few have found commercial application. They include solvent seasoning (Ellwood and Ecklund, 1963) and other chemical infusions to decrease sap-surface tension (Lantican, Cote, and Skaar, 1965), biological pre-treatments (Bauch, Liese, and Berndt, 1970), steaming (Kubinsky, 1971; Haslett and Kininmonth, 1975) and some mechanical techniques, such as incising (Banks, 1973, Perrin, 1978) and compression rolling (Goulet and

Cech, 1967).

Compression rolling, which has been the subject of a series of investigations over 20 years, is one mechanical process which offers the prospect of improving wood characteristics.

1.2 THE DEFINITION AND ORIGIN OF COMPRESSION ROLLING

The compression rolling of wood is a mechanical and physical process. According to published literature, the process, known as dynamic transverse compression rolling, originated and was developed in Canada (Goulet 1968). This technique involves feeding sawn timber boards through a pair of contra-rotating rollers. The control parameters of the compression rolling machine are the diameter of the rollers, feed speed and compression level, which depends on the gap between the rollers.

The initial research results using hardwood species (yellow birch) seemed to indicate that a hydraulic and mechanic combination during rolling induced pit membranes to rupture without causing damage to the cell wall itself. The timber appeared to be opened up for fluid flow, without a significant concomitant loss in mechanical strength (Goulet, Cech and Huffman, 1968; Cech and Huffman, 1970; Cech, 1971). Goulet (1968) claimed savings in the order of 60% in drying of yellow birch after compression rolling. Since Goulet (1968), most research conclusions have been less optimistic. Subsequent application of the process to several slow drying hardwoods did not produce the expected improvement

in drying behaviour. Thus the original claims of Goulet (1968) have yet to be broadly verified.

The research on compression rolling can follow one of two general themes.

1.3 The application of compression rolling to improve of the properties of wood and increase of treatability of timber.

1.4 The study on the theory of compression rolling

The first approach is interested in the effects of compression rolling on physical and mechanical properties and on the treatability of wood, such as drying time and quality, the variance of preservative uptake and penetration etc.. The second one concentrates on the compression rolling process itself. It seeks to explain the basic changes of wood structure during compression rolling and to explore the reasons for the change in the properties of wood. The latter approach will be used in the project.

1.5 AIMS AND TASKS OF THE RESEARCH

This research is based on a previous project (H. Helge Gunzerodt 1985). The present study is concerned with computerized data acquisition during the compression rolling process, in an attempt to understand the deformation of wood and the change of physical properties during compression rolling.

The aims and tasks of the research were developed as follows:

1.6 Installation and application of the instrumentation

The dynamometer elements was designed and installed on the compression rolling machine in order to measure load, torque and speed during compression rolling.

1.7 The application of the computer in the experimental process.

A microcomputer and analog-to digital converter were used to guarantee accurate data acquisition and processing.

1.8 The study of the mathematical and mechanical model during compression rolling.

A understanding of the mechanism required a knowledge of the following parameters during rolling:

1.9 Compression level

1.10 Feed speed

1.11 Roller diameter

1.12 Timber characteristics and their interactions with one another.

1.13 Experiments and results

The aim was to establish the factors which determine an effective compression rolling process and to determine the optimum operating parameters, in order to design and utilize compression rolling as a possible commercial operation.

CHAPTER TWO:

LITERATURE REVIEW

2.1 LITERATURE ON COMPRESSION ROLLING PROCESS

There is only a limited literature on the process of rolling of timber and very little attention has been given to the analysis of the compression and decompression cycle. Previous researches have simply stated that timber boards subjected to such a dynamic loading process behave in a different manner to other materials, such as metals or plastics. Although theories concerning the behaviour of these materials during rolling cannot be directly applied to timber, the principles developed for other materials are still worth examine.

Wusatowski has described systematically the principles of compression rolling of metals (Wusatowski 1969, Chapter 3.3).

It assumes that the process of rolling induces strain across the entire cross-section under compression rolling. The stresses in the various cross sections in the area of plastic deformation are different due in part to non uniform speed conditions in the compressed material (Figure 2.2): the metal accelerates while

passing between the rollers. The following simplifying assumptions are made in order to derive slip theories for metal during rolling.

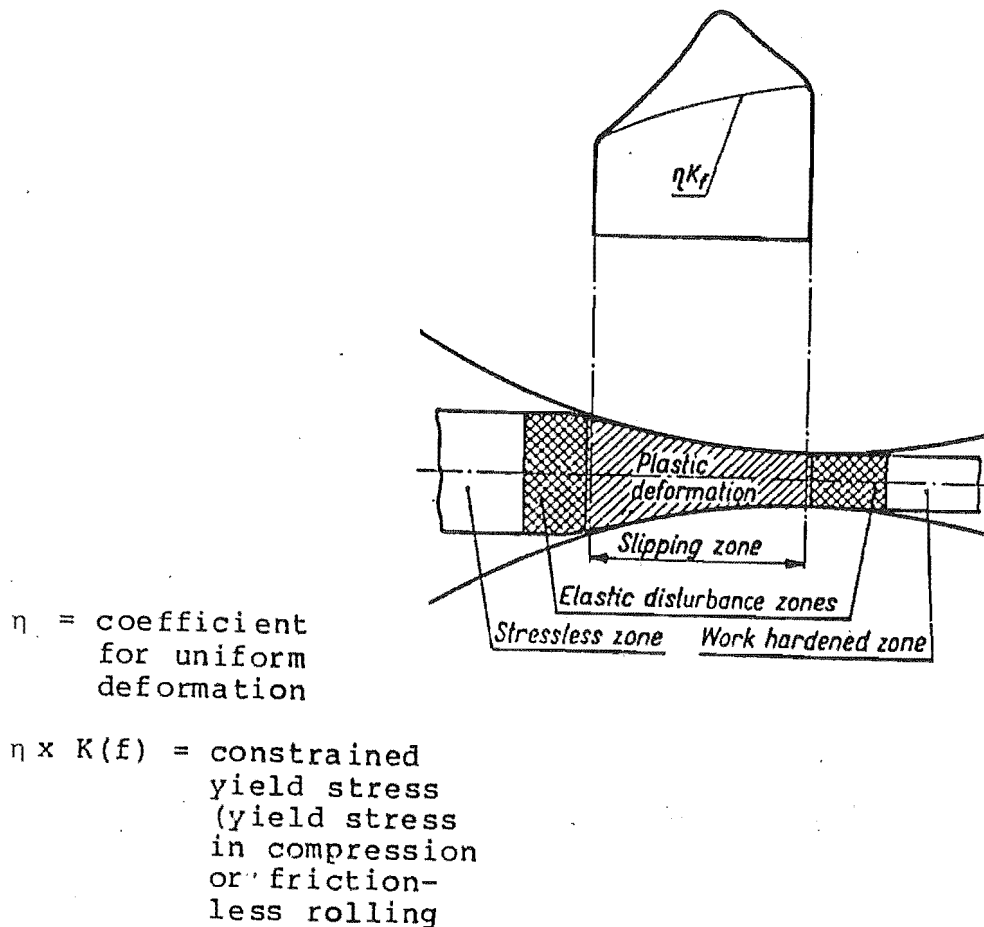
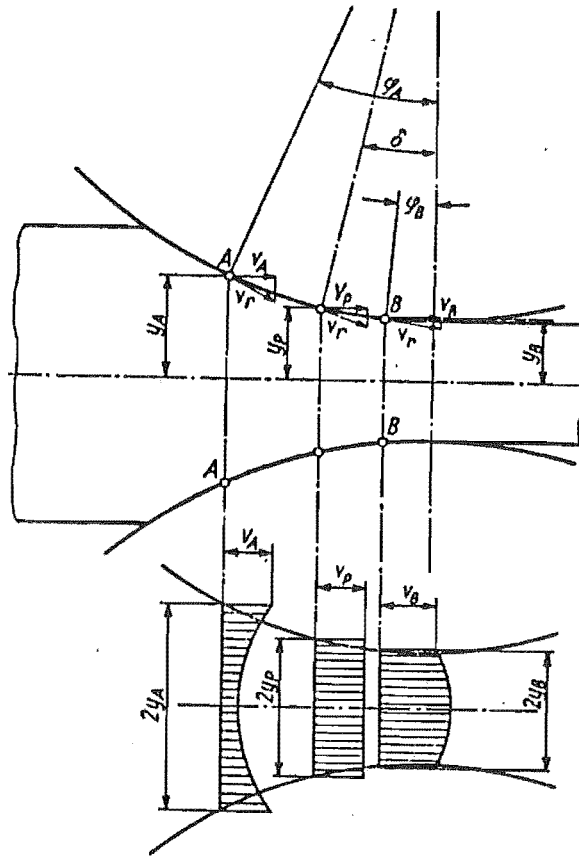


Figure 2.1 Scheme of compression cycle during cold metal rolling (According to Wusatowski, 1969, Pg.208)

1. Plane and perpendicular cross-sections of the initial stock remain also plane and perpendicular after rolling.
2. The rolled stock does not spread sideways in rolling.

3. The coefficient of friction between roll and surface of rolled stock is constant at every point along the



$V(r)$ = Peripheral speed of rolls (m/s)
 $V(p) = V(r) \times \cos \delta$
 $V(A) = V(r) \times \cos \phi_A$
 $V(B) = V(r) \times \cos \phi_B$
 $V(A_m)$ = Mean speed of stock in cross section AA
 $V(B_m)$ = Mean speed of stock in cross section BB
 AA, BB = Arbitrarily chosen planes one on each side of the neutral plane
 b = Unit width
 $2Y(A)$ = Height of rolled stock before
 $2Y(B)$ = Height of rolled stock after
 $V(S)$ = Volume per second of rolled stock
 $= 2 \times Y(p) \times \cos \delta$
 $V(A_m) < V(A)$
 $V(B_m) > V(B)$

Figure 2.2 Speed distribution of metal flow along its cross section (According to Wusatowski, 1969, Pg.209)

arc of contact.

4. The constrained yield stress is constant along the arc of contact.
5. The rolled material is homogeneous.
6. Rollers are rigid and are not deformed during rolling.
7. Stress is acting on each cubic element of any cross section between the rollers.

When analysing the process of compression rolling of timber board, some of these assumptions above-mentioned may be applied with some modification. In discussing the compression rolling process, Gunzerodt came to the following conclusions:

" The deformation of wood during rolling is very different to that observed with metals, because of wood's elastic and visco-elastic properties described previously. Also there is a volume change of the body when rolling wood, which does not occur with metals."

The following factors make the model derived for metal rolling inapplicable to timber, since elasto-plastic materials (timber represents such a material) behave differently when subjected to the multiaxial forces during compression rolling (Gunzerodt, 1985).

1. Constant volume may not be assumed.
2. Wood does not accelerate through the rollers as it is inextensible to a first approximation in the longitudinal direction and fibres are orientated parallel to the feed direction.
3. The rolled material is inhomogeneous and anisotropic in its three main directions.
4. Elastic deformation is substantially larger than plastic deformation.
5. The constrained yield stress across the thickness of the sample and along the arc of contact varies, because of the phenomenon of short term surface densification.
6. There are localized density variations in the wood with corresponding fluctuation in MOE, hence the strain is not uniformly distributed.

Furthermore, one of the main differences in the behaviour of a plastic or ductile material lies in the recovery phase of elasto-plastic materials. Timber must be regarded as a material displaying plastic and elastic characteristics. The proportion of visco-elastic recovery in the total recovery is a function of the loading rate. An increase in speed of loading leads not only to higher overall strength values (Kollmann, 1967), but also an increase in the proportion of elastic to visco-elastic recovery (Kollmann, 1961). The effects of loading rate on the instantaneous recovery are

represented in Figure 2.3.

The graph is derived from compression tests perpendicular to the grain of Picea spp. (Kollmann,

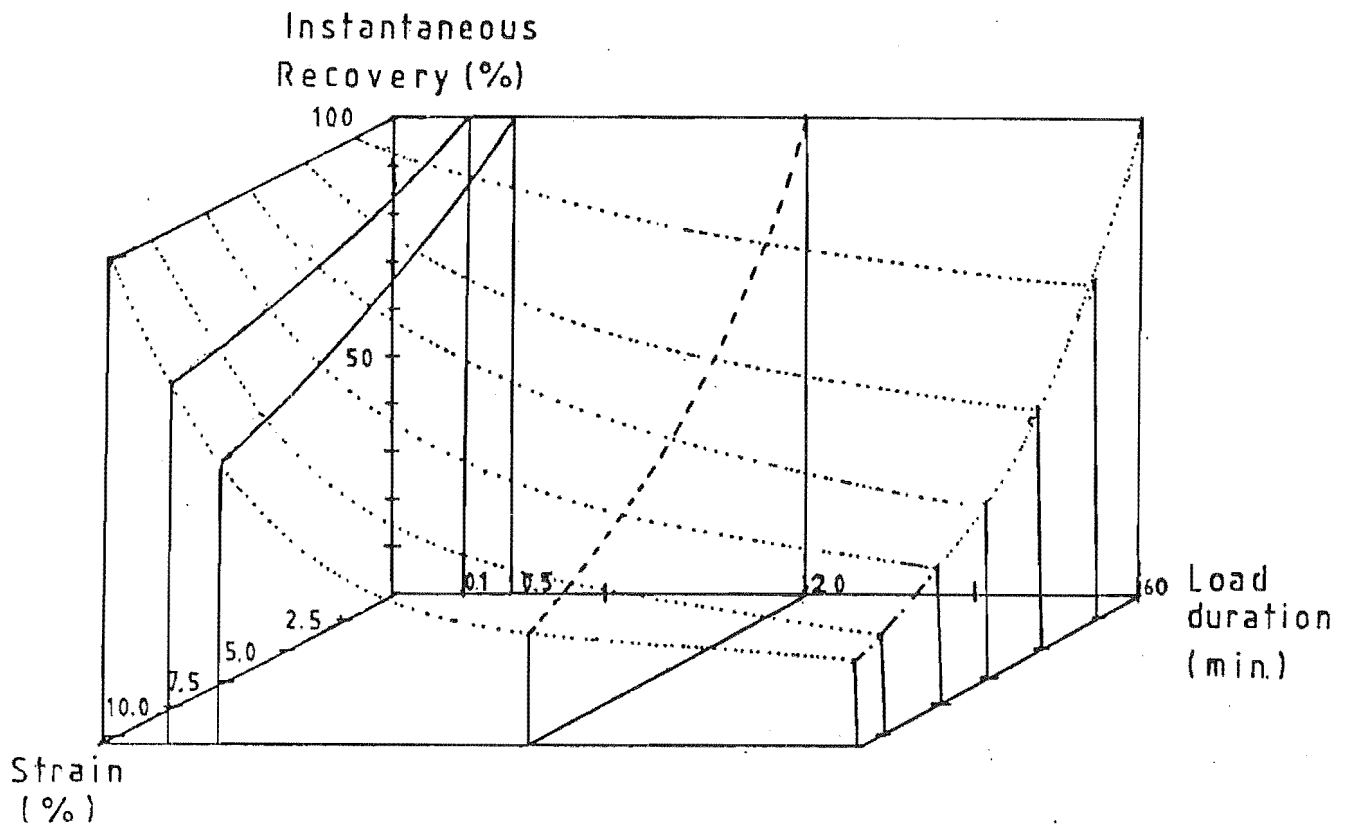


Figure 2.3 Effects of loading time and compression level on instantaneous recovery of timber compressed perpendicular to the grain (According to Gunzerodt, 1985)

Data for Nothofagus (Gunzerodt): ————
 Data for Picea (Kollmann): - - - - -
 Data for Populus (Koch):
 Extrapolated Data:

1961), Populus tremuloides (Koch, 1964) and Nothofagus fusca (Gunzerodt, 1985).

Figure 2.3 illustrates the relationship between load duration and instantaneous recovery as a function of the compression level. In the course of compression rolling experiments, the complete loading cycle never exceeds 3 seconds, depending on the feed speed and the roller diameter and would typically be of the order of 0.2 to 0.02 seconds. Typically, after dynamic compression to 85% of its original thickness the wood will recover to 98.5%. In other words only 10% of the dynamic compression is not recoverable (Cech, 1971). Thus, in the analysis of rolling of wood, Gunzerodt assumed that creep deformation can be neglected and that the cellwall matrix behaves as a perfect elastic material.

Previous studies (Gunzerodt, 1985 and Gunzerodt et. al., 1988) on the process of compression rolling of timber indicate that the particular distribution of the total deformation is restricted to the regions in immediate contact with the surface of the rollers. The concentrated deformation in the upper and lower surface of the timber board can be described as a surface phenomenon. This has been observed during wood deforming processes under static loading conditions (Kollmann, 1959; Doyle, 1980) and under dynamic loading processes (Johnston and St Laurent, 1978; Peters and Zenk, 1968; Grosditz, 1979; Cech, 1972 and Gunzerodt, 1985).

The moisture content of the timber board has a significant influence on the compression rolling process. The results of the experiments have revealed that:

High saturation level reduces the compressibility of the cell voids and fracture occurs in areas of stress concentration (Haslett and Kininmonth, 1975; Gunzerodt, 1985).

On the other hand, when the moisture content of the timber board is below fibre saturation, the cell voids are more compressible and same levels of compression as applied to the highly saturated samples do not increase the intra-cellular pressure during rolling to the same extent.

2.2 LITERATURE CONCERNED WITH EFFECT OF COMPRESSION

ROLLING OF THE TIMBER BOARDS

Compression rolling as a mechanical approach to overcome the resistance of impermeable timbers to moisture movement, either during drying or during preservative treatments, was developed in Canada (Goulet, 1968). The process, known as dynamic transverse compression rolling, had significant influence on the drying characteristics and permeability of species, which had been subjected to the rolling process.

Goulet (1968) supposed that during the compression cycle, damage is induced in the tissue at the microscopic level which has a positive influence on the subsequent drying characteristics and on the treatability of the timber. It was postulated that a combination of hydraulically and mechanically induced stresses ruptured pit membranes without causing substantial damage to the cell-wall itself. Cech's studies indicated that the pit

apertures were deformed due to the compression treatment, but no actual evidence of wall failure could be found. Thus, it was believed that opening up the wood structure to fluids during compression rolling does not produce significant concomitant losses in mechanical strength (Goulet, Cech and Huffman, 1968; Cech and Huffman, 1970 and Cech, 1971).

The previous researches on compression rolling of the timber mainly concentrated on the following two aspects:

- (1). Effect on the drying of timber.
- (2). Effect on the treatability of timber.

These studies have been undertaken by a number of workers, but the results vary. In summarizing the research, the following observations indicate why there are still doubts about the effectiveness and use of compression rolling, despite claims of very substantial improvements in both drying rate and timber quality after drying (Gunzerodt 1985).

1. These studies have been primarily concerned with the drying of hardwood.
2. Only hardwoods have been investigated for the influence of compression rolling on drying in most cases.
3. The technique has been almost always applied to fresh material.

4. There are contradictions in the published literature regarding the degree of acceleration in drying even for a single species, such as yellow birch (Goulet 1968, Goulet and Cech 1968, Cech 1971).
5. Disagreement exists regarding the effect of compression rolling on drying when differing drying schedules are applied (especially concerning the effects of high-temperature schedules).
6. The process proved to be unsuitable for more impermeable timber species such as New Zealand native beeches, Nothofagus fusca and Nothofagus truncata (Haslett and Kininmonth, 1975) partly contradicting an earlier study on drying (Cech, 1871), which had indicated that compression rolling could have a more pronounced effect on less permeable wood.
7. In most of the investigations only limited emphasis was placed on specific aspects of machine design and on the various process related parameters, such as feed speed, roller diameter and temperature.

Gunzerodt summarized comprehensively the effects of compression rolling on the treatability and drying of timber (Table 2.1).

Even though all of the studies on compression rolling of timber are basically concentrated on the effects of compression rolling on both drying rate and treatability, there is some literature dealing with prospect development and profits on compression.

Implication on surface densification of wood:
Tarkow and Seborg (1968) undertook research on surface

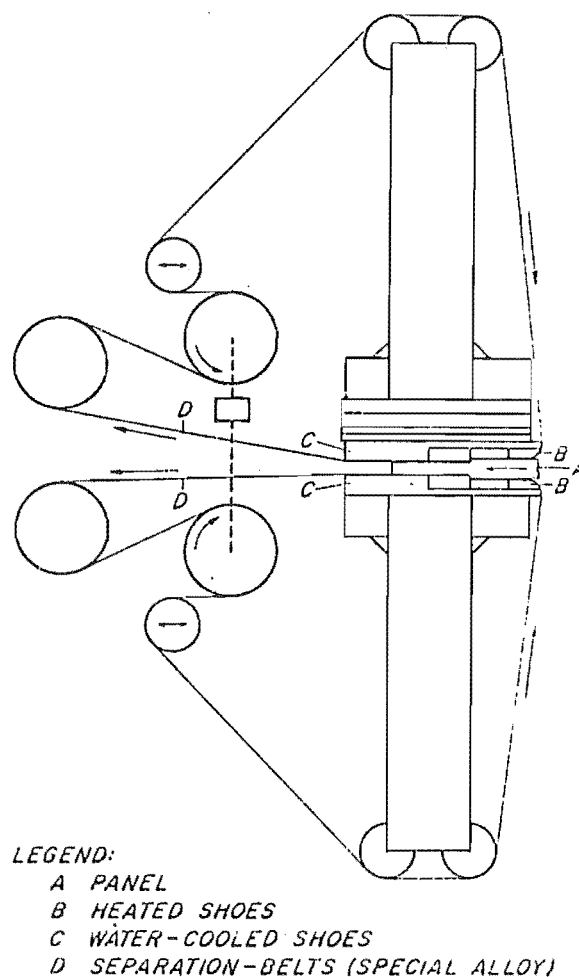


Figure 2.4 Equipment for continuously densifying the surface region of wood (According to Tarkow and Seborg, 1968)

densification of wood in 1968. They used a pair of endless special alloy belts driven by the rollers to press the solid wood panel. Moving at lineal speeds up to 25 feet per minute, the panel was subjected to a short period of intense heat and pressure and followed by a quick cooling while still under pressure (Figure 2.4).

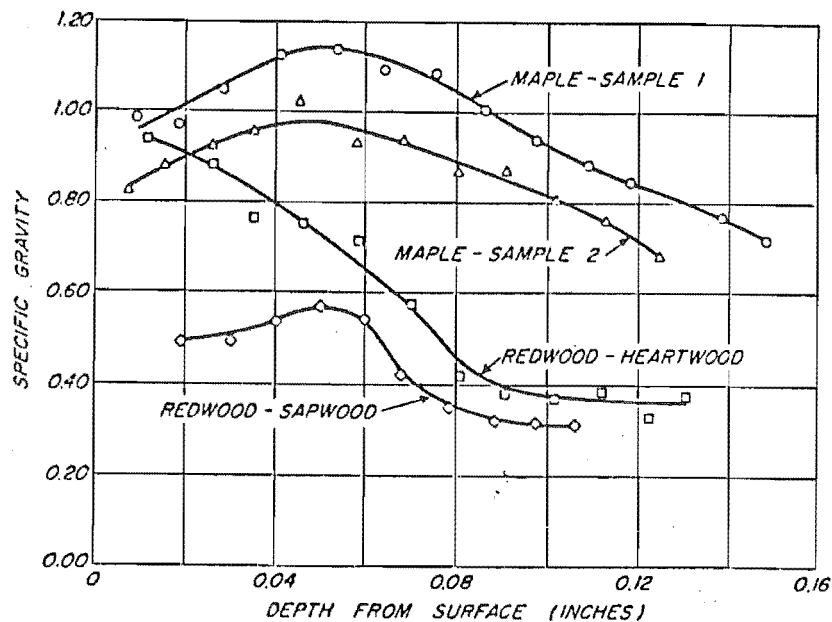


Figure 2.5 Specific gravity gradient of surface-densified wood
(According to Tarkow and Seborg, 1968)

The experiment results indicated:

The maximum specific gravity of the maple which occurred 0.04 inch from the surface, was slightly more than 1.0. The maximum specific gravity for redwood occurred within the first 0.01 inch and decreased to the normal value at about 0.10 inch

from the surface (Figure 2.5)

The abrasion resistance of wood increased at least 15 times with doubling of the density. The abrasion resistance of the surface-densified redwood is probably greater than that of normal hard maple.

There are differences between the research on surface densification of wood (Tarkow and Seborg, 1968) and studies on compression rolling of timber (Goulet and Cech, 1967; Goulet, 1968; Cech and Goulet, 1968; Cech, 1971; Cech and Pfaff, 1975, etc.), such as, different feed speed (compression rolling with higher speed), different processing temperature (compression rolling with normal temperature, surface densification with high temperature) and different type of compression. Even though there are some differences between the treatments of surface densification of wood and compression rolling, there are surface compression deformation in both case (Tarkow and Seborg, 1968 and Gunzerodt, 1985). They might be the cause to produce a certain surface densification.

Table 2.1 (1) Effects of compression rolling on sawn timber of softwood

EFFECTS OF COMPRESSION ROLLING ON SAWN TIMBER										
GYMNOSPERMEAE - SOFTWOODS										
Botanical Name	<u>Abies amabilis</u>	<u>Picea glauca</u>	<u>Picea glauca</u>	<u>Picea glauca</u>	<u>Pinus contorta</u>	<u>Pinus radiata</u>	<u>Pinus strobus</u>	<u>Pseudots. menziesii</u>	<u>Pseudots. menziesii</u>	<u>Tsuga heteroph.</u>
Common Name	Silver fir	Eastern w.spruce	Eastern w.spruce.	Eastern w.spruce.	Lodgepole pine	Radiata pine	Eastern w.pine	Douglas fir	Douglas fir	Western Hemlock
Density ³ (kg/m ³)	430	430	430	430	400	400	380	500	500	460
Wood maturity	Heart-wood	Heart-wood	Heart-wood	Heart-wood	Heart-wood	Sap-wood	Heart-wood	Heart-wood	Heart-wood	Heart-Sapwood
Grain orientation	Not consid.	Flat-sawn	Flat-sawn	Flat-sawn	Not consid.	Flat-sawn	Flat-sawn	Not consid.	Flat-quarter	Not consid.
Moisture cont. (%)	28 - 50	28 - 50	38.6	20	28 - 50	Dry, Redr.	50 - 70	28 - 50		28 - 50
Permeability	Resist.	Resist.	Resist.	Resist.	Resist.	Permeable	Moderate resist.	Resist.	Resist.	Moderate resist.
Process (Dr., Tr.)	Creosote CCA	Creosote CCA	Creosote CCA	CCA	Creosote CCA	Drying HT-Drying	?	Creosote CCA	CCA	Creosote CCA
Roller Size (mm)	152.4	152.4	114.3	114.3	152.4	?	114.3	152.4	?	152.4
Feed Speed (mm/s)	253.3	253.3	253.3	253.3	253.3	140.0	253.3	253.3	?	253.3
Opt. Compr. (%)	10	10	15	12.5 - 17.5	10	10 - 20	8 - 12	10	15	10
Results and Observations	CCA uptake signif. on faces. (no edge-penetration). EW > LW Satisfactory treatment	Creosote uptake improved. Face penetration improved. LW > EW Inadequate treatment with CCA	Increase Pen. 58 % Ret. 62 % upt. only surfacial (no edge) significant retention	3.5x increase in radial penetration, 4.5x in tang. direction Uptake is a surface phenomena	Improved creosote face penetration CCA uptake not improved LW > EW	Slight reduction in checks when rolled green. Not effective when dry rolled	Compression surface phenomena leads to stretch-of pit membranes	Improved creosote retention Face penetration increased collapse at CL > 15% Uptake of CCA not improved	Uptake improved 400 % in flatsawn boards due to damaged pit membranes	Creosote uptake improved, substant. on faces. High compression leads to collapse
Authors and Date	Cooper 1973	Cooper 1973	Cech et al 1972	Cech et al 1974	Cooper 1973	Berni et al 1979	Grozdzits e.a. 1981	Cooper 1973	Nicholas 1973	Cooper 1973
Country	Canada	Canada	Canada	Canada	Canada	Australia	Canada	Canada	USA	Canada
Remarks	Detailed Reference Apparent correlation: permeability and density. Influence of intra-specific variability, no explanation of mechanism	Detailed Rf, points out problems if CL > 15% Indicates role of axial permeability	Detailed Reference notes role of un-aspirated LW pits responsible for good LW-permeability. Suggested rolling at 20% MC. No explanations	Detailed Reference Indicates disproportion of CCA. Increased retention at lower MC. Problems if CL > 15% No explanation of mechanism	Detailed Rf, (see col. 2) Low treatment due to narrow LW layers No explanations of mechanism	Checking when redrying treated P. radiata cannot be prevented No explanations of mechanisms. Very limited infos	No Data about experim. methods. Conclusions based on unpubl. data	Very low uptake only on surface indicates that LW provides pathways, this causes low permeability (see column 2)	Conclusion based on unpublished data Very incomplete and short	LW > EW, uniform penetration pattern. Detailed report (see column 2)

Table 2.1 (2) of compression rolling on sawn timber of hardwood

EFFECTS OF COMPRESSION ROLLING ON SAWN TIMBER									
ANGIOSPERMEAE - HARDWOODS									
Botanical Name	<u>Acer sacchar.</u>	<u>Betula alleghan.</u>	<u>Betula papyrif.</u>	<u>Eucalypt. obliqua</u>	<u>Eucalypt. regnans</u>	<u>Nothofag. fusca</u>	<u>Nothofag. truncata</u>	<u>Populus tremuloi.</u>	<u>Quercus rubra</u>
Common Name	Hard maple	Yellow birch sp.	White birch	Messmate stringyb.	Mountain ash	Red Beech	Hard Beech	Trembling aspen	South. red oak
Density ³ (kg/m ³)	610	640	540	490	700	530	600	450	650
Wood maturity	Heart-wood	Heart-wood	Heart-wood	Heart-wood	Heart-wood	Heart-wood	Heart-wood	?	Heart-wood
Grain orientation	Flat-sawn	Flat-sawn	Flat-sawn	?	Not consid.	Flat-sawn	Not consid.	Flat-sawn	Flat-sawn
Moisture cont. (%)	Green	Green	Green	Green 113.2	Green 110	Green 87.9	Green 85.3	Green	Green 80
Permeability	Permeable	Moder. Resist.	Moder. Resist.	Very resist.	Very resist.	Very resist.	Resist.	Resistant	Resist.
Process (Dr., Tr.)	Drying	Drying	Drying	Drying	Drying	Drying	Drying	Drying	Drying
Roller Size (mm)	114.3	114.3	114.3	50	?	50	50	114.3	114.3
Feed Speed (mm/s)	253.3	253.3	253.3	16.4	?	16.4	16.4	253.3	253.3
Opt. Compr. (%)	8 - 12	8.5 - 12.5	8 - 12	10	?	10	10	8 - 12	7.5
Results and Observations	Moderate improvement of depth of deformation during rolling	Possible to dry at high temperat. slight reduction drying time	Deep distribution of deformation in board. Pits damaged due to small size	No improvement on drying time nor influence on shrinkage	No improvement on drying	Severe checks in 25% of boards, no decrease in drying time	Severe checks in 75% of bds, no decrease in drying time	No drying improvement. Pit membrane stretched no splits	Slight decrease in drying time, not of economic significance.
Author(s) and Date	Grozdzits e.a. 1981	Cech 1971	Grosditz 1981	Haslett e.a. 1975	Campbell 1978	Haslett e.a. 1975	Haslett e.a. 1975	Grozdzits 1981	Cech et al 1975
Country	USA	Canada	USA	N.Z.	Australia	N.Z.	N.Z.	USA	Canada
Remarks	Lacks detailed data. Indicates damage to pits improves drying through diffusion	21% increase in diffusion Evidence of shear and hydraulic pressure may rupture pit membranes	Lacks detailed data. Pit rupture accounts for high vapor diffusion Conclus. do not convince	Process not effective Machine not up to standard	Lacks detailed data. Main emphasis on other issues	Highly saturated boards may explain damage. Machine not adequate	Limited emphasis on rolling due to restrict. machine capacity	Stretched pit membranes not convincingly interpreted. Very limited data.	Lacks detailed data. Main emphasis on other issues

CHAPTER THREE:

ANALYSIS OF COMPRESSION ROLLING PROCESS

3.1 BASIC ASSUMPTIONS AND INFLUENCE FACTORS OF COMPRESSION ROLLING

Because of its natural origin, the physical properties of timber exhibit a wide degree of variability. These variations are in part the result of the growth conditions of timber brought about by environmental factors such as climate, soils, water supply, available nutriment, etc.. In addition, many properties of timber are in part heritable; consequently, a substantial portion of the natural variability of timber can be attributed to differences in genetic stock.

The physical properties of timber are further complicated by its complex internal structure, which gives rise to anisotropic behaviour. In addition to natural variability and anisotropy, timber is also porous and inhomogeneous. Because of the inhomogeneity of timber, there is a wide range of variability in density, strength properties, moisture content, hardness and frictional behaviour.

In order to simplify the analysis of a compression rolling process, the following basic assumptions have been made:

1. The width of timber boards remains constant during compression rolling.
2. The timber boards are homogeneous and of uniform density and strength properties.
3. Only a small plastic deformation occurs in the timber boards during rolling.
4. The rate of elastic recovery of the timber boards is invariant.
5. The elastic deformation of the timber boards is far greater than plastic deformation during compression rolling.
6. The coefficient of friction between the rollers and the timber boards is constant during compression rolling.
7. Both compression rollers are active rollers and have equal diameter and peripheral speed.
8. The compression rollers are rigid and are not deformed during compression rolling.
9. The weight of the timber boards is negligible.

3.2 SYMBOLS AND DEFINITIONS

h	height of the timber board in any point during rolling.
b	width of the timber board
D	diameter of the compression roller
h_1	height of the timber board before compression rolling
h_2	minimum height of the timber board during rolling
dh	absolute compression dimension ($dh=h_1-h_2$)
C	compression level (%)
σ	normal stress
L	load
E	elastic modulus
α	bite angle: the angle between the initial contact point and the minimum height point of the timber board
V	peripheral speed of the rollers
K	a constant which is a factor concerned with modulus of elasticity
H	hardness of timber
R	radius of the roller
t	the projection length of AC contact arc on the horizontal plane (refer Figure 3.1)
r	the rolling angle
τ	shear force
P	normal force
f_1	coefficient of slip friction
θ	angle of friction
Rh	compression deformation of timber in radial direction

p_i force on a small area of the contact arc
 m the feed speed factor
 n the hardness factor
 f_2 coefficient of friction during rolling
 z the distance between the centre of the normal force
and geometric symmetric centre of the contact arc
 τ_i a shear force on a small area of the contact arc

3.3 MATHEMATICAL RELATIONS ON COMPRESSION ROLLING

Figure 3.1 represents schematically the dynamic

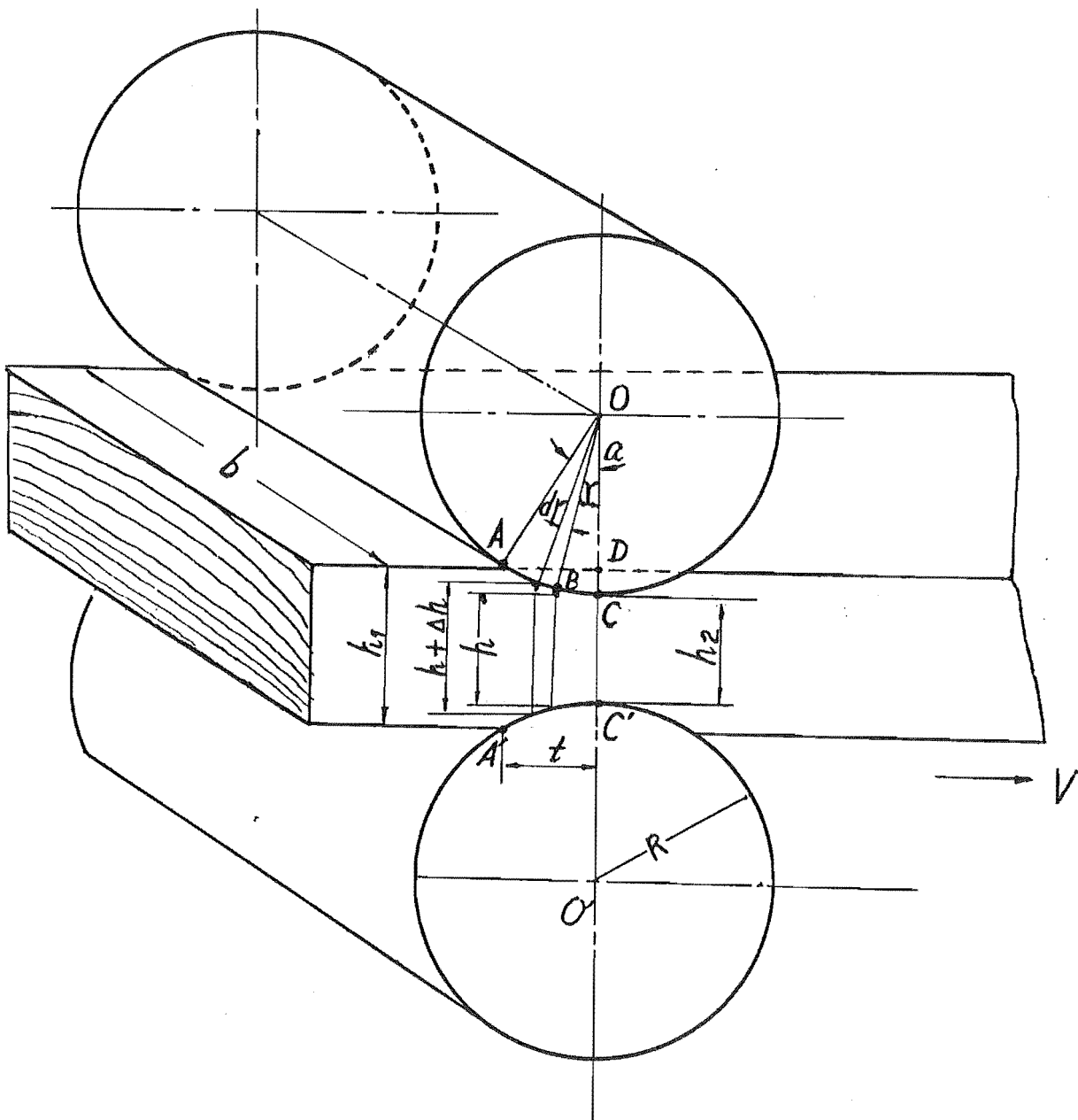


Figure 3.1 The Dynamic Compression Rolling of Wood

transverse compression rolling process of timber.

According to Figure 3.1, the absolute compression value of timber board is:

$$dh = h_1 - h_2 \quad (3.1)$$

where h_1 is height of the timber board before compression rolling

h_2 is minimum height of the timber board during rolling

thus, relative compression value of timber boards is defined as:

$$C = dh/h_1 \times 100\% \quad (3.2)$$

where C is also called compression level

From Figure 3.1, the basic formulae can be derived:

$$(D/2) \times \cos \alpha = D/2 - (h_1 - h_2)/2$$

and transposing

$$1 - \cos \alpha = (h_1 - h_2)/D$$

Hence the formula for calculating the angle of bite is found

$$\cos \alpha = 1 - dh/D \quad (3.3)$$

where α is the angle of bite which is one of the most important factors on compression rolling

D is the diameter of the rollers

Furthermore, from Figure 3.1

$$t^2 = OA^2 - OD^2$$

that is, $t^2 = R^2 - (R - dh/2)^2$

hence, $t = (dh \times R - (dh/2)^2)^{1/2} \quad (3.4)$

and neglecting higher-order term

$$t \approx (dh \times R)^{1/2} \quad (3.5)$$

From the simplified equation (3.5), the following formula can be deduced,

$$\sin \alpha = t/R \approx (dh \times R)^{1/2}/R = (dh/R)^{1/2} \quad (3.6)$$

Since the maximum bite angle is quite small, in order to simplify the calculation, the sinusoidal value of the bite angle could be replaced by the bite angle itself in radians. For example, in this study, the maximum compression level is 20%, the maximum thickness of the timber board is 33 mm and the diameter of the rollers is 206.8 mm, thus the maximum bite angle is 14.51 degrees. Obviously, the maximum error caused by the difference between the sinusoidal value and the radian value of the bite angle is less than 0.03. Finally, the calculation formula of the bite angle α is deduced as follows:

$$\alpha = (dh/R)^{1/2} \quad (\text{rad}) \quad (3.7)$$

From Figure 3.1, the formulae of the rolling angle r and the thickness of the timber board h at any point of contact arc can also be deduced:

$$\cos r = 1 - (h - h_2)/D \quad (3.8)$$

$$h = h_2 + D \times (1 - \cos r) \quad (3.9)$$

3.4 THE DYNAMIC PROPERTIES OF COMPRESSION ROLLING OF TIMBER BOARDS

3.4.1 MECHANISM OF BITE AND FRICTION IN THE COMPRESSION ROLLING PROCESS

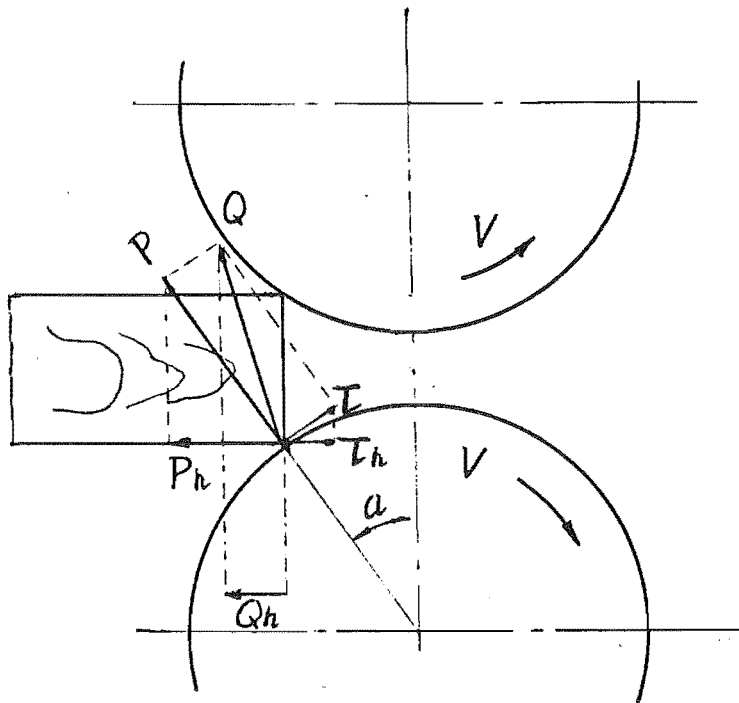


Figure 3.2 The timber board can not be fed by the rollers
($P \times \sin \alpha > \tau \times \cos \alpha$)

Compression rolling of the timber boards is a process of compression, shear and friction between the compression rollers and the timber boards. The feed of the timber boards is driven by two compression rollers, thus the feed conditions are of considerable importance.

Obviously, at the beginning of compression rolling (that is, when the timber board just contacts the rollers), the condition of bite is:

$$P \times \sin \alpha = \tau \times \cos \alpha \quad (3.10)$$

The equation 3.10 represents the critical

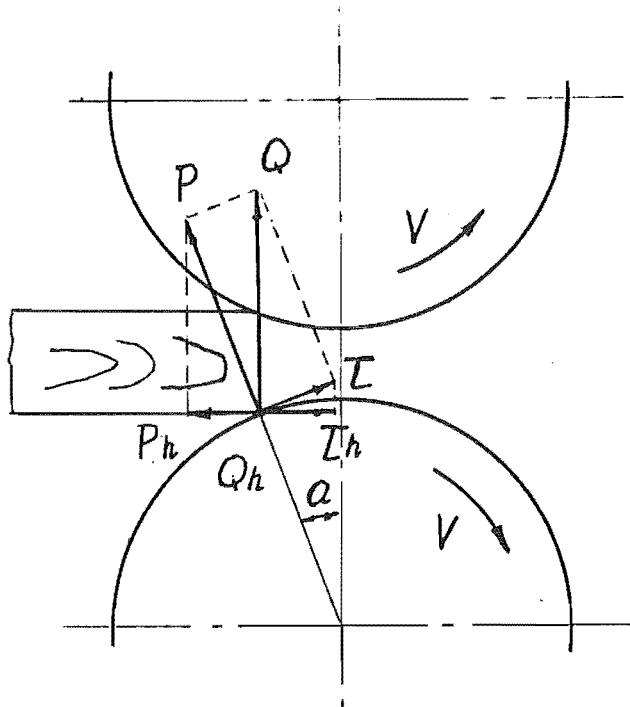


Figure 3.3 The timber board can be fed by the rollers $(P \times \sin \alpha < \tau \times \cos \alpha)$

condition during the feed of the timber boards.

where, P is normal force

τ is shear force

The equation (3.10) can be clearly depicted in Figure 3.2 and Figure 3.3.

In Figure 3.2, $P \times \sin\alpha$ is greater than $\tau \times \cos\alpha$, thus it is impossible to feed the timber board through the compression rollers; but in Figure 3.3, the timber boards can be fed by the rollers since $P \times \sin\alpha$ is less than $\tau \times \cos\alpha$. According to equation (3.10), we know that the value of $P \times \sin\alpha$ decreases and the value of $\tau \times \cos\alpha$ increases when the bite angle decreases, that is the possibility of bite increases when the bite angle decreases, thus we need to find out the maximum bite angle, which can set up the equation (3.10).

It is likely that the maximum angle of bite depends on the surface condition of the rollers and the timber boards, such as the moisture content of timber boards, the smoothness of the timber boards and rollers, the resin content etc..

Furthermore, the shear force can be represented:

$$\tau = f_1 \times P \quad (3.11)$$

where f_1 is coefficient of friction

The coefficient of friction can be represented as follows:

$$f_1 = \tan\theta \quad (3.12)$$

where θ is angle of friction

Substituting equation (3.11) into equation (3.10) gives:

$$P \times \sin\alpha = f_1 \times P \cos\alpha$$

hence,

$$f_1 = \sin\alpha / \cos\alpha = \tan\alpha \quad (3.12)$$

It is known that the coefficient of friction f_1 is equal to the tangent of the angle of friction, thus,

$$f_1 = \tan \alpha_{\max} = \tan \theta \quad (3.13)$$

and then,

$$\alpha_{\max} = \theta \quad (3.14)$$

From equation (3.14), the following conclusions can be drawn:

1. The timber boards can be fed by the rollers when the bite angle is less than or equal to the friction angle.
2. The range of the bite angle must be: $0 < \alpha < \theta$
3. Since the direction change of the resultant normal force, the feed condition is improved when the gap of the rollers is filled by timber boards.

The dynamic friction is caused by slipping between the timber board and the steel rollers at the initial period of feeding. The friction coefficient can be specified within 0.2-0.3 according to previous research results (McMillin etc. 1970, McKenzie and Karpovich 1968)

3.4.2 THE SPEED OF COMPRESSION ROLLING

The peripheral speed of the compression rollers can be calculated as follows:

$$V = (\pi \times D \times n)/60 \quad (\text{m/sec}) \quad (3.15)$$

where,

D is the diameter of the compression rollers in meters

n is the revolutions per minute of the rollers

Generally, the peripheral speed of the compression rollers represents the feed speed of the timber board. But we must recognize that the horizontal component of the peripheral speed of the compression rollers varies

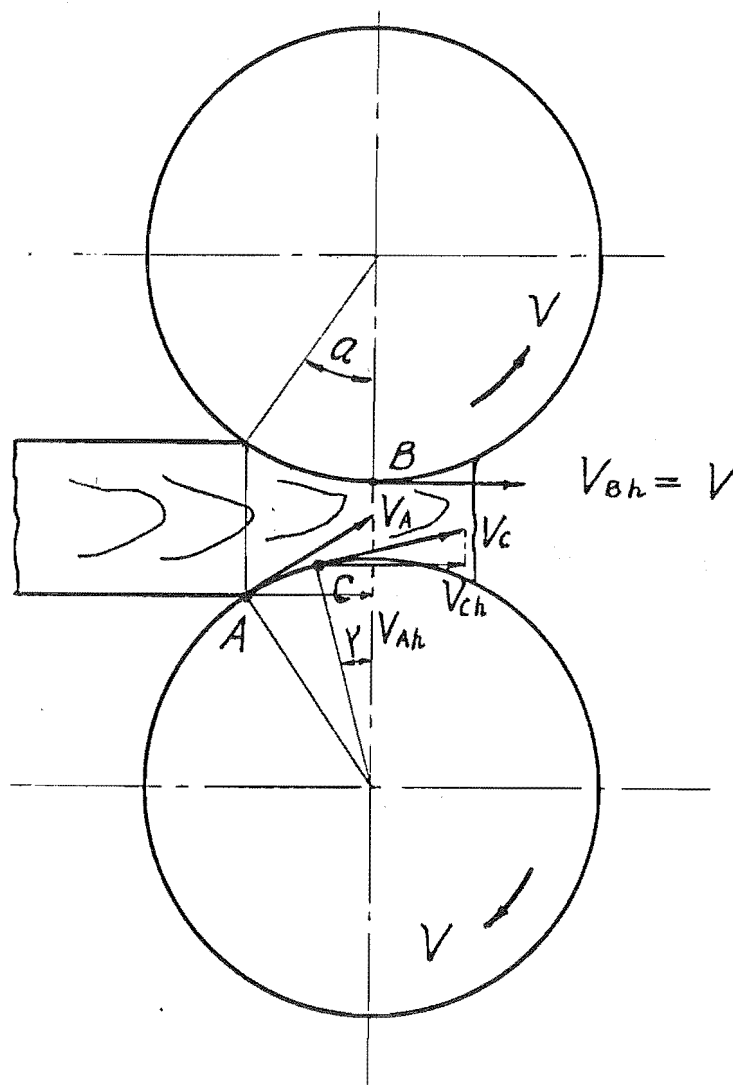


Figure 3.4 The change of feed speed at the different points

(Figure 3.4) during compression rolling. For instance, in Figure 3.4, the horizontal component of the peripheral speed of the point A is a minimum V_{Ah} , but in the point B, the horizontal component of the peripheral speed is a maximum V_{Bh} . Thus, in the arc of the rolling of any point C between A and B, the relationship will be:

$$V_{Ah} < V_{Ch} < V_{Bh} \quad (3.16)$$

The change of the horizontal component of the

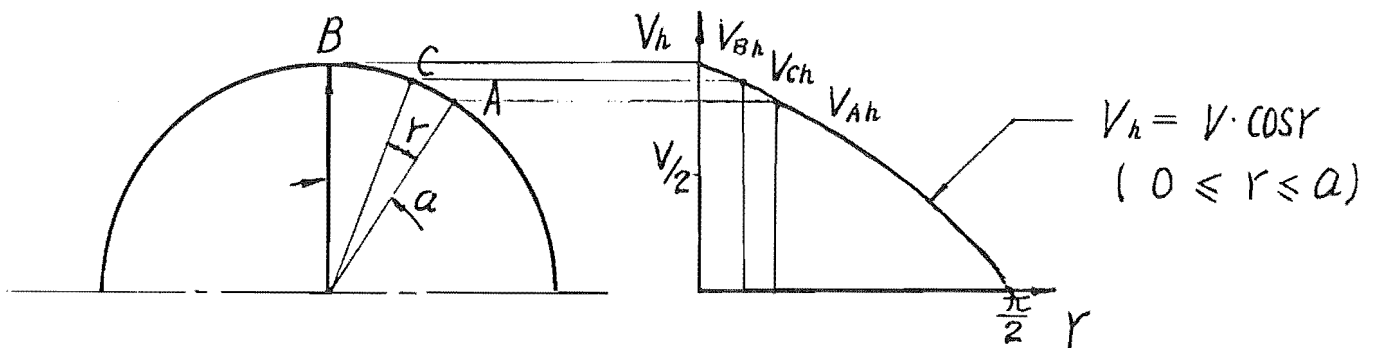


Figure 3.5 Sketch of change of the horizontal component on peripheral speed

peripheral speed can be represented schematically in Figure 3.5

From Figure 3.5, we can observe that there is a difference between V_{Ah} and V_{Bh} . It is the maximum difference of the feed speed, so the maximum relative difference of the feed speed is:

$$V_d = (V_{Bh} - V_{Ah})/V_{Bh} \times 100\% \quad (3.17)$$

In Figure 3.5, at a certain point, the horizontal component of the peripheral speed can be represented as follows:

$$V_h = V \times \cos r \quad (3.18)$$

where r is the rolling angle $(0 \leq r \leq \alpha)$

thus, $V_{Bh} = V \quad (3.19)$

$$V_{Ah} = V \times \cos \alpha \quad (3.20)$$

Substituting equations (3.19) and (3.20) into equation (3.17) and simplifying yields,

$$V_d = (1 - \cos \alpha) \times 100\% \quad (3.21)$$

To sum up, it is likely that there is a slight slip between the timber boards and compression rollers during rolling.

3.4.3 LOAD AND TORQUE DURING COMPRESSION ROLLING

According to the basic assumptions, we suppose the elastic deformation is far greater than plastic deformation of the timber boards during compression rolling, thus the timber boards are elastic bodies and Hooke's law can be used.

To simplify the calculations, the following hypothesis is made.

1. The strain and stress at a point during rolling have a constant relation.

2. The projection length between any two points of the timber board on the horizontal plane is not changed during rolling.
3. The width of the timber board is supposed to be of a unit width.
4. During compression rolling, the relationship of load and normal force, speed and hardness is represented as follows:

$$L = P \times V^m \times H^n \quad (3.22)$$

where,

L is the working load of compression rolling

P is the normal force caused by deformation of wood

V is the feed speed

m is feed speed factor

H is the value of wood hardness

n is the hardness factor

In equation (3.22), P is the principal parameter which basically determines the range of the load. Item V^m indicates the following fact: The compression rolling process is affected by the recovery rate of the timber board. Under the same compression level and treatment condition (include the moisture content of the board, diameter of rollers and the density of the timber, etc.), if the feed speed increases up to a certain value, the recovery rate of the timber boards is relatively lower than the feed speed (the recovery rate is not change, refer basic assumptions 5), so the dynamic contact arc is shorter than static contact arc of the timber boards and

the rollers.

Figure 3.6 describes schematically this phenomenon during the compression rolling process.

In Figure 3.6, all of the compression rolling

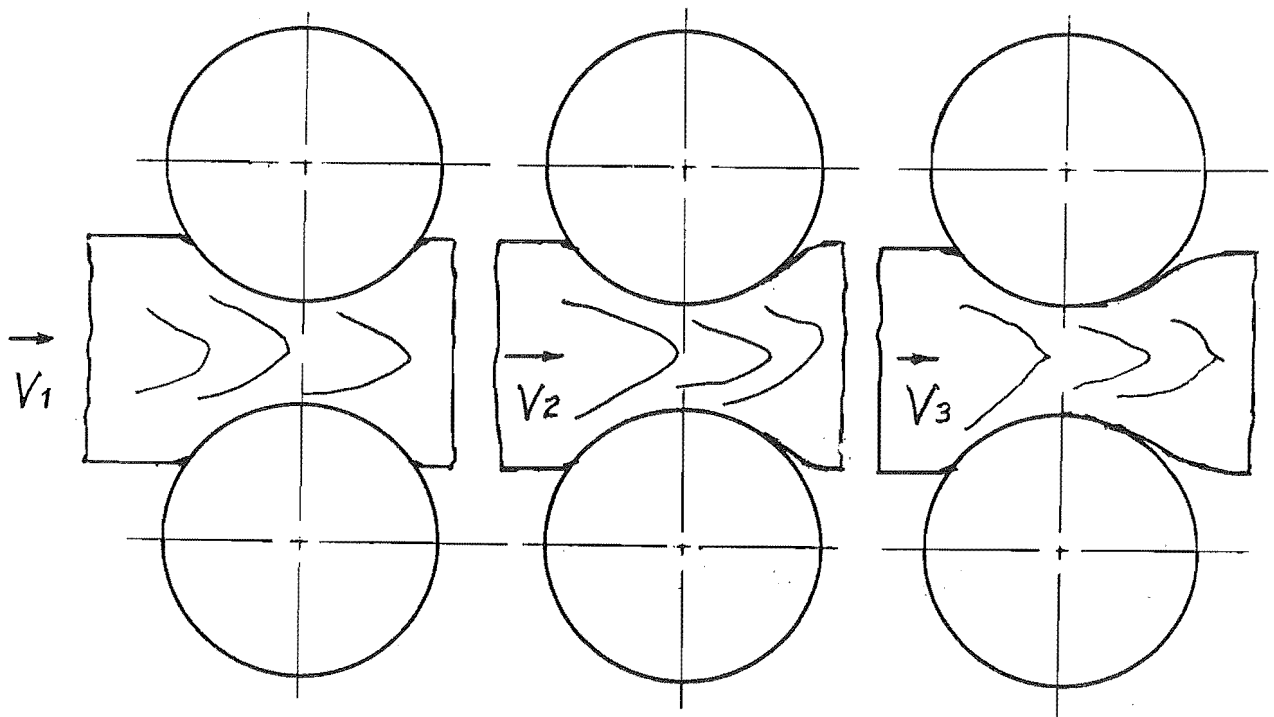


Figure 3.6 The effect of the feed speed on the process of deformation recovery ($V_1 < V_2 < V_3$)

conditions are the same except for the feed speed: $V_1 < V_2 < V_3$

Item H^n is a correction of the hardness change of the timber boards. In fact, the hardness of the timber boards can represent the general physical properties of

the timber boards during compression rolling (such as density of wood, moisture content etc.).

In order to simplify the analysis of compression rolling process and to compare easily the result of the experiments, we take the logarithm of both sides of the equation (3.22), that is,

$$\text{Ln}L = \text{Ln}P + m \times \text{Ln}V + n \times \text{Ln}H \quad (3.23)$$

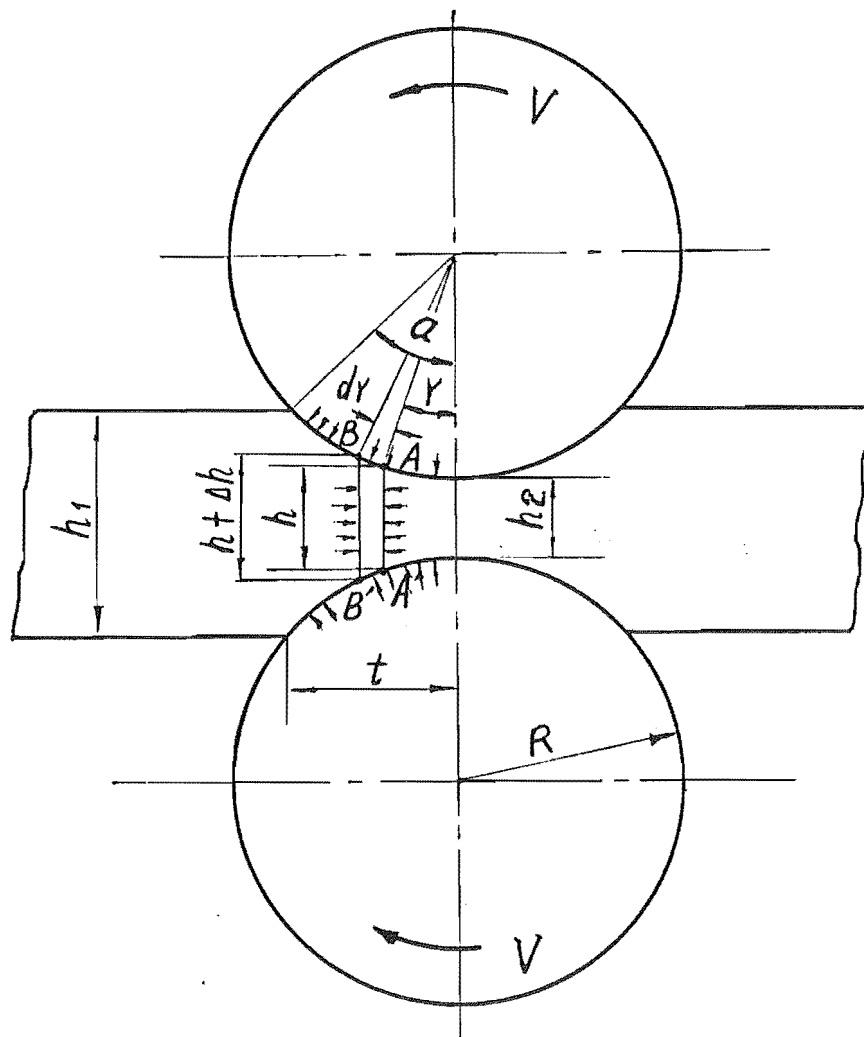


Figure 3.7 The distribution of the force during compression rolling

Furthermore,

$$P = \Sigma (p_i) \quad (3.24)$$

where, p_i is a force on a small area of the contact arc

Figure 3.7 represents schematically the distribution of the force during compression rolling. From Figure 3.7, we observe that at the point of A,

$$p_A = \sigma_A \times M_A \quad (3.25)$$

where,

σ_A is the normal stress of the timber boards at the point A

M_A is the area of the small element

According to the basic principle of the theory of elasticity (Bodig and Jayne, 1982), the normal stress of the timber board can be written as follows:

$$\sigma = K \times R_h \quad (3.26)$$

where,

K is a constant which is a factor concerned with modulus of elasticity

R_h is compression deformation of timber along the radial direction

Substituting equation (3.26) into equation (3.25) yields,

$$p_A = K \times R_{hA} \times M_A \quad (3.27)$$

In equation (3.27), the area of the small element M_A can be represented as follows:

$$M_A = R \times dr \quad (3.28)$$

and

$$Rh_A = \frac{dh_A}{\cos r} \quad (3.29 \text{ a})$$

Since the maximum bite angle is quite small and $0 \leq r \leq \alpha$, in order to simplify the calculation, Rh could be replaced by dh , that is, equation (3.29 a) can be rewritten as follows:

$$Rh_A \approx dh_A = (h_1 - h_2)/2 - R(1 - \cos r) \quad (3.29 \text{ b})$$

and the relative error can be indicated:

$$d_f = (Rh_A - dh_A)/Rh_A = 1 - \cos r \quad (3.30)$$

In this research, this relative error is less than 0.03. Substituting equations (3.28) and (3.29 b) into equation (3.27) and simplifying yield,

$$p_A = K \times R \times (dh/2 - R \times (1 - \cos r))dr \quad (3.31)$$

p_A represents a normal force on a small element which includes the point A of contact arc between the timber board and the roller. In fact, the point A represents any point on the contact arc, so summing up all of the force elements on the contact arc and taking into account the symmetry of the contact arc and the width of the timber board, we get the following equation,

$$P = 2xbxKxR \int_0^\alpha (dh/2 - R \times (1 - \cos r))dr \quad (3.32)$$

that is,

$$P = 2xbxKxRx(dh/(2\alpha) - Rx\alpha + Rx\sin\alpha) \quad (3.33)$$

where,

b is the width of the timber board

We can further analyse the equation (3.33). Since the maximum bite angle is very small, the sinusoidal value of the bite angle can be replaced by the bite angle itself in radian, that is,

$$\alpha \approx \sin \alpha$$

Substituting the above equation into equation (3.33) yields:

$$P = b \times K \times R \times dh \times \alpha \quad (3.34)$$

Furthermore, substituting equation (3.7) into equation (3.34) and simplifying yields:

$$P = b \times K \times \sqrt{R} \times (dh)^{3/2} \quad (3.35)$$

Using the same principle, we can deduce:

$$\tau = \Sigma (\tau_i) \quad (3.36)$$

where τ is the resultant shear force caused by friction

τ_i is shear force of any small element on the contact arc

During compression rolling of timber boards, the output side portion of the contact arc does not provide the full portion of its normal reaction so that the point at which the centre of normal force is applied always deviates from the geometric centre of the roller. If this distance is z , there is a retarding couple $L \times z$ which must be overcome by the torque of hydraulic motor. Neglecting other friction and the drop of efficiency, the

following equation can be deduced (Bowden and Tabor, 1963):

$$T = L \times z \quad (3.37a)$$

Furthermore, comparing equation (3.11), we can get the following equation:

$$T = \tau \times R \quad (3.37b)$$

where R is the radius of the roller
 z is the distance between the centre of the normal force and geometric symmetric centre of the contact arc
 T is the compression rolling torque
 L is the working load
 τ is the resultant shear force caused by resistant friction force

Equation (3.37a) is deduced by considering the following factors:

1. The timber is not perfect elastic material, so the recovery of compression deformation is a function of time.
2. The contact arc is not geometrically symmetrical during compression rolling (Figure 4 Gunzerodt etc. 1988).
3. The influence of the feed speed and hardness is considered.

From equations (3.37a) and (3.37b), we believe that there are two basic methods to calculate the torque.

1. First method: the torque based on the resultant shear force

The same principle as equation (3.24), we have,

$$\tau = \Sigma (\tau_i)$$

where τ_i is shear force on a small area of the contact arc

$$\tau_i = f_2 \times p_i \quad (3.11a)$$

where p_i is a force on a small area of the contact arc

f_2 is friction coefficient during compression

Because many factors influence the friction (such as smoothness of the contact surface, moisture content and the condition of the compression rolling), it is very difficult to determine the friction coefficient.

Generally, the friction coefficient during rolling is varied: it is greater than the rolling friction coefficient and smaller than sliding friction coefficient (Knudson and Schniewind 1971). It is likely that this friction coefficient is as a modified rolling friction coefficient. It is caused by two different factors:

- (1) slip at the contact arc during rolling.

- (2) deformation of compression rolling

(Johnson and Tabor 1968)

2. Second method: the torque is based on the retarding couple $L \times z$

Based on the previous research, we believe that the contact arc is not geometrically symmetrical during rolling (Gunzerodt 1985 and Gunzerodt etc. 1988): the

pattern of the contact arc has already been described in Figure 3.6

We believe the following equation is basically correct with limited experiments:

$$t_2 = (1/2 \sim 3/4) \times t_1$$

where t_1 is the projection length of the contact arc on the input side

t_2 is the projection length of the contact arc on the output side

The pattern and length of the contact arc and the distribution of the force can be described in Figure 3.8

If we suppose that: the distance between the geometrical centre line of the rollers and the centre of the resultant normal force at input side contact arc is $1/3 \times t_1$ and the distance between the geometrical centre line of the rollers and the centre of the resultant normal force at output side contact arc is $1/3 \times t_2$, then we have the following equation:

$$T = (0.08 - 0.566)t_1 \times L$$

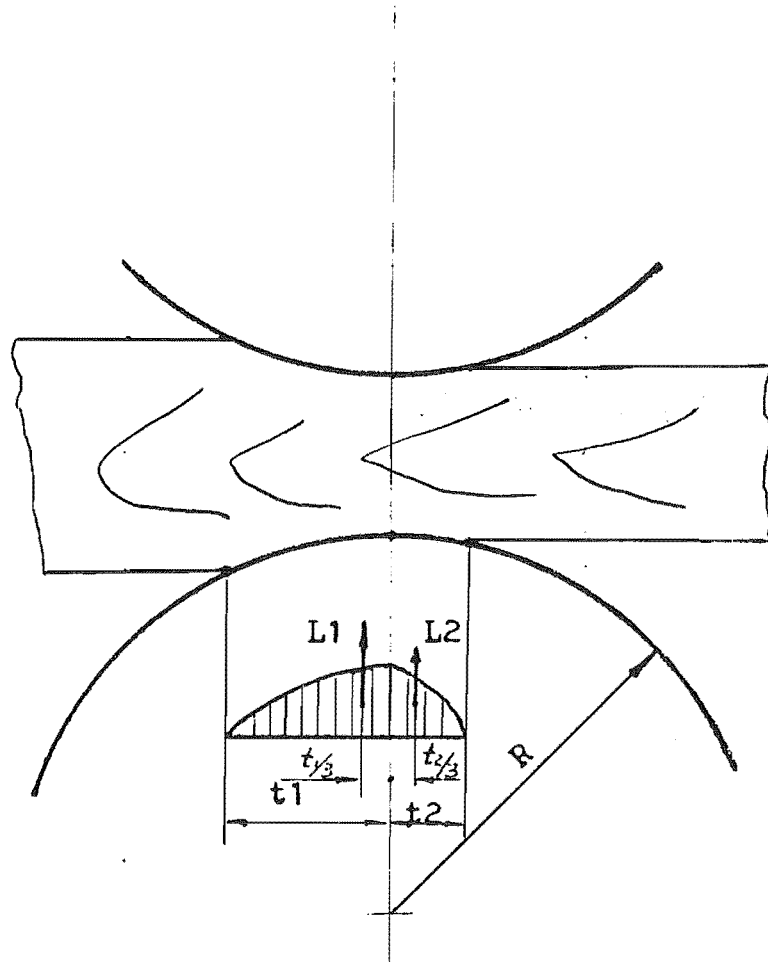


Figure 3.8 Resultant rolling force and torque arm

Referring to equation (3.35), the normal force P is the function of the width of timber boards, elastic property of timber, the diameter of rollers and compression level. In the experiments, the item $b \times K \times R^{1/2}$ can be thought of as a single factor and be written as:

$$\beta = b \times K \times R^{1/2}$$

Thus, the normal force can be represented as follows:

$$P = \beta \times (dh)^{3/2} \quad (3.38 \text{ a})$$

We generalize the equation (3.38 a), then we deduce the following formula:

$$P = \beta \times (dh)^j \quad (3.38 \text{ b})$$

Equation (3.38 b) is the mathematical generalization formula of equation (3.38 a). Substituting equation (3.38 b) into equation (3.22) yields:

$$L = \beta \times dh^j \times v^m \times H^n \quad (3.39)$$

Thus, the equation (3.23) can be also represented as:

$$\ln L = \ln \beta + j \times \ln(dh) + m \times \ln V + n \times \ln H \quad (3.40)$$

The equations (3.37a), (3.37b), (3.39) and (3.40) are the basic calculation formulae for analysing compression rolling in term of the working load and torque.

CHAPTER FOUR:

THE COMPRESSION ROLLING MACHINE

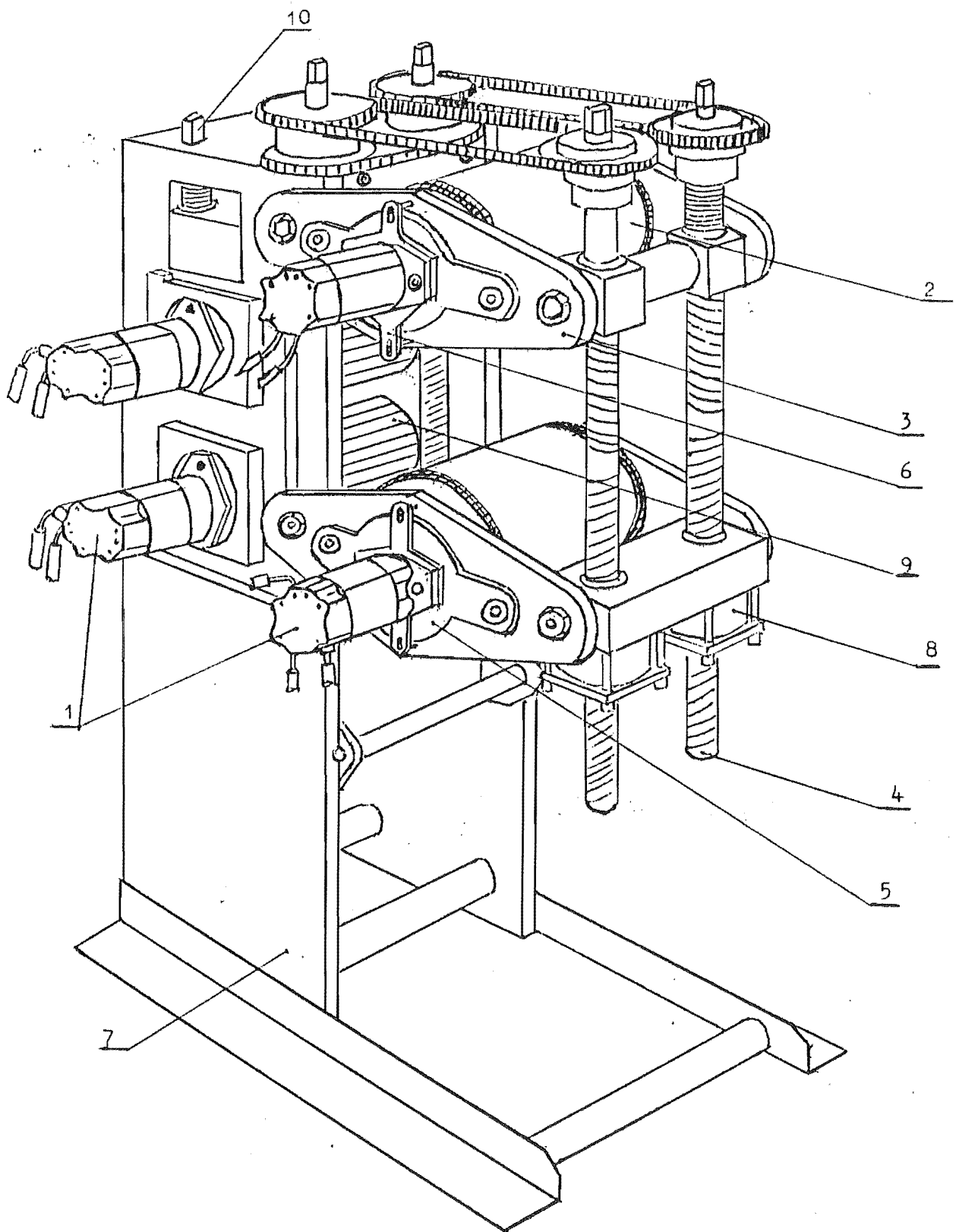
4.1 GENERAL FUNCTION AND FEATURE OF COMPRESSION ROLLING DEVICE

Figure 4.1 represents schematically the configuration of the compression rolling device used in this research. This compression rolling machine provides the following functions and features for compression rolling of timber boards.

1. The machine is easy to operate because the structure of the machine is very simple.
2. The adjustment of the feed speed is reliable, simple and flexible. The hydraulic motors are used to accomplish speed control with infinite and smooth speed change over a wide range and in either direction.
3. The design of the machine considers fully a possibility of installation and usage of measurement instrumentation. With this configuration, the compression rollers are left unenclosed giving good access to the nip area for observation and measurement of the timber boards during compression rolling.

Figure 4.1 The compression rolling device

1. Hydraulic motors
2. Compression rollers
3. The main brackets
4. Load screws
5. Load beams
6. Torque arms
7. The main frame
8. Limited load cylinders
9. The infeed rollers
10. Adjustment screws of feed
rollers.



The compression rolling machine consists of a compression rolling device and a hydraulic power system. Their functions and features are explained as follows:

1. Hydraulic motors: Four low speed and high torque hydraulic motors are used on the compression rolling device. The motors are mounted directly on the ends of the shafts of the compression and infeed rollers. These motors are connected to a variable displacement pump system. The application of the hydraulic motors provides the following advantages and features:

(A). The hydraulic motors can operate at a low speed that remains constant even when the load varies.

(B). Infinite and smooth speed control is accomplished easily and economically.

(C). The rotation direction of the motors can be changed instantly with a simple and economic control system. They can rotate continuously and provide equal power output in either direction.

2. Compression rollers: Three pairs of compression rollers are provided. Their diameters are 206.8 mm, 156 mm and 51.8 mm. 206.8 mm diameter compression rollers are called the main compression rollers. The others are the auxiliary compression rollers. The design and installation of the compression rollers permit the maximum compression thickness is up to 140 mm.

As shown in Figure 4.1, the main compression rollers are installed on the main brackets. The duplex chain is fixed on both sides of the main compression rollers in order to drive other auxiliary compression rollers at the same peripheral speed as the main rollers.

3. The main brackets: They are used to connect and support the compression rollers and the hydraulic motors. The main brackets are connected and supported by four long screws rather than a heavy frame. This is one of the features of this compression rolling device. With this structure, the operators have access to the nip area to measure and observe the compression rolling process at close range.
4. Load screws: Four long load screws link the main brackets. This configuration has the advantage of not needing a heavy external structure. The set of four load screws are reverse threaded at the top and bottom, so the top screw nuts and bottom screw nuts remove in reverse direction when the set of four load screws is turned in the same direction. The screw nuts connect with the main brackets. The main brackets are closed or further apart by the load screws. The screws are linked by a chain and sprocket system to give easy and convenient adjustment of the roller gap.

5. Load beams: On both sides of the two main compression rollers, there are four load beams, which are used for the installation of the strain gauges and for measuring the load values.
6. Torque arms: As shown in Figure 4.1 and Figure 4.2, there are two torque arms connected to the main brackets and the hydraulic motors. Because of the connection method of the torque arms, they bear pure

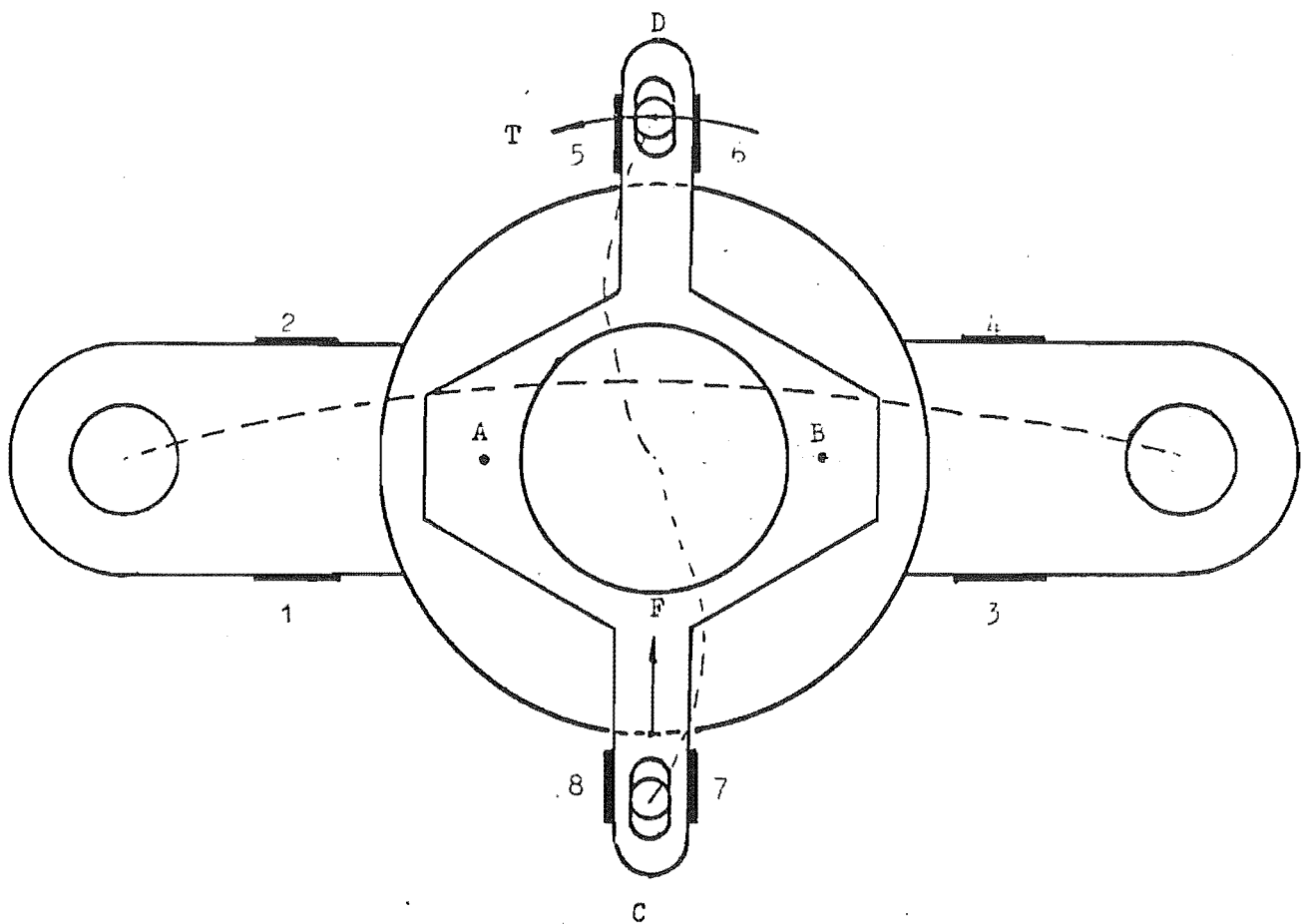


Figure 4.2 Sketch of Load Beam and Torque Arm

torque, thus the torque during the compression rolling of timber board is measured accurately. Each torque arm is connected to each of the hydraulic motors of the main compression rollers at A and B. At same time, it is attached to each of the main brackets on the side of the hydraulic motors through simple supports at C and D. A and B are fixed connections carry loads in all three planes, but C and D are suspended supports and bear torque only. Thus the deformation of the torque arms during compression rolling is the "S"-shape type deflection (Figure 4.2).

7. The main frame: It connects the other parts of the device and supports the compression rollers and the infeed rollers.
8. Load hydraulic "cut out" cylinders: They are designed and used for the purpose of safety and protection. The working pressure of the cylinders can be pre-adjusted to supply hydraulic overload protection against large, hard knots in the timber.
9. The infeed rollers: There is a pair of grooved infeed rollers on the device. Each roller is driven by a hydraulic motor.
10. Infeed rollers adjustment screws: the screws are used for adjusting the gap of the infeed rollers.

4.2 THE FUNCTIONS AND FEATURES OF HYDRAULIC POWER SYSTEM

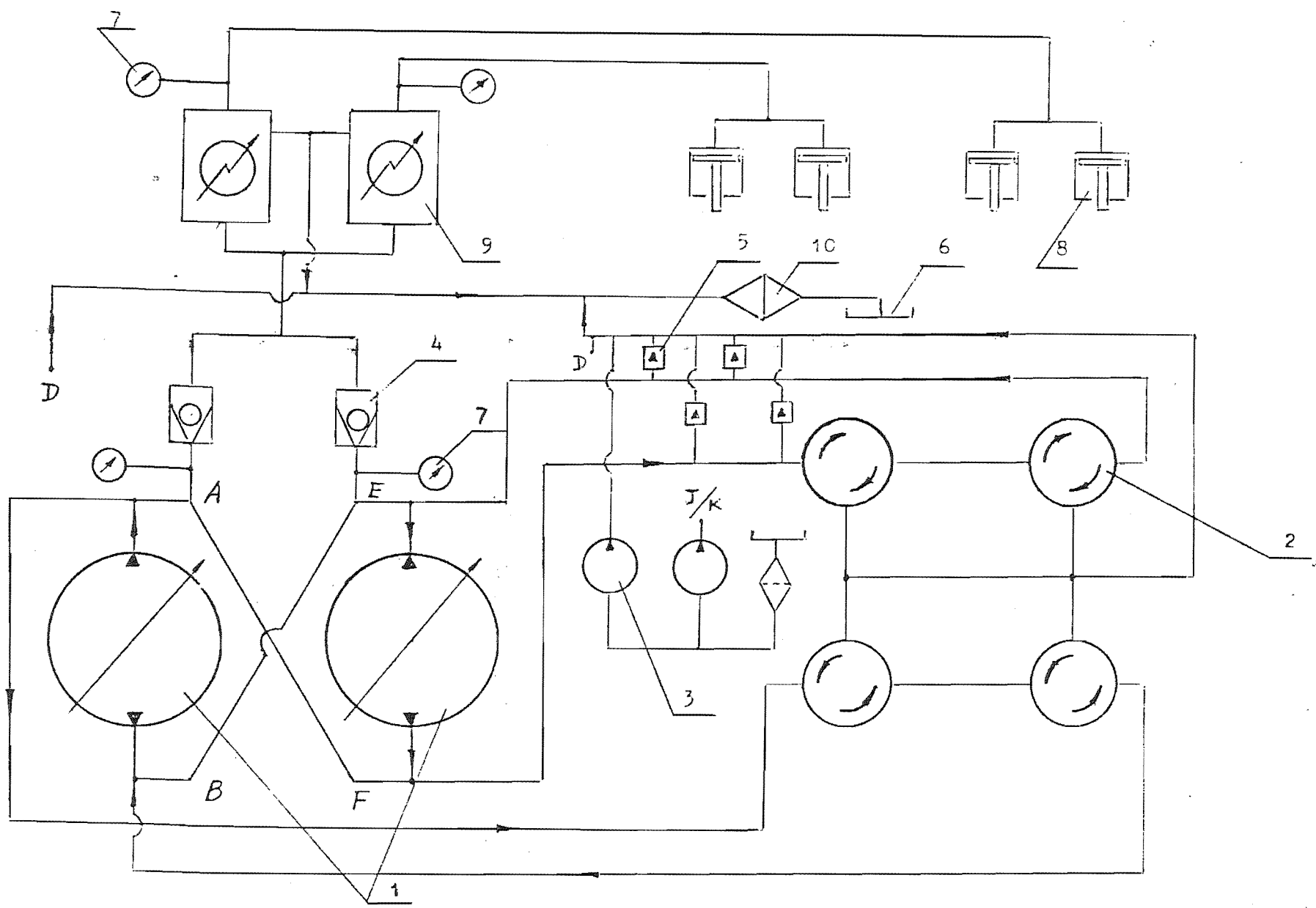
The hydraulic power system consists of the electric motor, the flywheel, the clutch, the VPT 3333 hydrostatic transmission primary unit, the adjustment mechanism (control of displacement of double pump), the filter, the safety valve, the oil reservoir and electric control parts. The principle of the hydraulic system is described schematically in Figure 4.3. The hydrostatic transmission primary unit is composed of two variable displacement hydraulic pumps, check valves, low pressure relief valve, four differential piston type high pressure relief valves and charge pump.

4.3 SPECIFICATION

The power of electric motor	18 kw
Maximum design compression force	50 KN
Diameter of compression rollers	51.8 mm
	156 mm
	206.8 mm
Diameter of infeed rollers	206.8 mm
Maximum working width	110 mm
Maximum gap between the principal rollers	140 mm
Feed speed	0-3500mm/s
Dimension of the device (mm)	1100x760x1400
Dimension of the hydraulic system (mm)	1310x1200x1440

Figure 4.3 The principle of the hydraulic system

1. Variable displacement hydraulic pumps
2. High torque hydraulic motors
3. The charge pump unit
4. Check valves
5. Relief valves
6. Oil tank
7. Pressure gauges
8. Limiting load hydraulic cylinders
9. Throttle valves
10. Filter



CHAPTER FIVE:

THE APPLICATION OF INSTRUMENTATION AND MICROCOMPUTER FOR MEASUREMENTS AND DATA ACQUISITION

5.1 THE AIMS AND RANGE OF THE APPLICATION

Figure 5.1 is a diagram, which explains schematically the principle and range of application of the computer and the instruments.

The object of the instrumentation is mainly to measure speed, torque and load during compression rolling and capturing digital values.

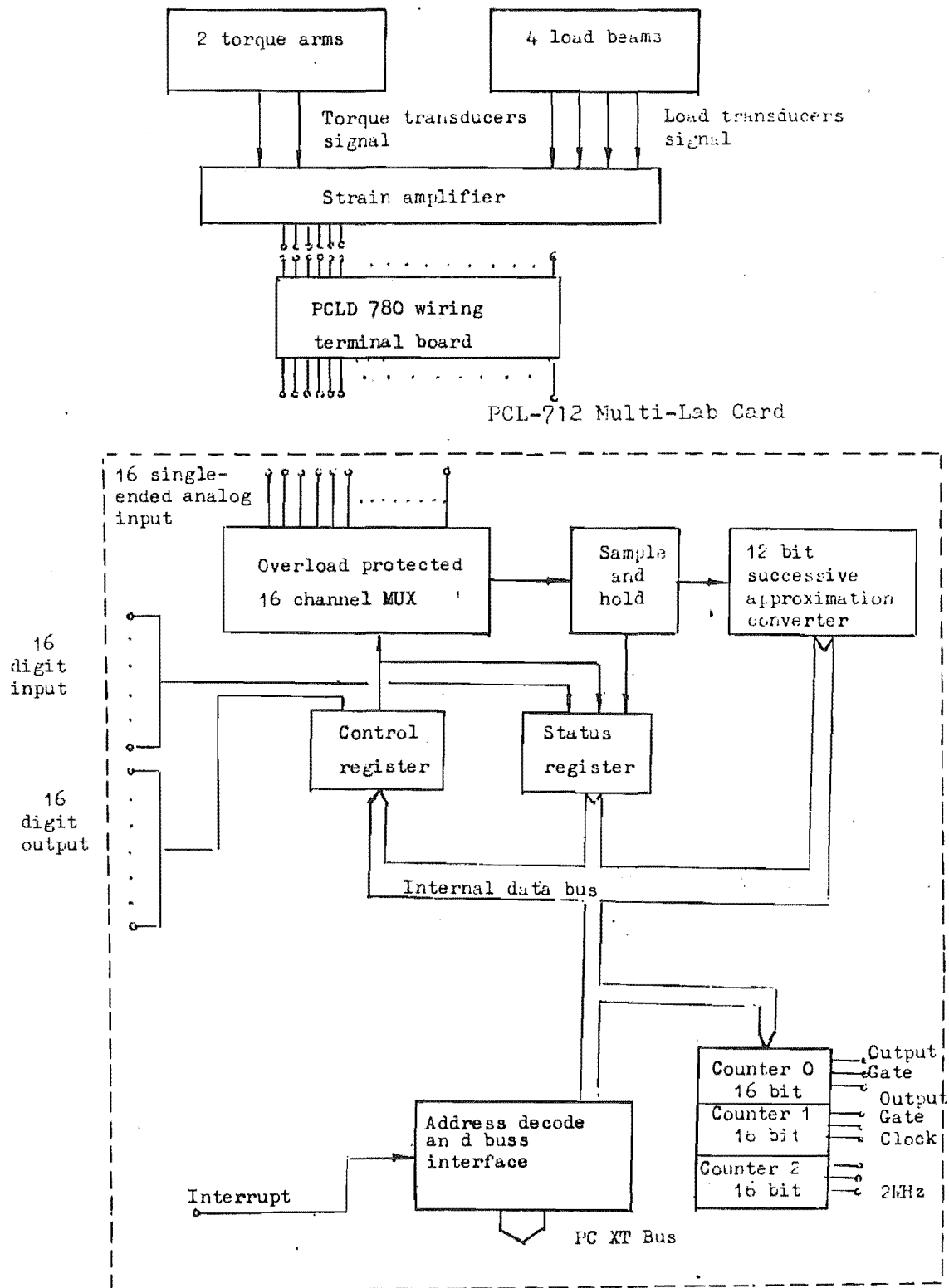


Figure 5.1 The principle of application of the computer and the instruments

5.2. MEASUREMENT OF TORQUE AND LOAD

5.2.1 BASIC PRINCIPLE OF THE MEASUREMENT

The measurement elements of the load and torque-- torque arms and load beams have been described in Chapter 4 (Figure 4.2). Each torque arm is part of a torque dynamometer. Each load beam is one of the elements of a load dynamometer. A torque dynamometer consists of a torque arm, 4 resistance-type strain gauges, direct current power device and the signal amplifier. Similarly, a load dynamometer is composed of a load arm, 4 strain gauges, DC power device and the signal amplifier. The position of the torque arms and load beams and the distribution of the strain gauges are shown in Figure 4.1 and Figure 4.2. A group of four resistance-type strain gauges is glued onto each of the torque arms and each of the load beams. Each group is connected and wired up to a Wheatstone bridge with a temperature compensating circuit as shown in Figure 5.2 and Figure 5.3.

Since the change of electric resistance is directly proportional to the change of the strain in the strain gauge and the strain gauges are closely glued to the torque arms or the load beams, the change in the resistance in the strain gauges represents the change in the strain in the torque arms or the load beams, which is caused by torque or load during compression rolling. Thus, the load of compression rolling represented by the

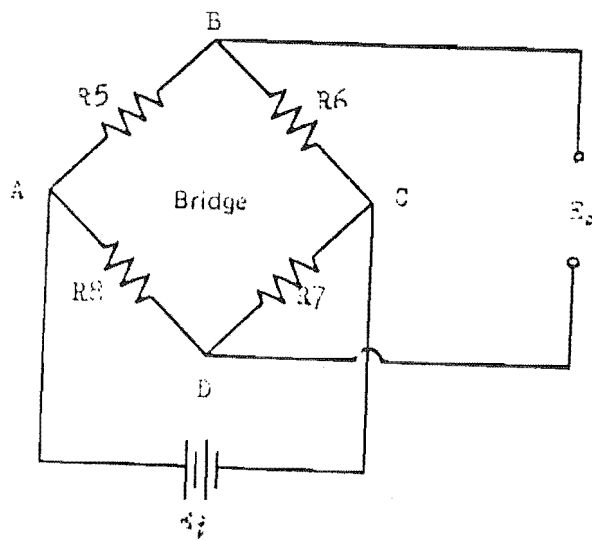


Figure 5.2 Wheatstone bridge circuit on the torque arm

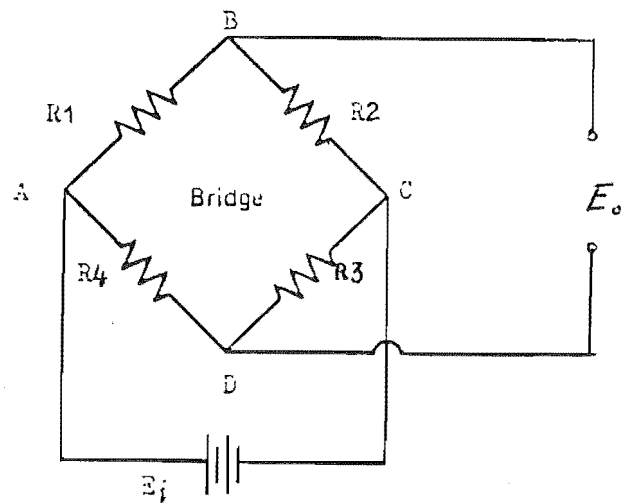


Figure 5.3 Wheatstone bridge circuit on the load beam

strain of the load beam can be expressed by the change of resistance of the strain gauges on the load beam. The same applies to the measurement of the torque. The principle of the torque dynamometers and the load dynamometers is indicated clearly in Figure 5.4.

5.2.2 SIGNAL CONDITIONING CIRCUIT -- THE WHEATSTONE BRIDGE

One of the Wheatstone bridges on the load arms is analyzed as follows. The rest of the Wheatstone bridges have the same principle.

Figure 5.3 represent a Wheatstone bridge on a load beam. The output voltage E_o of the bridge can be determined by treating the top and bottom parts of the bridge as individual voltage dividers. Thus,

$$E_{AB} = E_i \times R_1 / (R_1 + R_2) \quad (5.1)$$

$$E_{AD} = E_i \times R_4 / (R_3 + R_4) \quad (5.2)$$

The output voltage E_o of the bridge is :

$$E_o = E_{BD} = E_{AB} - E_{AD} \quad (5.3)$$

Substituting equations (5.1) and (5.2) into equation (5.3) yields:

$$E_o = (R_1 \times R_3 - R_2 \times R_4) / ((R_1 + R_2) \times (R_3 + R_4)) \quad (5.4)$$

Equation (5.4) indicates that the initial output voltage will vanish ($E_o = 0$) if

$$R_1 \times R_3 = R_2 \times R_4 \quad (5.5)$$

When equation (5.5) is satisfied, the bridge is said to be balanced. With an initially balanced bridge, an output voltage dE_o develops when the resistances R_1 , R_2 , R_3 and R_4 are varied by amounts dR_1 , dR_2 , dR_3 and dR_4 respectively. From equation (5.4), with these new values of resistance,

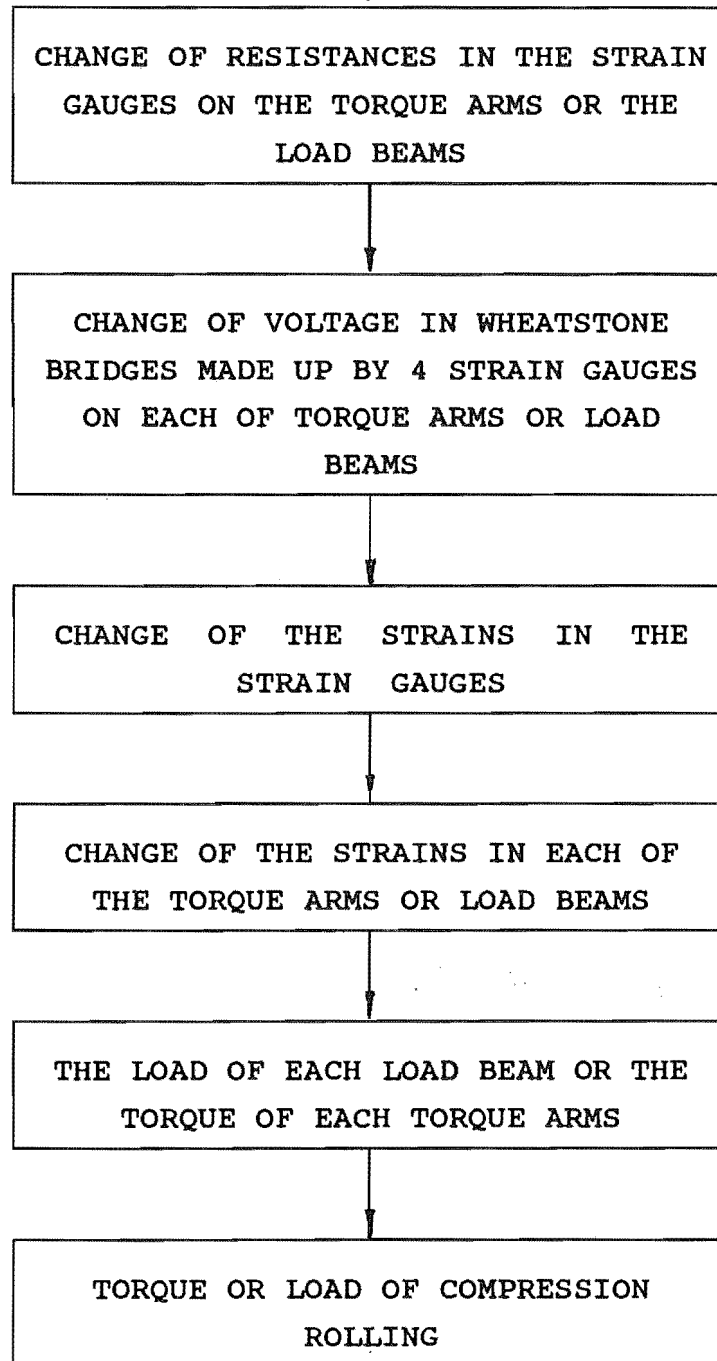


Figure 5.4 Principle of the torque dynamometers and the load dynamometers

$$\frac{(R_1+dR_1) \times (R_3+dR_3) - (R_2+dR_2) \times (R_4+dR_4)}{(R_1+dR_1+R_2+dR_2) \times (R_3+dR_3+R_4+dR_4)} \times E_i \quad (5.6)$$

Expanding, neglecting higher-order terms and substituting equation (5.5) yields:

$$dE_o = \frac{R_1}{(R_1+R_2)^2} \times \left(\frac{dR_1}{R_1} - \frac{dR_2}{R_2} + \frac{dR_3}{R_3} - \frac{dR_4}{R_4} \right) \times E_i$$

Equation (5.7) indicates that the output voltage from the bridge is a linear function of the resistance changes. This apparent linear results from the fact that higher-order terms in equation (5.6) are neglected. If the higher-order terms are retained, the output voltage dE_o is a nonlinear function. Since the resistances of each of the strain gauges on the load beam are same, the equation (5.7) can be deduced:

$$dE_o = ((dR_1+dR_3) - (dR_2+dR_4)) / (4 \times R) \quad (5.8)$$

where $R=R_1=R_2=R_3=R_4$

Since the distribution of the strain gauges on the load beam is symmetrical, the strains on gauge 1 and gauge 3 are the same and the strains on gauge 2 and gauge 4 are also the same, that is,

$$dR_1 = dR_3 = dR_C$$

$$dR_2 = dR_4 = dR_T$$

where dR_C is the change of resistance in gauge 1 or gauge 3 due to uniaxial compression.

dR_T is the change of resistance in gauge 2 or gauge 4 caused by uniaxial tension.

According to symmetry, from equation (5.8) the following equation is deduced:

$$|dE_o| = (2x|dR_C| + 2x|dR_T|) / 4xR \quad (5.9)$$

then,

$$|dE_o| = dR/R \quad (5.10)$$

By neglecting the installation error of the strain gauges and the error caused by the strain gauges performances, the strain of the load beam can be deduced from Appendix 1, that is:

$$\delta = 1/GF \times dR/R \quad (5.11)$$

To sum up: the resistance change of the strain gauges of the load beam is converted into the change of voltage by the Wheatstone bridge and this change expresses the change of strain on the surface of the load beam. The load of compression rolling can be represented as a linear function of the strain. Finally, by means of

calibration, we can set up a relationship between the load and the voltage of the Wheatstone bridge.

For the principle of the resistance-type strain gauges also refer to Appendix 1. For the selection and installation of the strain gauges refer to Appendix 2 in detail.

5.2.3 RELATED MEASURING DEVICE

The following devices are used for the measurement of load and torque.

- (1). The strain gauge amplifier.
- (2). DC power device
- (3). Terminal Block
- (4). PCL-712 Multi-Lab Card
- (5). PC XT
- (6). PCLD-780 Wiring terminal board

The principle and application of these devices will be described separately.

5.2.4 CALIBRATION

Before the measurement of the torque and load, the dynamometers need to be calibrated. The principle of calibration is very simple. The known load or torque is applied to the dynamometers and the voltage values are recorded under the different levels of load or torque. The voltage-load curve and the voltage-torque curve are drawn according to calibration test data. The linear regression equations of load and voltage or of torque and

voltage can be deduced by data processing.

The calibration procedure of each of the two load dynamometers was described as follows:

- (1). First of all, a load cell must be calibrated. It is connected with the strain gauge indicator in the full Wheatstone bridge and loaded up by means of uniaxial compression on the universal testing machine from 0 KN to 50 KN at interval of 5 KN. The readings of the strain values from the strain gauge indicator are recorded. These readings correspond to each load.
- (2). Secondly, the load cell is placed between the two compression rollers. Both top and bottom surface of the load cell are in contact with the aluminium blocks as shown in Figure 5.5.

(3). The load cell is placed under load by closing the gap between two compression rollers. A hand pump is connected to the two "limit load" cylinders at the bottom of the two long screws (Figure 4.1) and need to pump the hydraulic oil into the

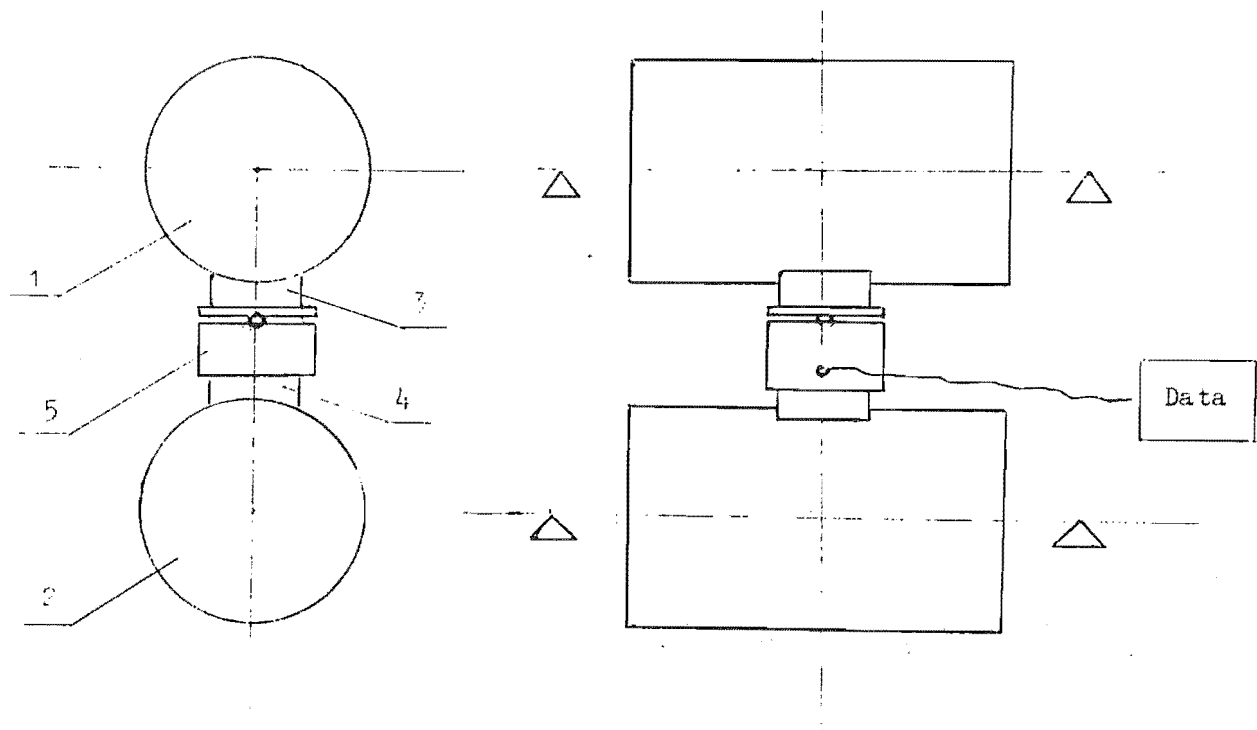


Figure 5.5 Calibration of the load dynamometers

Legend: 1, 2 The compression rollers
 3, 4 Aluminium Blocks
 5 Load cell and measurement system

cylinders. The two cylinders push the bottom compression roller upwards and so place the load cell under load. The voltage values of each of load dynamometers are recorded when the load is separately 0, 5, 10, 50 KN.

(4). The results of data processing and the load-voltage curve are shown in Table 5.1, Table 5.2, Figure 5.6 and Figure 5.7.

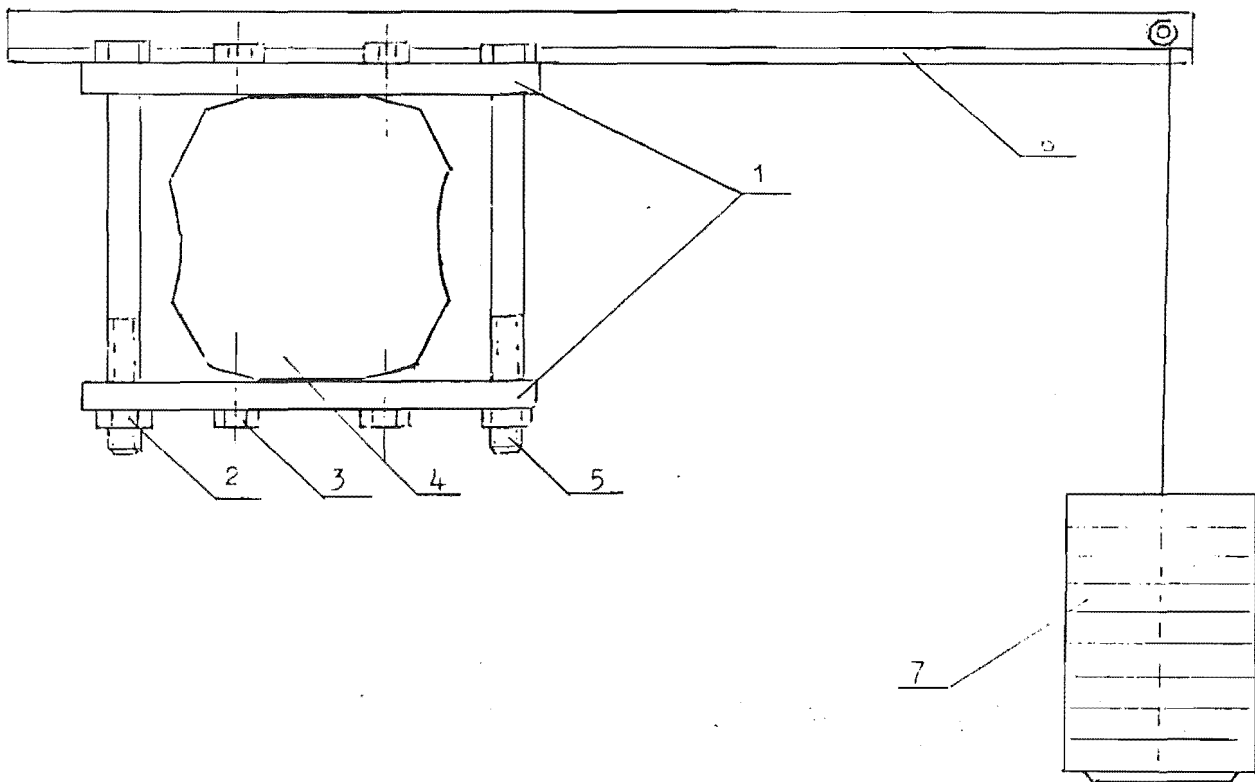


Figure 5.8 Calibration of the torque dynamometers

Legend: 1 Steel plates 2 Nut
3 Auxiliary adjust screw
4 Hydraulic motor 5 Long bolts
6 Load arm 7 Weight

The calibration procedure of the two torque dynamometers was as follows:

1. A special clamp was designed and used for loading the known torque on the torque dynamometer. The

clamp consists of two steel plate and 4 bolts as shown in Figure 5.8.

Two steel plates are clamped on the hydraulic motor by 4 bolts and 8 adjustable auxiliary screws. The load arm used for calibration is installed on the top plate. The weights are put on the end of the load arm to produce the torque.

2. The different weights are added and the voltage readings are recorded. The torque-voltage curves are set up by data processing. The calibration result of the two torque dynamometers is listed in Table 5.3, Table 5.4, Figure 5.9 and Figure 5.10.

Table 5.1 Calibration of Load Beam 1

No.	Load(KN)	Voltage(v)	D A T A		P O C E S S
	X	Y	X*X	Y*Y	X*Y
1	0.0	3.296	0	10.864	0.000
2	5.0	3.483	25	12.131	17.415
3	10.0	3.692	100	13.631	36.920
4	15.0	3.893	225	15.155	58.395
5	20.0	4.095	400	16.769	81.900
6	25.0	4.292	625	18.421	107.300
7	30.0	4.409	900	19.439	132.270
8	35.0	4.603	1225	21.188	161.105
9	40.0	4.810	1600	23.136	192.400
10	45.0	4.998	2025	24.980	224.910
SUM	225	41.571	7125	175.715	1012.615

Regression Analysis Results:

Constant	3.314181818
Std Err of Y Est	0.025055453
R Squared	0.998268023
No. of Observations	10
Degrees of Freedom	8
X Coefficient(s)	0.0374630
Std Err of Coef.	0.0005517

Table 5.2 Calibration of Load Beam 2

No.	Load(KN)	Voltage(v)	D A T A		P O C E S S
	X	Y	X*X	Y*Y	X*Y
1	0	3.577	0	12.795	0.000
2	5	3.395	25	11.526	16.975
3	10	3.214	100	10.330	32.140
4	15	3.030	225	9.181	45.450
5	20	2.848	400	8.111	56.960
6	25	2.666	625	7.108	66.650
7	30	2.484	900	6.170	74.520
8	35	2.304	1225	5.308	80.640
9	40	2.118	1600	4.486	84.720
10	45	1.957	2025	3.830	88.065
11	50	1.765	2500	3.115	88.250
SUM	275	29.358	9625	81.960	634.370

Regression Analysis results:

Constant	3.574181818
Std Err of Y Est	0.005421990
R Squared	0.999926630
No. of Observations	11
Degrees of Freedom	9
X Coefficient(s)	-0.036210
Std Err of Coef.	0.0001033

Figure 5.6 CALIBRATION OF LOAD DYNAMOMETER (LOAD BEAM 1)

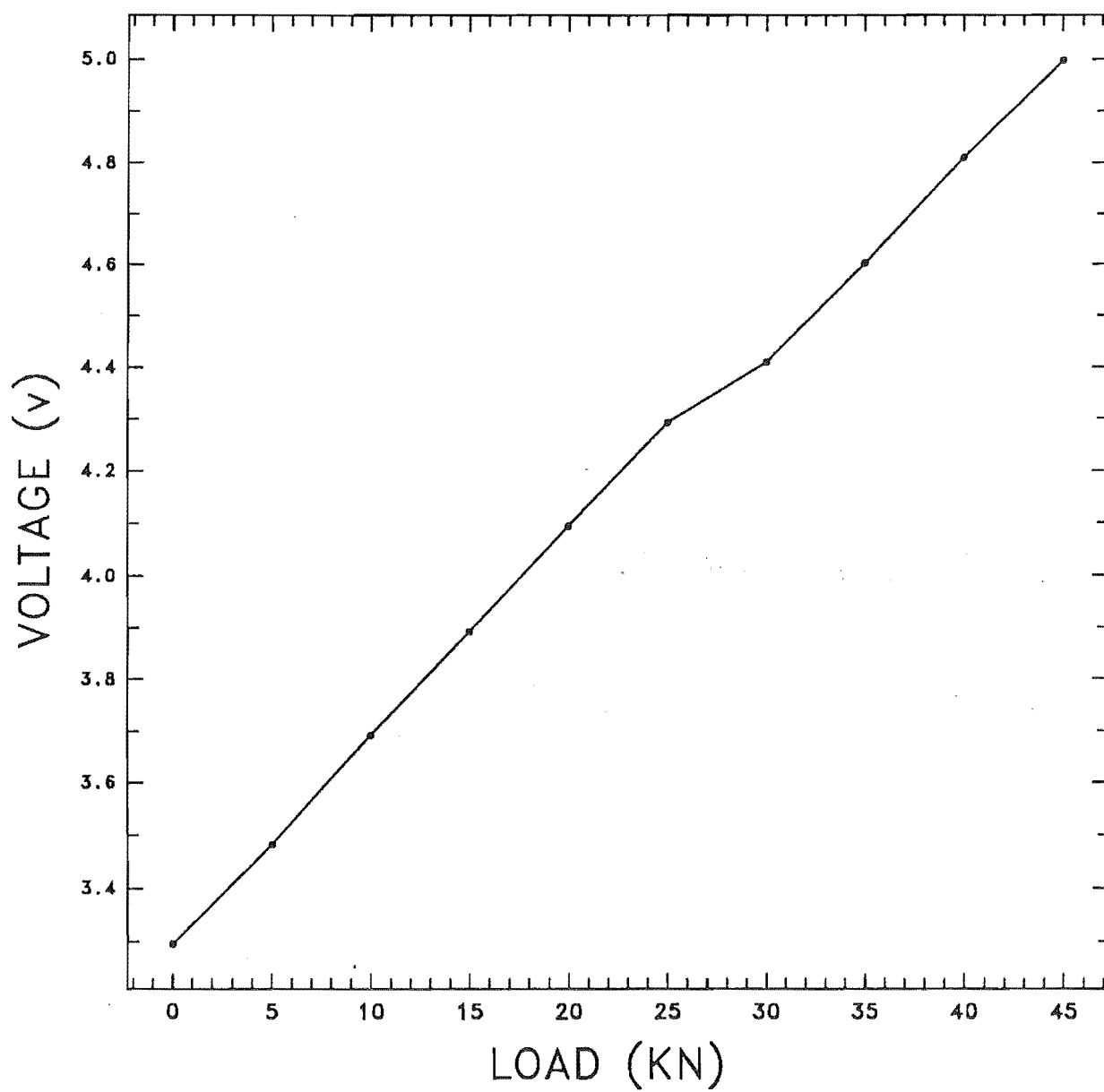


Figure 5.7 CALIBRATION OF LOAD DYNAMOMETER (LOAD BEAM 2)

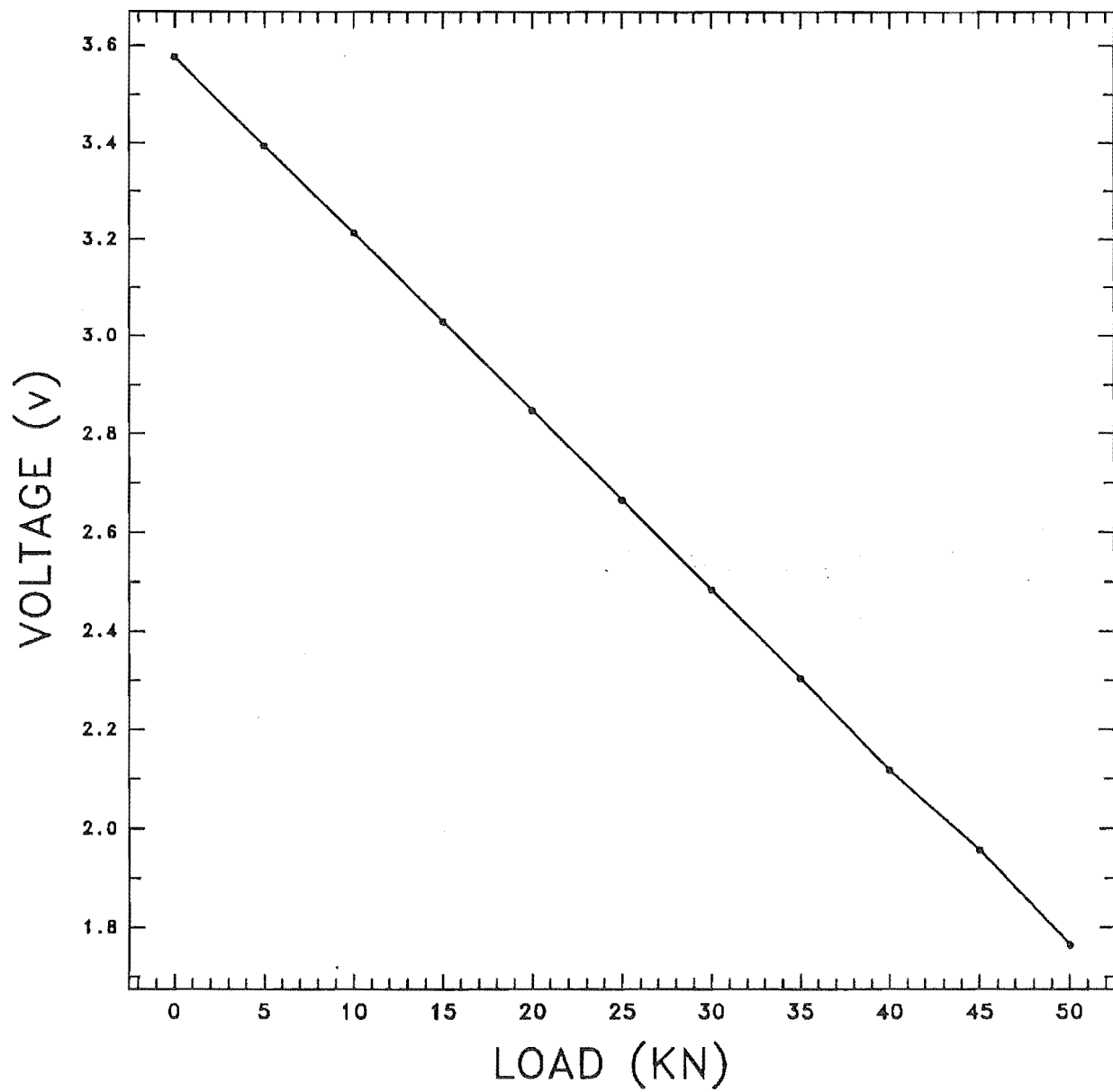


Table 5.3 Calibration of Torque Arm 1

No.	Length(m)	Weight(Kg)	Torque(Kg*m)	Voltage(v)
1	0.455	0.00	0.000	3.617
2	0.455	0.44	0.200	3.609
3	0.455	0.84	0.382	3.604
4	0.455	1.24	0.564	3.602
5	0.455	2.04	0.928	3.600
6	0.455	2.84	1.292	3.578
7	0.455	3.64	1.656	3.563
8	0.455	4.44	2.020	3.543
9	0.455	5.24	2.384	3.525
10	0.455	6.04	2.748	3.510
11	0.455	6.84	3.112	3.493
12	0.455	7.64	3.476	3.474
13	0.455	8.44	3.840	3.463
14	0.455	9.24	4.204	3.448
15	0.455	10.04	4.568	3.434
16	0.455	10.84	4.932	3.414
17	0.455	11.64	5.296	3.401
18	0.455	12.44	5.660	3.385
19	0.455	13.24	6.024	3.372
20	0.455	14.04	6.388	3.355
21	0.455	14.84	6.752	3.340

Regression Analysis Results:

Constant	3.625619754
Std Err of Y Est	0.005184888
R Squared	0.997008061
No. of Observations	21
Degrees of Freedom	19

X Coefficient(s-0.042300
Std Err of Coef0.0005316

Table 5.4 Calibration of Torque Arm 2

No.	Length(m)	Weight(Kg)	Torque(Kg*m)	Voltage(v)
1	0.455	0.00	0.000	3.581
2	0.455	0.56	0.255	3.595
3	0.455	1.76	0.801	3.606
4	0.455	2.96	1.347	3.625
5	0.455	4.16	1.893	3.643
6	0.455	5.36	2.439	3.663
7	0.455	6.56	2.985	3.684
8	0.455	7.76	3.531	3.704
9	0.455	8.96	4.077	3.723
10	0.455	10.16	4.623	3.742
11	0.455	11.36	5.169	3.763
12	0.455	12.56	5.715	3.787
13	0.455	13.76	6.261	3.810
14	0.455	14.96	6.807	3.830
15	0.455	16.16	7.353	3.846
16	0.455	17.36	7.899	3.865
17	0.455	18.56	8.445	3.902
18	0.455	19.76	8.991	3.922
19	0.455	20.56	9.355	3.932

Regression Analysis Results:

Constant	3.574353402
Std Err of Y Est	0.005880589
R Squared	0.997496724
No. of Observations	19
Degrees of Freedom	17
X Coefficient(s)	0.0376346
Std Err of Coefficient	0.0004572

Figure 5.9 CALIBRATION OF TORQUE DYNAMOMETER 1

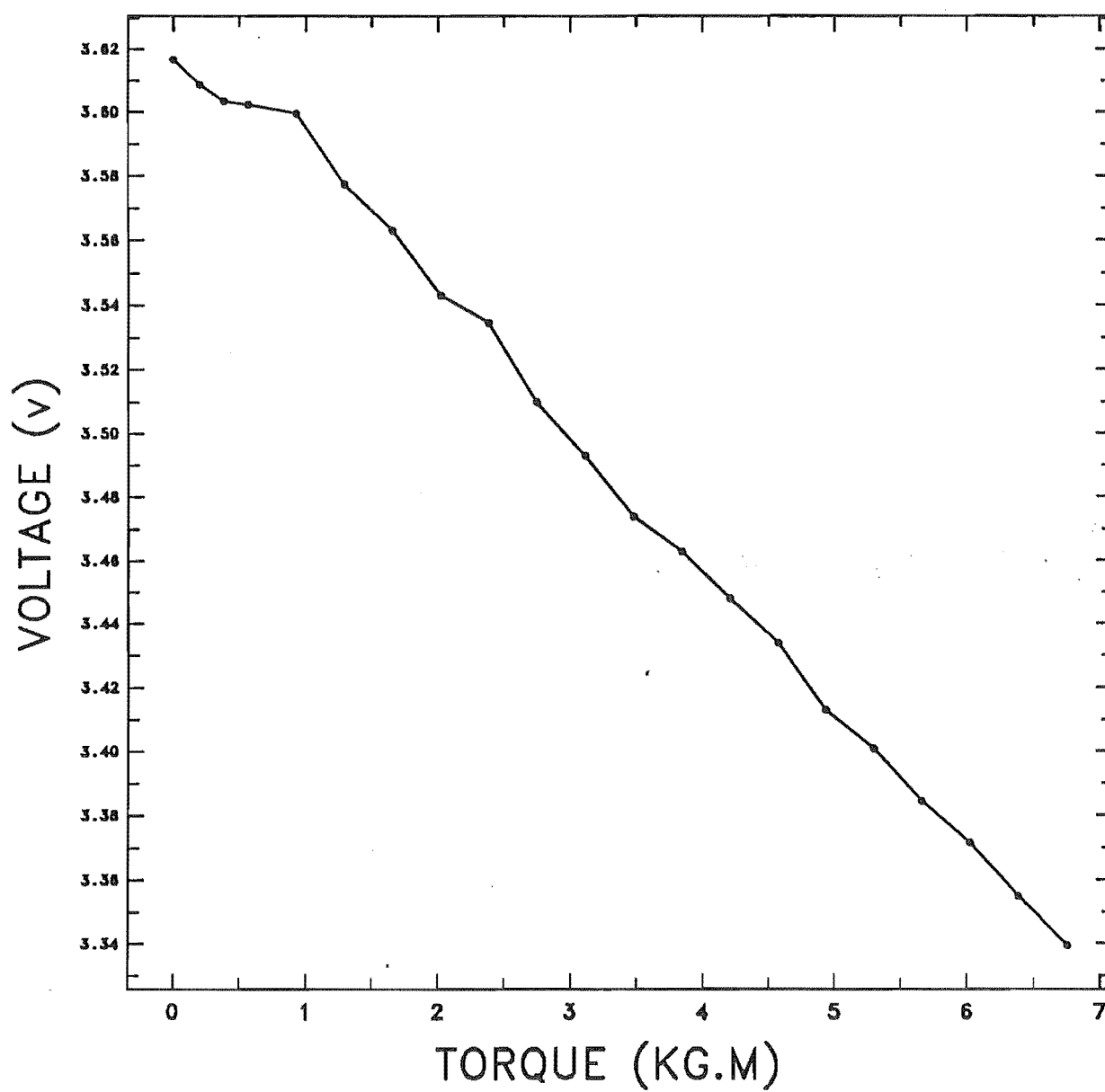
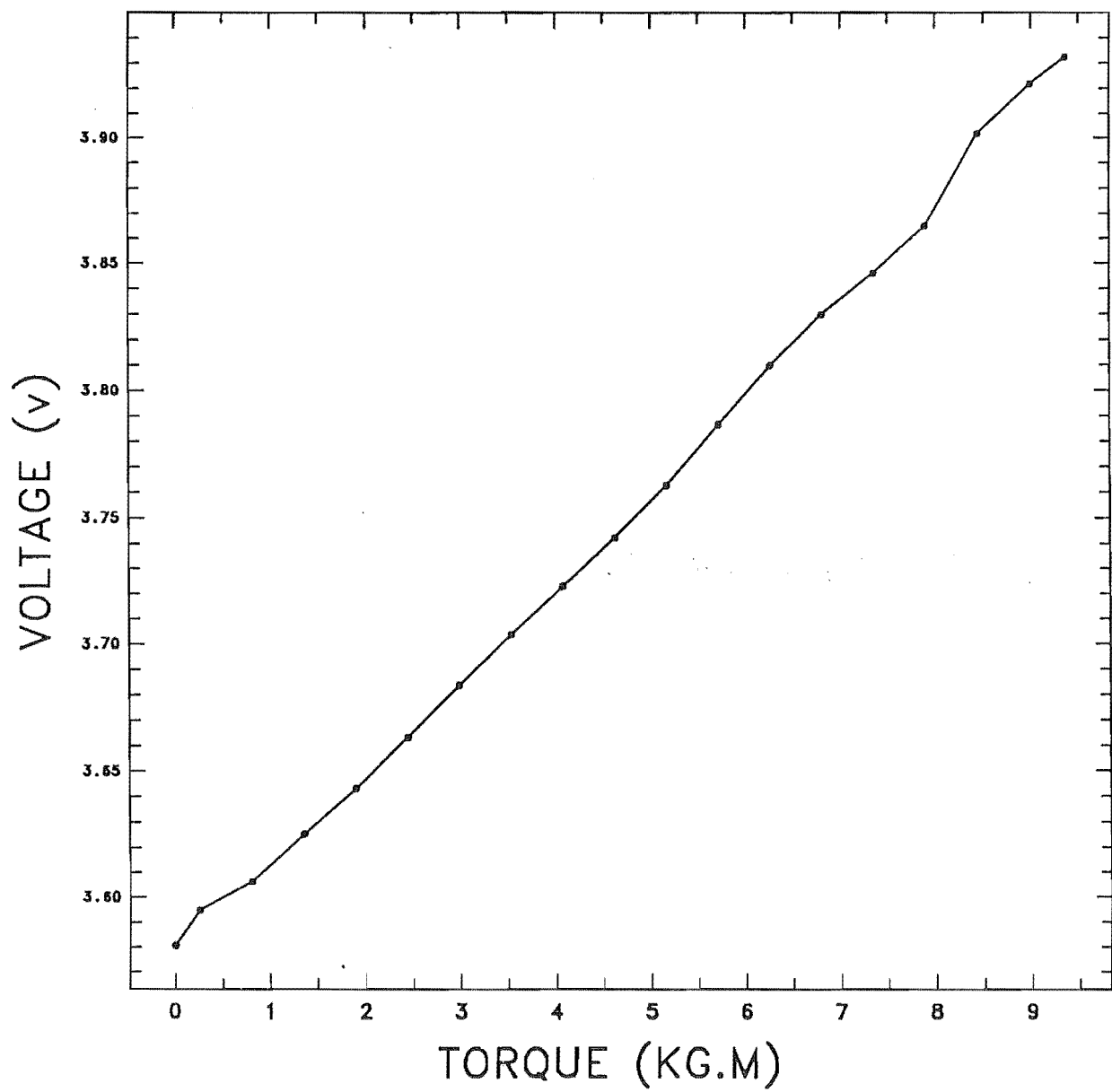


Figure 5.10 CALIBRATION OF TORQUE DYNAMOMETER 2



5.3 MEASUREMENT OF THE SPEED

The devices for measuring speed consist of a reflective object sensor, a reflecting disk, a DC power device and a counter. The reflective object sensor consists of an infra-red emitting light emitting diode (L.E.D.) and a phototransistor. The phototransistor responds to radiation from the diode when a reflective

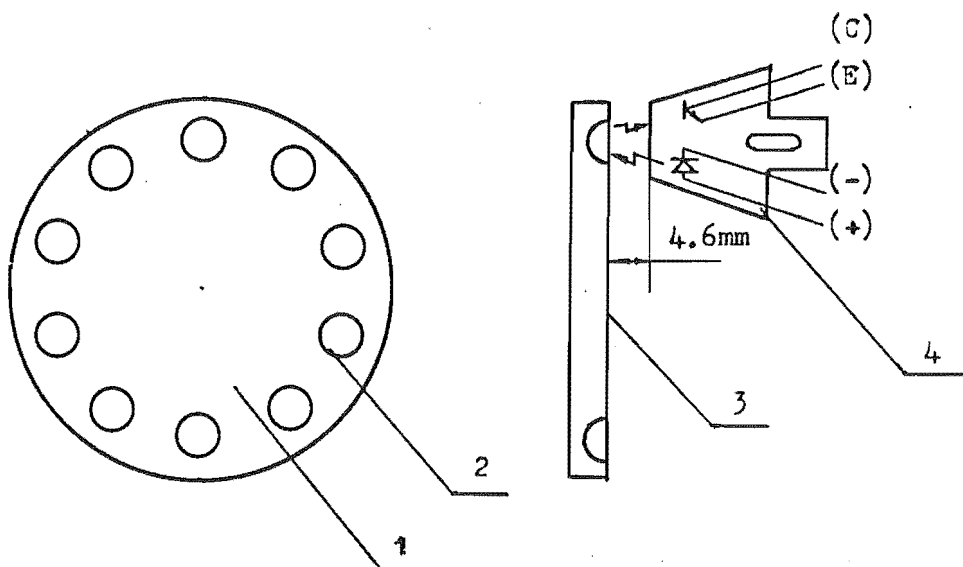


Figure 5.11 The Scheme of Principle of Speed Measurement

1. Reflecting Disk 2. Blind Hole
3. Reflective Surface 4. Reflective Object Sensor

object is placed within the field of view. The optimum sensing distance of the reflective object sensor is 4.6 mm. The reflecting disk is designed as shown in Figure 5.11.

The distance between the reflective object sensor and the outside surface of the reflecting disk is about 4.6 mm, thus, there is a higher current in the emitter of the phototransistor and the output of voltage, V_{out} , is

high level when the light is reflected by the outside surface of the reflecting disk. Conversely, V_{out} is at a low level when the light is reflected by the blind hole of the reflecting disk. The reflecting disk with 10 holes (Figure 5.11) is fixed on the end of the shaft of compression rollers, thus this signal of the output voltage varies as shown in Figure 5.12.

The output of voltage, V_{out} , is connected to the counter. The digital display of the counter represents

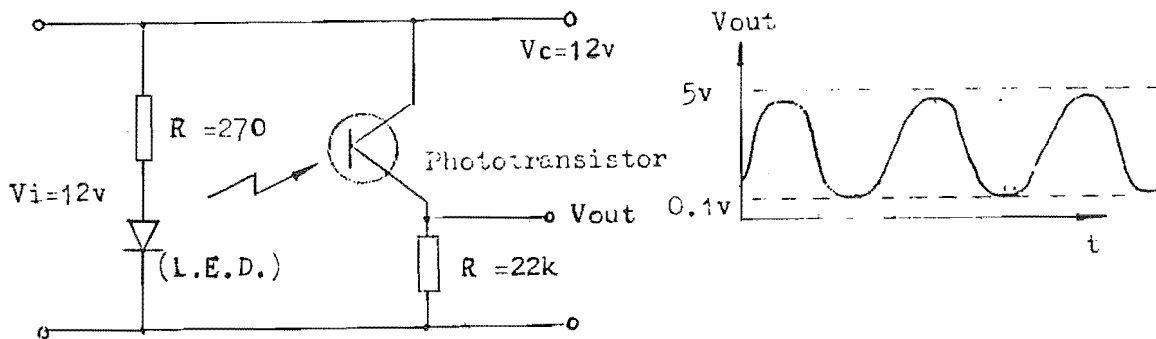


Figure 5.12 The circuit and signal of the reflective object sensor used for speed measurement

the speed of compression rollers.

5.4 COMPUTER-AIDED EXPERIMENT

5.4.1 THE PRINCIPLE OF ANALOG TO DIGITAL CONVERSION

The measurement method of torque and load has been described in this chapter, but it is necessary to capture and record data of load and torque during compression

rolling. A PC was used to realize data acquisition and data processing. In order to use the computer, it is necessary to transfer the analogue representing torque or load value into a digital value using an analog-to-digital converter. It connects the voltage signal representing the load or the torque to the computer.

The principle of analog-to-digital conversion is simply described as follows:

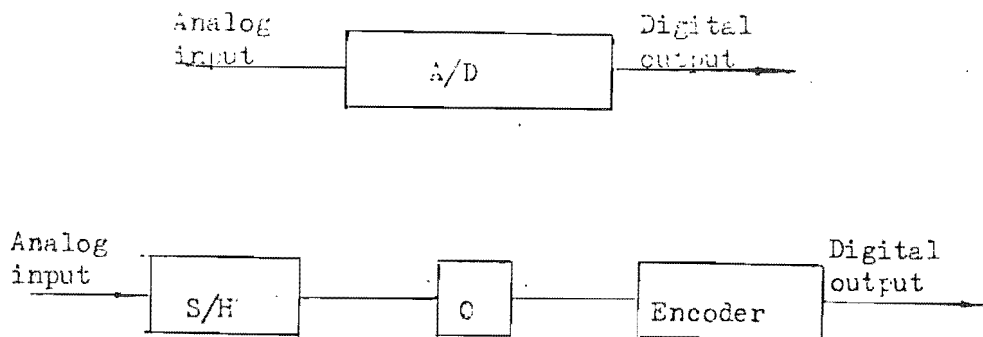


Figure 5.13 The block diagram of A/D Conversion

Analog-to-digital conversion consists of transforming the numerical information contained in an analog signal into a digital-coded word. The A/D usually performs the following sequential operations: sample-and-hold, quantization and encoding.

A sampling operation is needed to sample the analog signal at certain periodic intervals. Theoretically the holding operation is not needed;

however, the conversion time from analog to digital data of is not zero. In order to reduce the effect of signal variation during conversion, the sampled signal is held until the conversion is completed. Figure 5.13 gives the block diagram representations of an A/D.

From Figure 5.13, we know that one of the major operations in the A/D conversion is quantization. Since the digital output can assume only a finite number of levels, it is necessary to quantize or round off the analog number into the nearest digital level. Figure 5.14 illustrates the relationship between the analog and digital binary integral code (in order to simplify, a three-bit word is used for this example instead of 12-bit word).

As shown in Figure 5.14 the analog signal has decision levels at the values of $0.5q$, $1.5q$, $2.5q$, $6.5q$. It must be noted that the analog-to-digit conversion shown in Figure 5.14 is not generally a one-to-one relation. The parameter q which is equal to the least significant bit (LSB) is known as the quantization level. For example, the three-bit digital word, the LSB is $1/8$ of full scale (FS), as indicated in Table 5.5. The difference between the analog signal and the digital output is called the quantization error. The quantization error in general depends on the number of quantization level or the resolution of the quantizer.

Table 5.5 Relation Between Analog and Digital
Numbers for A Three-bit A/D Conversion

Analog Number	Binary-Coded	Digital Number
A	Binary Number	
	MSB LSB	
$ A < 0.5q$	0 0 0	0
$0.5q < A < 1.5q$	0 0 1	$1/8FS = q = LSB$
$1.5q < A < 2.5q$	0 1 0	$1/4FS = 2q$
$2.5q < A < 3.5q$	0 1 1	$3/8FS = 3q$
$3.5q < A < 4.5q$	1 0 0	$1/2FS = 4q$
$4.5q < A < 5.5q$	1 0 1	$5/8FS = 5q$
$5.5q < A < 6.5q$	1 1 0	$3/4FS = 6q$
$6.5q < A < 7.5q$	1 1 1	$7/8FS = FS - LSB = 7q$

As shown in Table 5.5, for a three-bit binary-coded digital number, the MSB has a weight of $1/2$ of full scale (FS); the second bit has a weight of $1/4$ FS; and the LSB has a weight of $1/8$ FS. In general, for an n-bit binary number, the MSB still has a weight of $1/2$ FS, but the LSB has a weight of 2^{-n} FS, that is, an n-bit A/D converter defines 2^n distinct states. Thus the A/D converter provides a resolution of one part in 2^n . The quantization level of the 12-bit A/D converter with ± 5 v input range in PCL-712 is:

$$q = (1/2^n)FS = 1/2^{12} \times (5 - (-5)) = 10/4096 \quad (5.12)$$

The quantization error is: $\pm 0.5q = \pm 0.00122$ v

The A/D converter in PCL-712 Multi-Lab Card is successive-approximation type. Its basic conversion process is briefly described in Figure 5.15.

Figure 5.15 shows the block diagram of a successive approximation type A/D converter. Basically,

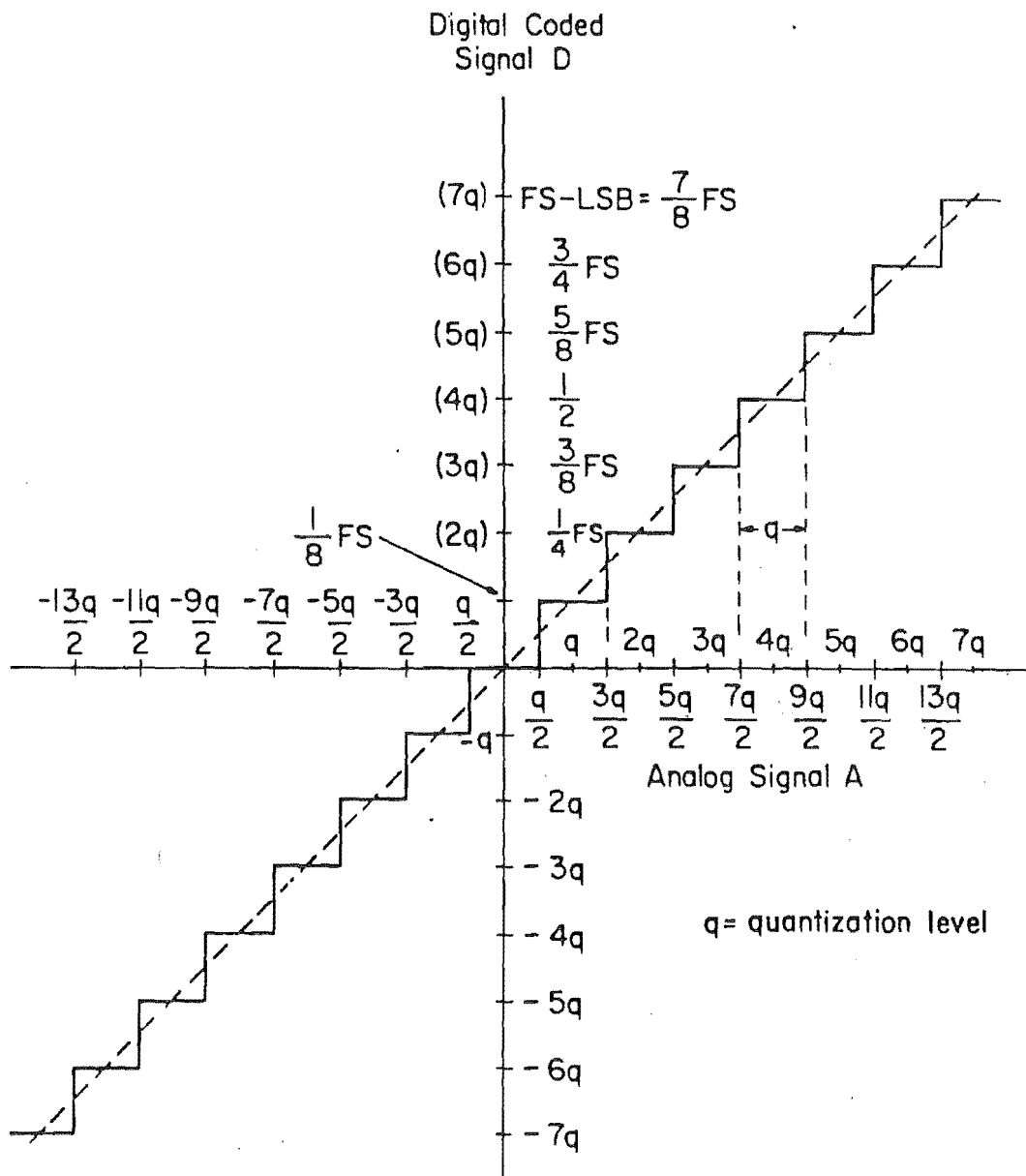


Figure 5.14 Relationship between analog signal and digital coded signal

it consists of a comparator, a D/A converter and some associated control logic.

At the start of the conversion, all the bits of the output of the A/D are set to zero and the MSB is then set to 1. The MSB, which represents one-half of full

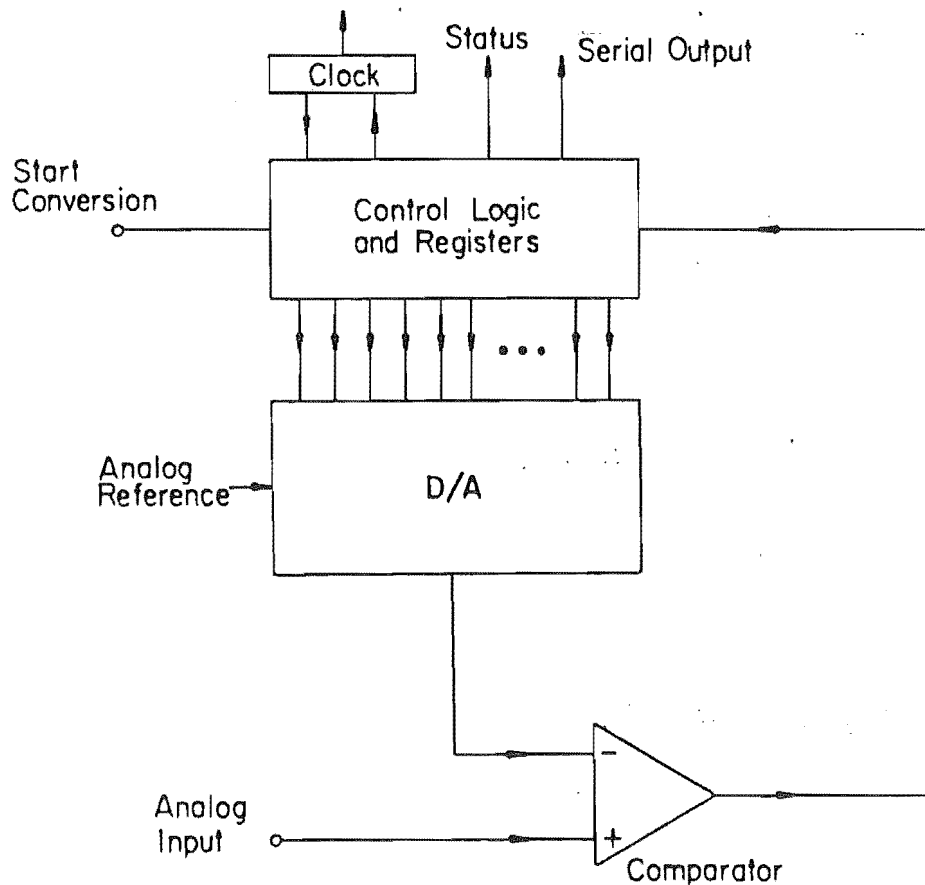


Figure 5.15 Principle of a successive approximation A/D converter

scale, is then converted by the D/A internally and compared with the analog input. If the input is greater than the converted MSB, the MSB=1 is left on; otherwise, it is set to 0. The next significant bit is then turned on and the comparison is repeated. The process is continued until the LSB has been compared and set, then a

status line indicates that comparison is completed and the digital output is available for transmission.

5.4.2 THE METHODS AND DEVICE INTERFACING TO THE COMPUTER

The following devices are used for data acquisition.

- (1). PC XT IBM compatible.
- (2). PCL-712 Multi-Lab card.
- (3). PCLD-780 Wiring Terminal Board

The PCL-712 Multi-Lab card is a low cost multifunction analog/digital I/O card. It provides 16 single-ended analog inputs with 2 analog outputs, 16 digital inputs, 16 digital outputs and a programmable interval counter. The input range of the A/D converter is +/- 5v or +/- 1v. A/D conversion time is less than 30 microseconds and can be triggered by software, programmable pacer or external pulses.

The I/O port base address for the PCL-712 is selectable by a 5 position DIP switch. Valid addresses are from hex 200 to hex 3F0. The manufactory sets hex 220-22F.

The PCLD-780 is a universal screw terminal board which provides convenient connection points for two 20-pin flat cable connector ports. The PCLD-780 provides straight connections for analog or digital I/O signals when it connects to PCL-712 Multi-Lab card with two flat ribbon cables.

5.4.3 COMPUTER PROGRAMME DESIGN FOR THE EXPERIMENT

The following form registers are used to perform the A/D conversion.

BASE+4: This byte, together with bit 0-3 of the bite at BASE+5, forms a 12 bit number which is the result of the A/D conversion. The number can be from 0 to 4095.

BASE+5: The use of bit 0-3 is described as above. Bit 4 reflects the status of the conversion, 0=ready, 1=not ready.

READ	Bit	7	6	5	4	3	2	1	0
BASE+4		D7	D6	D5	D4	D3	D2	D1	D0
BASE+5		0	0	0	NRDY	D11	D10	D9	D8

D11 to D0 is A/D data

NRDY: 0 A/D data ready
 1 A/D data not ready

BASE+10 Bit 0-3 of this register are used to select the desired A/D channel on which the A/D conversion will be performed. Bit 4-7 are ignored.

WRITE	Bit	7	6	5	4	3	2	1	0
BASE+10		x	x	x	x	c3	c2	c1	c0

c3 to c0: channel number.

x: Don't care.

BASE+11 Trigger mode control. This register is used to make a direct trigger or to enable or disable pacer trigger.

WRITE	Bit	7	6	5	4	3	2	1	0
BASE+11		x	x	x	x	x	x	T1	T0

T0: 0 No direct trigger.
1 Make a direct trigger.
T1: 0 disable pacer trigger.
1 Enable pacer trigger.

BASE+1	R LSB or MSB of counter 1
	W LSB or MSB of counter 1
BASE+2	R LSB or MSB of counter 2
	W LSB or MSB of counter 2

Counter 1 and counter 2 are configured to be a pacer to offer A/D converter trigger pulses with precise period in pacer trigger mode. To enable the pacer, a byte with bit 1 is written to set 1 to the register BASE+11.

BASE+3 Control byte.
Before loading or reading any of the individual counters, the control byte must be loaded.
The format of the control byte is:

WRITE	Bit	7	6	5	4	3	2	1	0
BASE+3		SC1	SC2	RL1	RL0	M2	M1	M0	BCD

SC1-0: Select counter

SC1	SC0	Counter
0	0	0
0	1	1
1	0	2
1	1	Illegal

RL1-0: Select the read or load operation

RL1	RL0	Operation
0	0	Counter Latch
0	1	Read/Load LSB
1	0	Read/Load MSB
1	1	Read/Load LSB first, and then MSB

M2-0: Select the operating mode

M2	M1	M0	Mode	Function
0	0	0	0	Interrupt on terminal count
0	0	1	1	programmable one slot
x	1	0	2	Rate Generator
x	1	1	3	square wave rate generator
1	0	0	4	software triggered strobe
1	0	1	5	hardware triggered strobe

BCD: Selects binary or BCD counting

BCD	Type
0	Binary counter 16-bits
1	BCD counter

According to the above, the control byte defines counter mode of read or load operation, mode of trigger and counting mode (BCD or binary). Further, the sampling period and the sampling rate can be calculated as follows:

$$Sp = (HB1 * 256 + LB1) * (HB2 * 256 + LB2) * 0.5 \text{ } (\mu s)$$

(5.13)

$$Sr=2/((HB1*256+LB1)*(HB2*256+LB2)) \text{ (MHz)} \quad (5.14)$$

If the sampling period is 50 microseconds, then LB1=1, HB1=0, LB2=100 and HB2=0. The following programme section written in my experimental programme is to sample 4 A/D channels of load and torque (channel 2-5) at the sampling rate of 20 KHz. The programme is written in Turbo Basic (Appendix 4).

p%=&H220	base address
	:
	:
60 for k%=1 to sam%	sam% is the sampling number of each channel decided by feed speed
for ch%=2 to 5	
80 out p%+10,ch%	select the channels
out p%+3 &H74	the control byte selects counter 1,loads LSB and then MSB, trigger mode=2,binary counting.
out p%+1,1	LB1=1
out p%+1,0	HB1=0
out p%+3, &Hb4	select counter 2, LSB and then MSB,mode=2, binary counter 16-bit.
out p%+2,100	LB2=100
out p%+2,0	HB2=0
out p%+11,2	trigger mode control
h%(ch%,k%)=inp(p%+5)	read the A/D high byte

```
if h%(ch%,k%)>=16 then 80
if h%(ch%,k%)<12 then 80
l%(ch%,k%)=inp(p%+4)      read the A/D low byte
next ch%
next k%
:
:
:
```

CHAPTER SIX:

EXPERIMENT PROCEDURE

6.1 MATERIAL

The material used in this experiment is radiata pine purchased from Baigents mill, Eves Valley, Nelson, New Zealand. The greensawn timber containing pith is dried in a high temperature kiln to a target moisture content of 15 percent.

The clear timber boards are crosscut into 200 to 500 mm long and then the finger joints are cut and assembled according to New Zealand Standard NZ3616:1978. (A. Tsehay, 1989)

After proof testing, the finger jointed clear timber boards are crosscut into two different lengths, 800 mm and 1200 mm, to eliminate any kind of broken or splintered parts caused by the tension and bending test. Finally, the timber boards are planed and reduced to their final dimension. They are divided into four groups. For dimension and treatment parameters of each group see Table 6.1 and Table 6.2.

6.2 METHODS

6.2.1 DIGITAL IDENTIFICATION SYSTEM

A digital identification system set up according to all of the experiment factors and designed experiment procedures makes the whole experiment reliable and accurate.

The system is used for general purposes, thus, some digits are not used in this experiment. The system is showed in Table 6.3.

6.2.2 COMPRESSION ROLLING TREATMENTS

The compression rolling treatment is carried on after a series of compression trials and hardness testing. Before compression a small piece of timber board is cut off from the end of every timber board for a hardness test (shown as Figure 6.1).

Compression level is set up by adjusting the distance between the two compression rollers by means of measuring gauges. Every piece of timber board is measured to give its length, width, thickness and the positions of any finger joints. The result of measurement is sketched in the experiment data sheets. The moisture content of the timber boards is also measured by an electric resistance type moisture meter. The values lie between 10.5 - 14.5 percent.

Every piece of timber board is compressed at a defined compression level, diameter of rollers and feed speed according to the Table 6.1 and Table 6.2. The load, torque and speed are recorded by the computer during compression rolling. After compression, every piece of timber board is observed with the naked eye to judge any macroscopic change on the surface. A 50 mm length section is cut from each piece after compression to test hardness.

6.2.3 MEASUREMENT OF LOAD AND TORQUE DURING ROLLING

In order to record the data of load and torque, the code of every piece of timber board must be input into the computer; the data file for load and torque will be set up by running the programme in the computer. When a timber board is fed into and contacts the two compression rollers, the output voltage of load and torque measurement (Wheatstone bridges) increases abruptly; the data acquisition and recording programme are started by this higher voltage signal. After compression the signal is at a lower level, so the data acquisition and record are terminated. By running the programme in the computer, every piece of timber board is given its own data file titled with its own code. It is convenient to process and analyse the load and torque values after experiment.

The amount of data in each channel depends on the feed speed and the length of timber board. Normally it is up to 600 1/s. The values of load and torque are

their mean value.

6.2.4 MEASUREMENT OF HARDNESS OF TIMBER BOARD

Hardness is measured not only to obtain such values but also to compare the hardness change after compression. In fact, hardness is measured in order to search for the positive result of timber board compression rolling process and to observe the effect of compression on hardness

Since there is a relationship between hardness and density, the degree of densification of timber board can be surveyed by observing changes in hardness.

The hardness measurement is concentrated on the comparison of changes in hardness of the compression

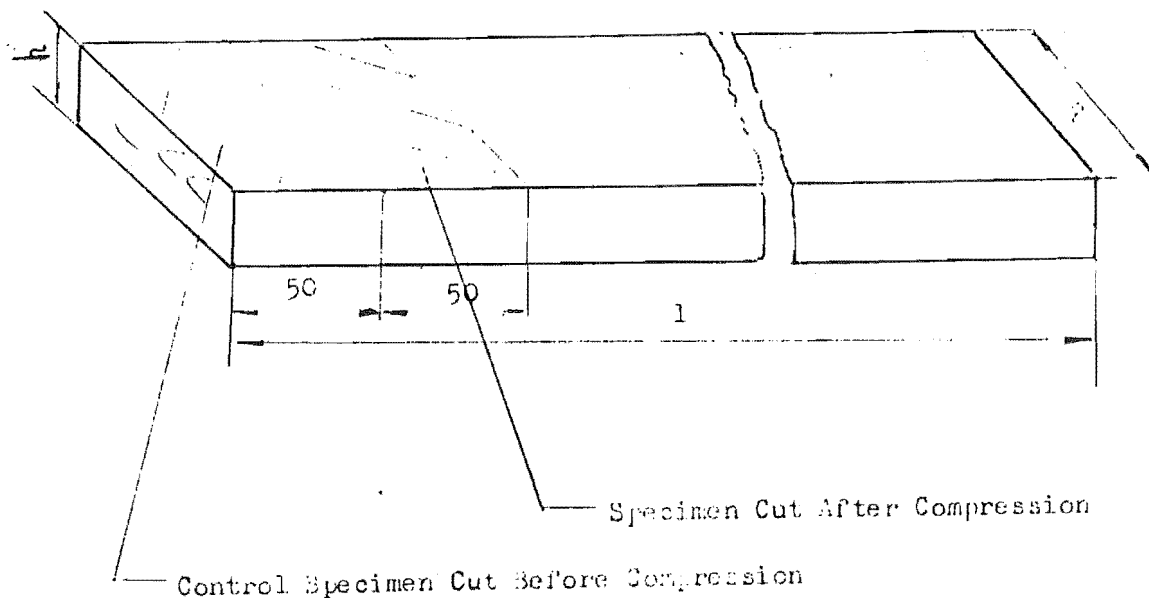


Figure 6.1 Specimens of Hardness Test

surface. Two small specimens are cut off separately from each piece of timber board before and after compression (Figure 6.1). These two specimens are matched with each other. The choice of testing points is described in Figure 6.2.

For the specimen before compression (specimen 1), two testing points are chosen on both surfaces

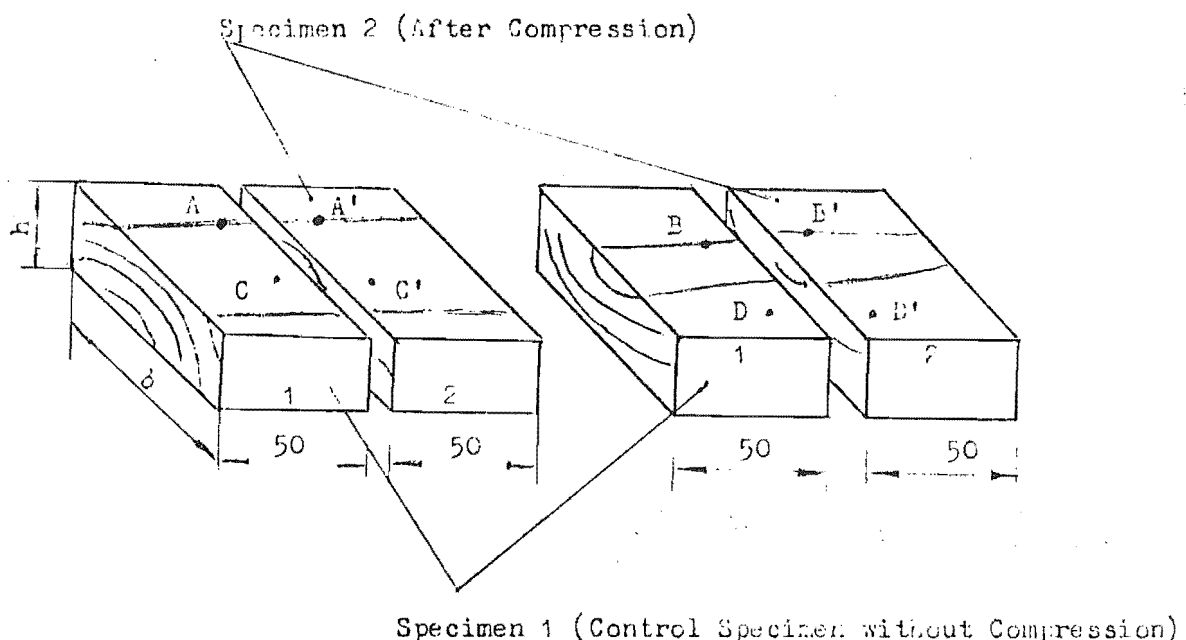


Figure 6.2 The positions of testing points in the specimens

corresponding to compression surface. The points A and B are in spring wood. The points C and D are in summer wood. For the specimen after compression (specimen 2), two testing points are on each of both compression surfaces. A' corresponding to A is on spring wood and in the same layer as A. C' corresponding to C is on summer wood and in the same layer as C. So are the points B'

and D'. The testing hardness result of every specimen is mean value of values of four point.

The test method is based on ASTM - Designation: D143-83, but the size of specimens and number and position of penetrations are modified because of the limit of the thickness of timber board and the different purpose of testing. A modified Brinell-hardness test

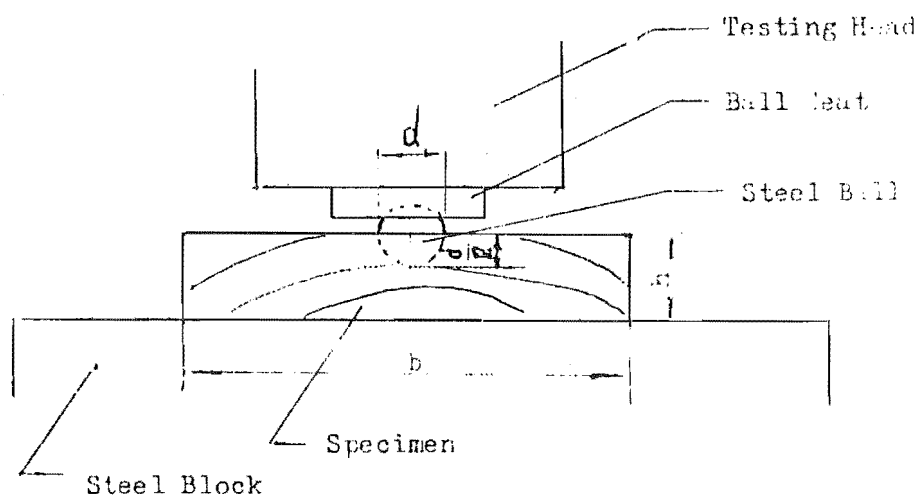


Figure 6.3 The Principle of Brinell - hardness test

method is used in this test. A 11.3 mm diameter steel ball is penetrated into the surface of the board at chosen points (Figure 6.3). The depth of penetration is half of the diameter of the steel ball and the loading speed is 6 mm/min. They are controlled by the microprocessor.

The hydraulic materials testing machine (Model

M200 HVL-1045) is used in this hardness test. It is dependable, accurate and flexible for controlled materials testing. The automatic control of loading speed and penetration stroke is realized by a hydraulic pumping system and a microprocessor-based control system. The control parameter required is established by keyboard input and the testing result is printed out in alphanumeric or graph form.

6.3 METHOD AND PROCEDURE OF DATA PROCESSING

Data are processed in the computer. The IBM SAS and Lotus are used for data processing.

1. The data file of load and torque for each piece of timber board is withdrawn and reproduced. The data are listed in the table and drawn X-Y graph to observe the range and change of load and torque against time during compression.
2. The maximum, minimum and mean values of each dynamometer are calculated.
3. The mean value of mean values of two load dynamometers and the mean value of mean values of two torque dynamometers are calculated.
4. The hardness values of both specimens from each timber board are calculated. These values are used for comparing the hardness changes and observing a relationship with load.
5. All of the data processed is listed in the Chapter

7 and Appendix 4 as well.

6. These data are graphed and used for regression analysis.

The analysis results of the experiment and graphs will be described in Chapter Seven.

Table 6.1 Treatment Factors (1)

TREATMENT FACTORS		DIMENSION OF TIMBER BOARDS	
ITEM	VALUES	1200X85X25	800X85X25
Speed (mm/s)	2000		*
	2500		*
	3000	*	
	3500	*	
Compression	10	*	*
Level (%)	15	*	*
Diameter of Rollers (mm)	206.8	*	*
Feed Condition	Without Feed Rollers	*	*
Wood Maturity	Unidentified	*	*
Replicate	5	*	*

NOTE:

1. This table is used in first experiment only.

Table 6.2 Treatment Factors (2)

TREATMENT FACTORS		DIMENSION OF TIMBER BOARDS	
ITEM	VALUE	1200x85x33	800x85x33
Speed (mm/s)	1000		*
	1500		*
	2000		*
	2500	*	
	3000	*	
	3500	*	
Compression Level (%)	5	*	*
	7	*	*
	10	*	*
	13	*	*
	15	*	*
	17	*	*
	20	*	*
Diameter of Rollers (mm)	206.8	*	*
Feed Condition	Without Feed Rollers	*	*
Wood Maturity Unidentified		*	*
Replicate	6	*	*

NOTE:

1. This table is used in the second experiment only.

2. The timber boards distribute as follows:

126 pieces: 800x85x33 mm

126 pieces: 1200x85x33 mm

Table 6.3 Numerical Identification System of the Board

DIGIT	TREATMENT FACTORS	NUMBER	VALUE
1	Feed Speed (mm/s)	1	1000
		2	1500
		3	2000
		4	2400
		5	2500
		6	3000
		7	3500
2	Compression Level (%)	0	0
		1	5
		2	7
		3	10
		4	13
		5	15
		6	17
3	Diameter of Roller (mm)	1	206.8
		2	116
4	Feed Condition	1	With Feed Rollers
		2	No Feed Rollers
5	Wood Maturity	1	Sapwood
		2	Heartwood
		3	Unidentified
6	Replicate	0,1,...,9	

CHAPTER SEVEN:

RESULTS OF THE EXPERIMENTS

7.1 THE MEASURING RESULTS OF COMPRESSION ROLLING OF TIMBER BOARDS

The results of the experiments are divided into two groups:

1. The first group data result is produced from the first group of experiment. The load and torque are mean values. The results of the first group data are shown in Table 7.1.
2. The results of the second group of data are listed in Table 7.2. The experiment condition is as follows:
 - (1) The thickness of timber board is 33 mm.
 - (2) The width of timber board is 85 mm.
 - (3) The moisture content is 12%-15%.
 - (4) The diameter of the compression rollers is 206.8 mm.

Each load or torque in the table is a mean value of six piece of timber boards under the same compression level and feed speed. So is the hardness value. Each original reading of hardness is from the last section of each timber board before compression rolling.

7.2 HARDNESS CHANGES DURING COMPRESSION ROLLING

The results of hardness testing are summarised in Table 7.3. The data are produced from the second group of experiments. The change of hardness can be indicated and estimated by a hardness coefficient, that is,

$$q = (H_2 - H_1) / H_1 \times 100\%$$

where q is the hardness coefficient

H_1 is the hardness of the control specimen
before compression

H_2 is the hardness of the specimens after
compression treatment

q represents the percent of decrease of hardness if the value is negative. q represents the percent of increase of hardness if the value is positive.

7.3 RELATIONSHIP BETWEEN MECHANICAL PROPERTIES AND TREATMENT CONDITIONS

The analysis results of the experiments are listed in Table A.4.1 and Table A.4.2. Table A.4.1 is the analysis results of the first group of experiments. The data analysis results of the second group experiments are shown in Table A.4.2. On the basis of the mathematical model in Chapter 3, after taking the logarithm of load, compression level, hardness and speed, the multiple regression analysis is considered to compare equation (3.40). The analysis results indicate: The experiment data is approached to the mathematical model. It is estimated by R squared (coefficient of determination). The value of R squared is from 0 to 1. The more R

squared approaches to 1, the more the experiment data close to the theoretical model (Maxwell, 1983) . Referring to Table A.4.1 and Table A.4.2 of Appendix 4, R squared is 0.804 for first group experiment and 0.953 for second experiment. The results of analysis indicate: There is a higher fit between the experiments and the theoretical model. Since the timber board is an inhomogeneous material, the changes of mechanical properties are found in timber board. Thus, during processing the data of the experiments, this factor must be considered.

TABLE 7.1 RESULTS OF EXPERIMENT (1)

COMPRESSION (%)	SPEED (M/S)	HARDNESS (Kg)	LOAD (KN)	TORQUE (Kg.M)
10	2.0	172.5	20.02	8.14
10	2.0	185.0	23.25	8.51
10	2.0	195.0	20.72	6.28
10	2.0	210.0	27.26	10.23
10	2.0	216.0	26.00	10.32
10	2.5	180.0	18.11	6.28
10	2.5	205.0	21.40	7.25
10	2.5	235.0	25.40	8.85
10	2.5	252.5	28.62	10.85
10	2.5	285.0	30.77	12.28
10	3.0	177.5	17.75	10.14
10	3.0	180.0	18.59	10.67
10	3.0	182.5	18.87	10.30
10	3.0	195.0	19.44	11.53
10	3.0	237.5	19.91	11.66
10	3.5	162.5	12.61	5.20
10	3.5	200.0	18.79	8.67
10	3.5	247.5	18.84	12.11
10	3.5	250.0	20.07	13.26
10	3.5	262.5	20.10	12.52
15	2.0	167.5	28.91	13.85
15	2.0	210.0	29.51	14.35
15	2.0	212.5	29.33	14.46
15	2.0	245.0	29.99	14.53
15	2.0	255.0	31.36	16.98
15	2.5	165.0	27.74	13.43
15	2.5	187.5	28.74	13.56
15	2.5	200.0	28.98	14.62
15	2.5	222.5	29.44	14.89
15	2.5	230.0	29.53	14.97
15	3.0	192.5	28.77	20.75
15	3.0	225.0	31.08	20.92
15	3.0	240.0	31.54	14.72
15	3.0	242.5	29.84	16.39
15	3.0	307.5	32.33	17.69
15	3.5	175.0	26.05	13.96
15	3.5	192.5	29.50	12.95
15	3.5	192.5	29.75	15.05
15	3.5	212.5	29.27	14.07
15	3.5	237.5	32.56	16.79

TABLE 7.2 RESULTS OF THE EXPERIMENT (2)

COMPRESS (%)	HARDNESS (Kg)	SPEED (m/s)	LOAD (KN)	TORQUE (Kg*M)
5	236.0	1.0	18.3	7.9
5	238.0	1.5	18.4	8.1
5	196.0	2.0	16.5	4.3
5	219.0	2.5	17.9	6.9
5	194.0	3.0	16.1	4.9
5	226.0	3.5	18.1	6.3
7	225.0	1.0	18.9	7.7
7	189.5	1.5	17.9	5.7
7	203.5	2.0	18.4	7.8
7	196.5	2.5	18.1	6.1
7	231.0	3.0	19.1	8.0
7	217.0	3.5	18.6	6.9
10	217.5	1.0	26.2	10.4
10	203.5	1.5	24.5	8.9
10	196.7	2.0	22.4	7.6
10	231.5	2.5	27.9	13.2
10	198.5	3.0	23.2	8.1
10	224.5	3.5	27.1	12.1
13	226.5	1.0	26.9	16.9
13	189.0	1.5	24.2	11.1
13	227.5	2.0	27.1	13.2
13	235.0	2.5	27.7	13.8
13	213.5	3.0	24.3	11.9
13	243.5	3.5	28.6	15.4
15	198.0	1.0	26.1	15.1
15	235.0	1.5	30.0	18.4
15	213.0	2.0	29.3	16.6
15	201.0	2.5	28.7	15.4
15	241.5	3.0	30.1	17.9
15	202.0	3.5	29.1	15.9
17	224.5	1.0	33.5	20.9
17	243.0	1.5	34.1	21.7
17	187.5	2.0	31.6	17.9
17	218.5	2.5	33.3	19.4
17	237.0	3.0	33.7	22.8
17	204.0	3.5	32.8	17.2
20	184.0	1.0	34.0	20.3
20	199.5	1.5	36.4	21.8
20	189.5	2.0	35.7	21.1
20	229.0	2.5	36.9	22.7
20	235.0	3.0	37.1	23.4
20	217.0	3.5	36.8	23.7

TABLE 7.3 RESULTS OF HARDNESS TESTING

COMPRESSION		5%	7%	10%	13%	15%	17%	20%
S P E E D m/s	Hardness Value of Control Samples Before Compression							
	1	236.0	225.0	217.5	226.5	198.0	224.5	184.0
	1.5	238.0	189.5	203.5	189.0	235.0	243.0	199.5
	2	196.0	243.5	196.7	227.5	213.0	187.5	189.5
	2.5	219.0	196.5	231.5	235.0	201.0	218.5	229.0
	3	194.0	231.0	198.5	213.5	241.5	237.0	235.0
	3.5	226.0	217.0	224.5	243.5	202.0	204.0	217.0
	Hardness Value of the Samples after Compression							
	1	234.5	225.0	209.0	228.0	204.0	233.5	191.0
	1.5	236.0	187.0	197.5	191.0	244.0	256.0	203.5
	2	192.5	244.0	189.0	228.0	221.5	198.5	187.5
	2.5	220.0	195.0	236.5	239.0	211.5	231.0	223.0
	3	193.5	234.0	193.0	220.0	257.0	261.0	230.5
	3.5	226.5	215.0	221.0	248.0	207.0	221.0	219.5
	Hardness Coefficient q (%)							
	1	-0.64	0.00	-3.91	0.66	3.03	4.01	3.80
	1.5	-0.84	-1.32	-2.95	1.06	3.83	5.35	2.01
	2	-1.79	0.21	-3.91	0.22	3.99	5.87	-1.06
	2.5	0.46	-0.76	2.16	1.70	5.22	5.72	-2.62
	3	-0.26	1.30	-2.77	3.04	6.42	10.13	-1.91
	3.5	0.22	-0.92	-1.56	1.85	2.48	8.33	1.15

Figure 7.3.1 Relationship between Hardness and Load

1. The thickness of timber board is 25mm.
2. Compression level is 10%.
3. Feed speed is 2.5 m/s.
4. Hardness values are mean values of each timber board after compression rolling.
5. Load values are mean value of each timber board.
6. Moisture content is 12% -14%.

Figure 7.3.1

Relationship between Hardness and Load ($h=25\text{mm}$, $\text{Com}=10$ $\text{Sp}=2.5\text{m/s}$)

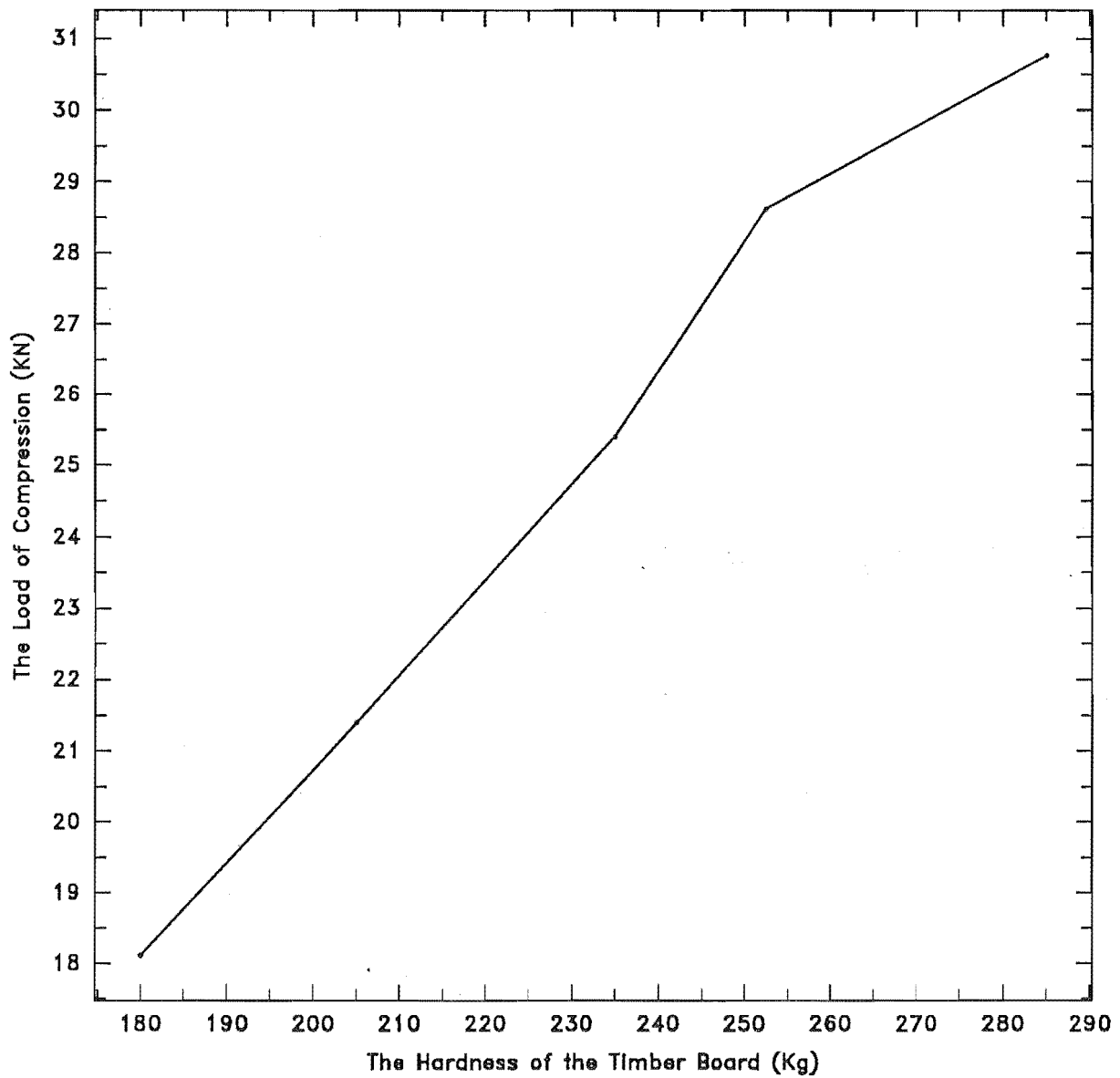


Figure 7.3.2 Relationship between Hardness and Torque

1. The thickness of timber board is 25mm.
2. Compression level is 10%.
3. Feed speed is 2.5 m/s.
4. Hardness values are mean values of each timber board after compression rolling.
5. Torque values are mean values of two compression rolling motors for each timber board.
6. Moisture content is 12% - 14%.

Figure 7.3.2

Relationship between Hardness and Torque(h=25mm, Com=10 percent, Sp=2.5m/s)

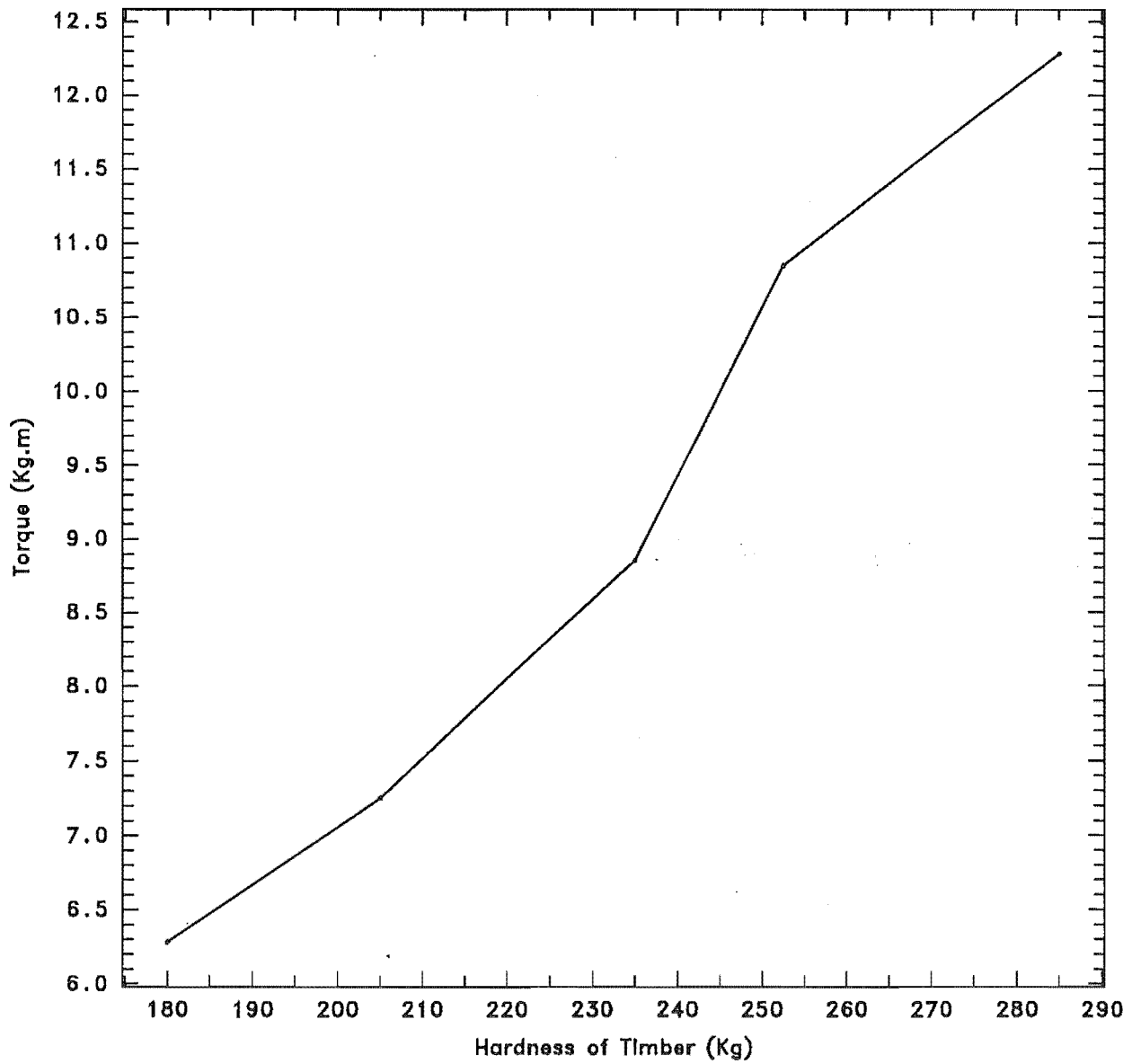


Figure 7.3.3 Relationship between Hardness and Load

1. The thickness of timber board is 25mm.
2. Compression level is 15%.
3. Feed speed is 2.5 m/s.
4. Hardness values are mean values of each timber board after compression rolling.
5. Load values are mean value of each timber board.
6. Moisture content is 12% -14%.

Figure 7.3.3

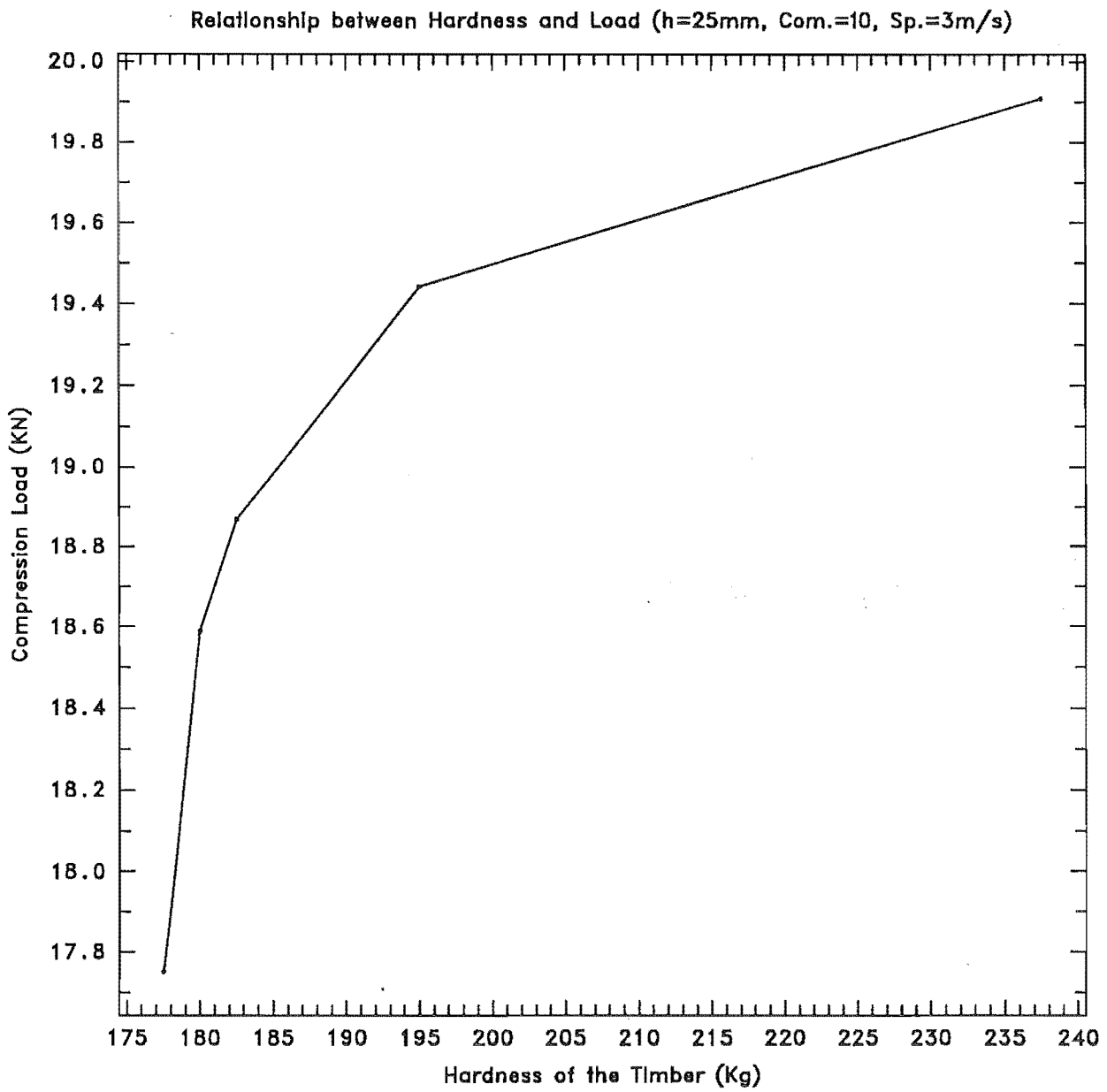


Figure 7.3.4 Relationship between Hardness and Torque

1. The compression level is 15%.
2. The thickness of timber board is 25mm.
3. Feed speed is 2.5 m/s.
4. Hardness values are mean values of each timber board after compression rolling.
5. Torque values are mean values of two compression rolling motors for each timber board.
6. Moisture content is 12% - 14%.

Figure: 7.3.4

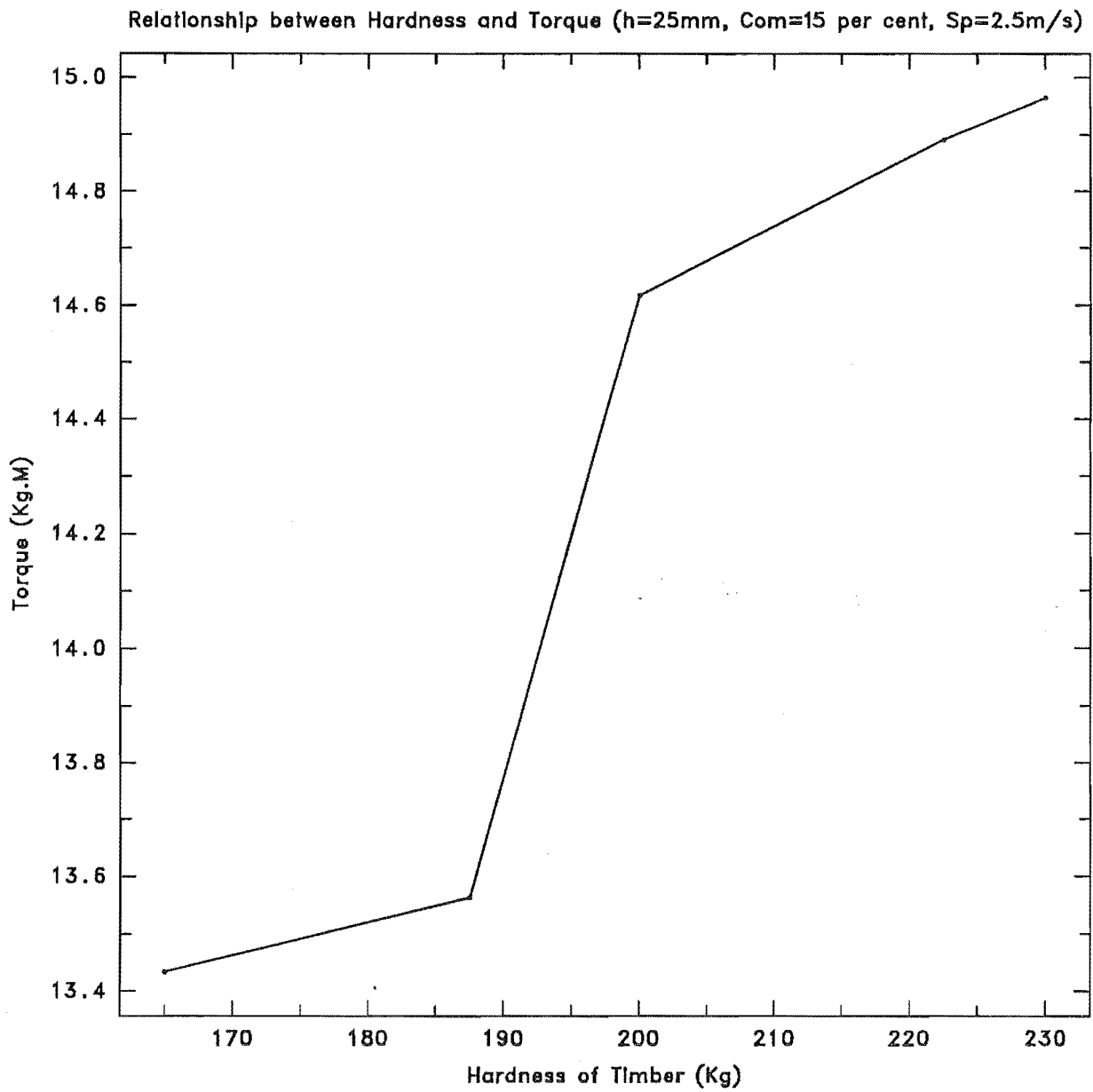


Figure 7.3.5 (a) Effect of Compression on Load

1. The thickness of the timber board is 33mm.
2. Moisture content is 11.5% -14%.
3. The feed speed and hardness are mean values.
4. The load values are mean values under the same
compression level.

Figure 7.3.5 (a)

Effect of Compression on Load ($h=33\text{mm}$)

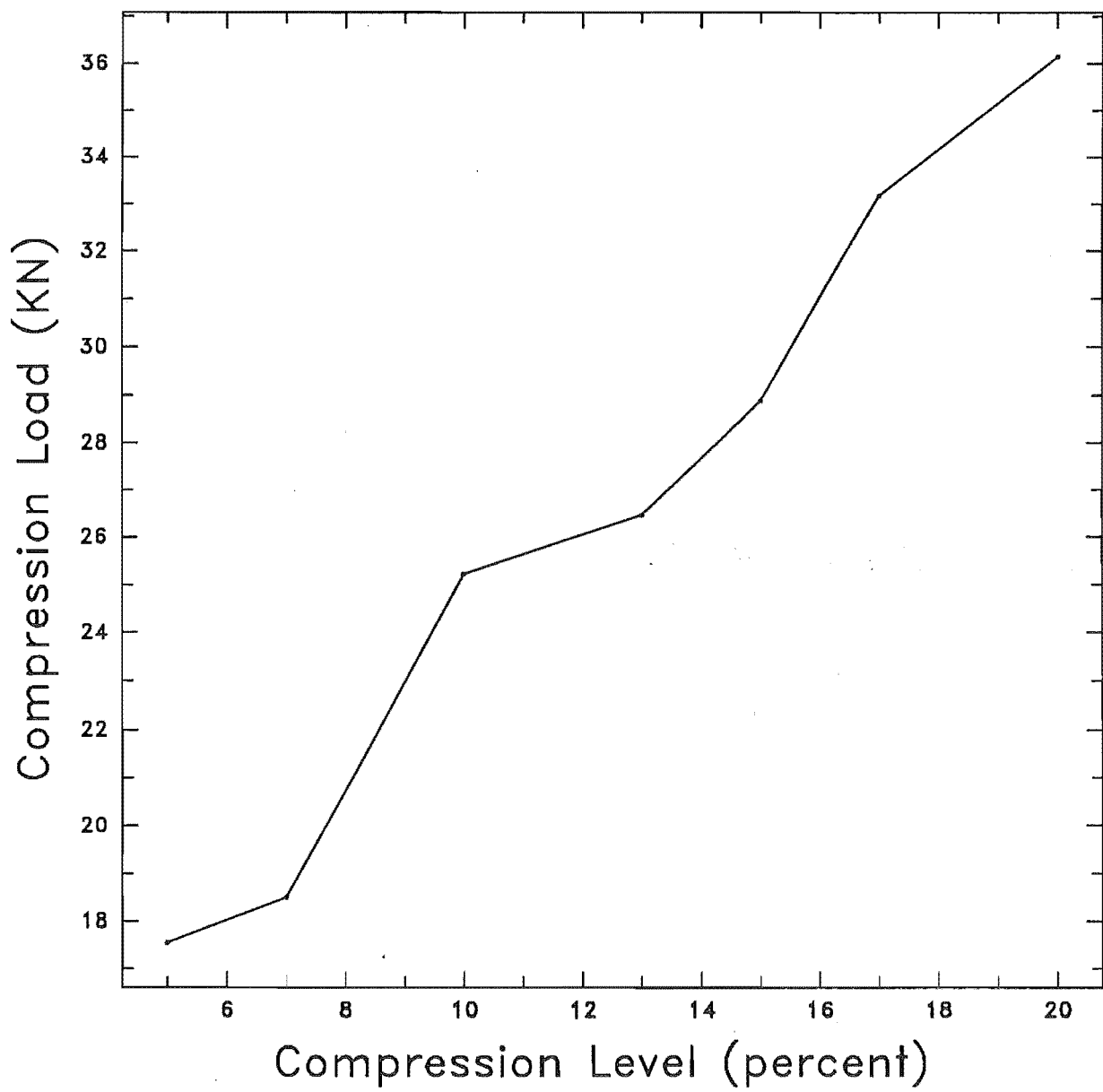


Figure 7.3.5 (b) Effect of Compression on Torque

1. The thickness of the timber board is 33mm.
2. Moisture content is 11.5% -14%.
3. The feed speed and hardness are mean values.
4. The torque is mean value under the same compression level.

Figure 7.3.5 (b)

Effect of Compression on Torque ($h=33\text{mm}$)

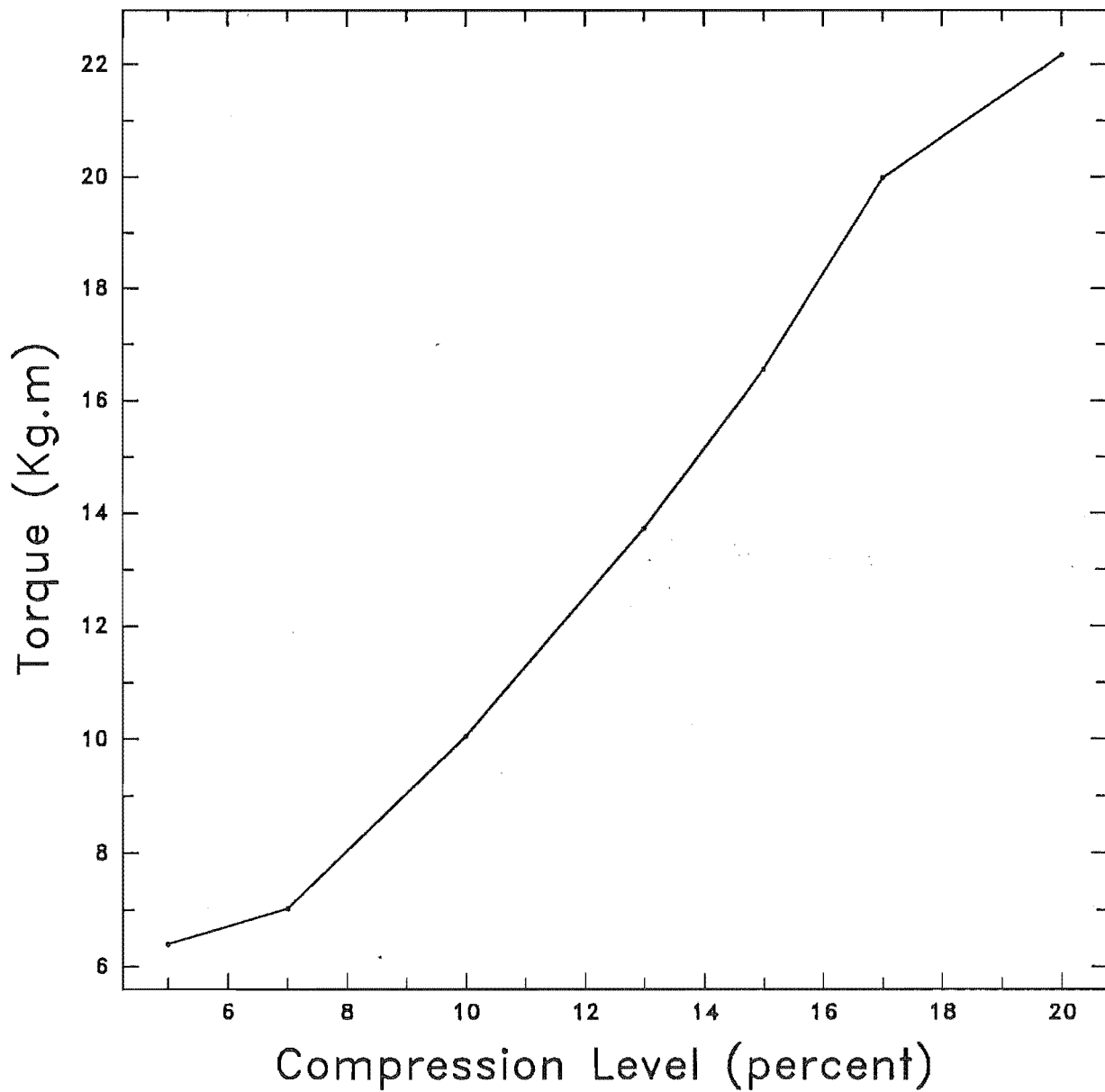


Figure 7.3.6 (a) Effect of Speed on Load

1. The thickness of the timber board is 25mm.
2. The compression level is 15%.
3. The range of hardness is from 230 to 255 (Kg).
4. Moisture content is 12% - 14%.
5. The load values are mean values under the different feed speed and 15% compression level.

Figure 7.3.6 (a)

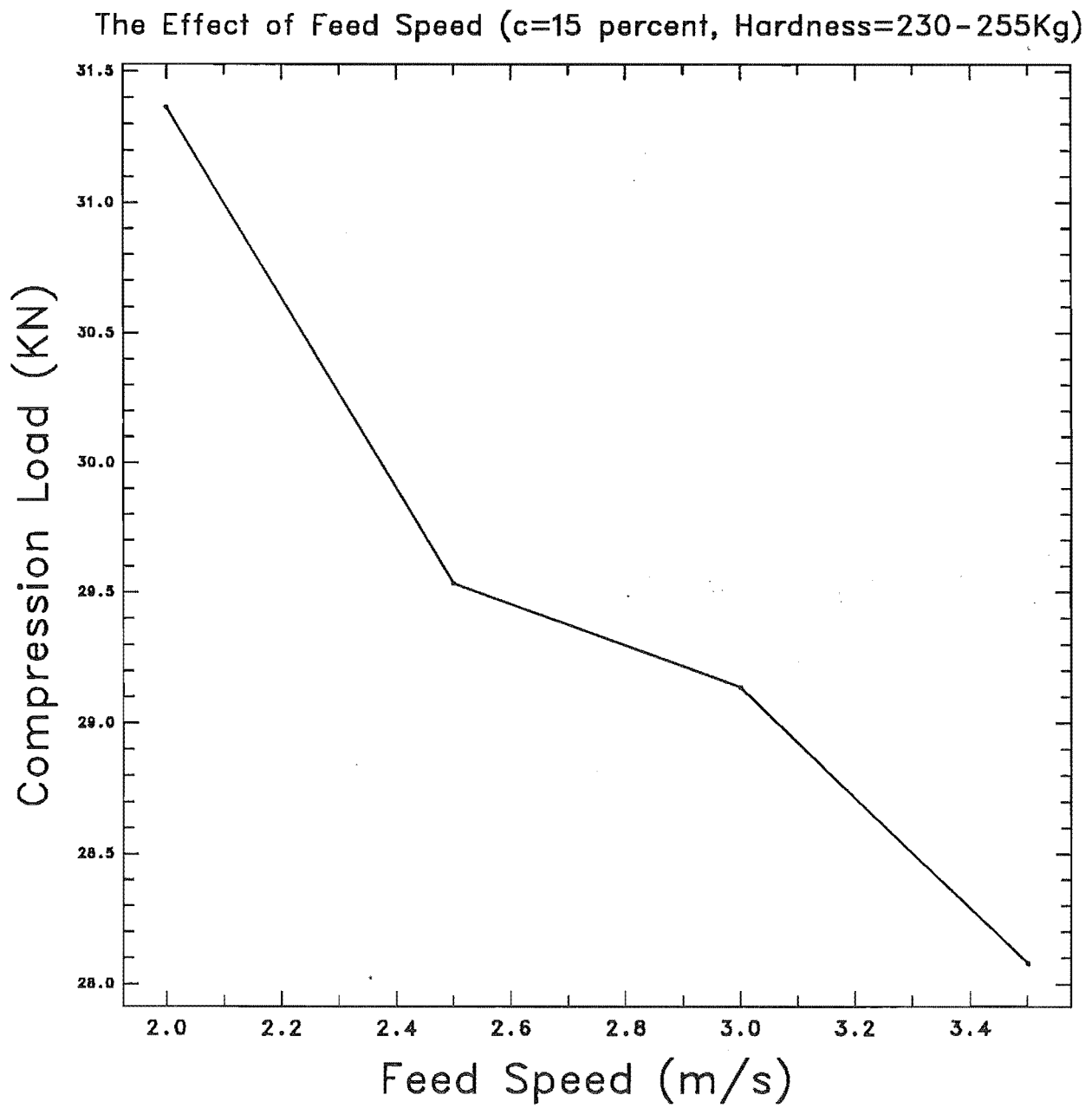


Figure 7.3.6 (b) Effect of Feed Speed on Torque

1. The treatment conditions are same as
 Figure 7.3.6 (a).
2. The torque values are mean values under the
 different feed speed and 15% compression level.

Figure 7.3.6 (b)

The Effect of Feed Speed

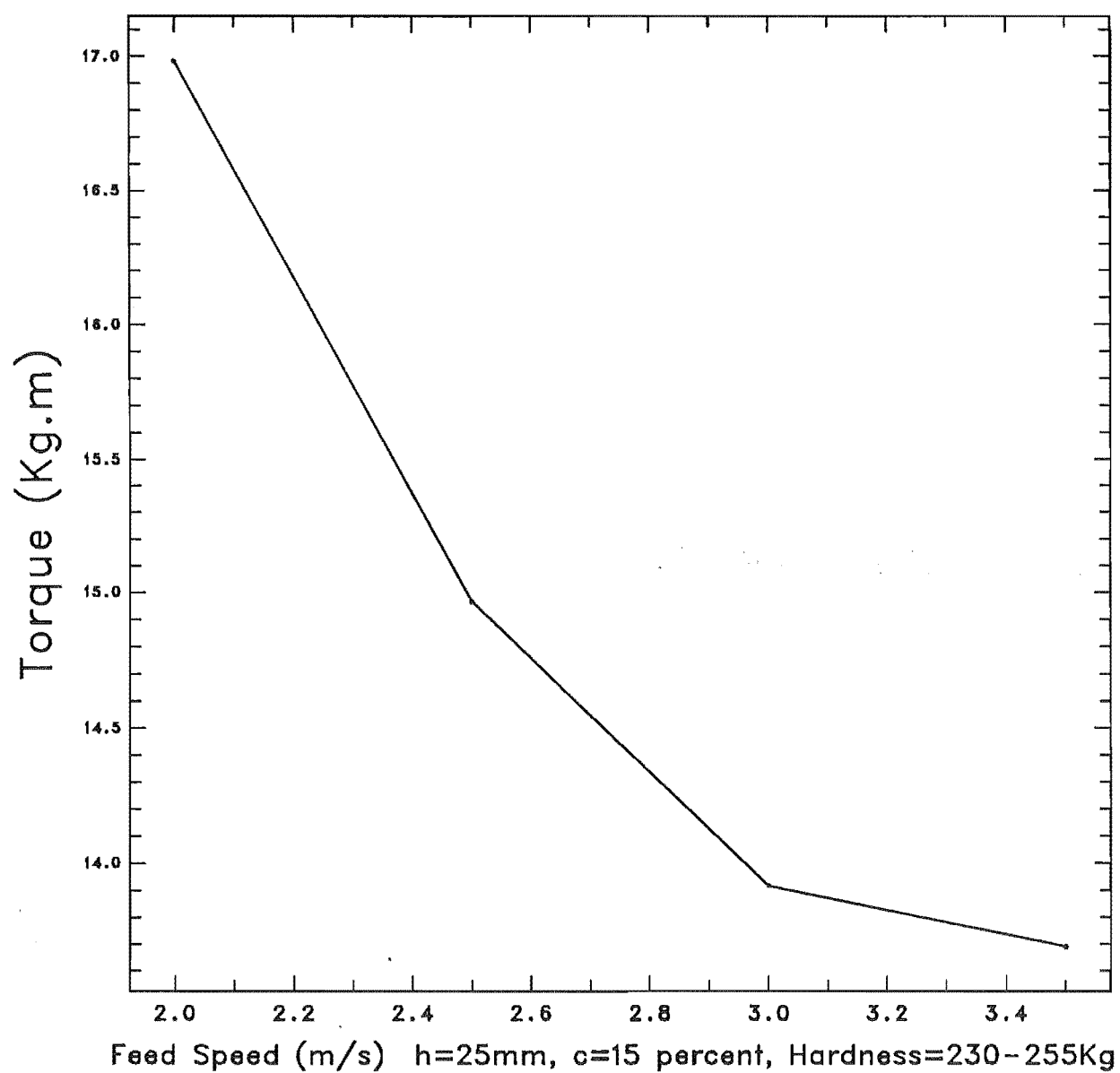


Figure 7.3.7 (A) Effect of Hardness on Load

1. The data is from the first group of the experiment.
2. The hardness values are mean values of each timber board after compression rolling.
3. The load values are mean values of each timber board.
4. The thickness of timber board is 25mm.
5. Moisture content is 12 -14%.
6. The compression level is 10% or 15%.
7. The feed speed is from 2m/s to 3.5 m/s.

Figure 7.3.7(A) EFFECT OF HARDNESS ON LOAD

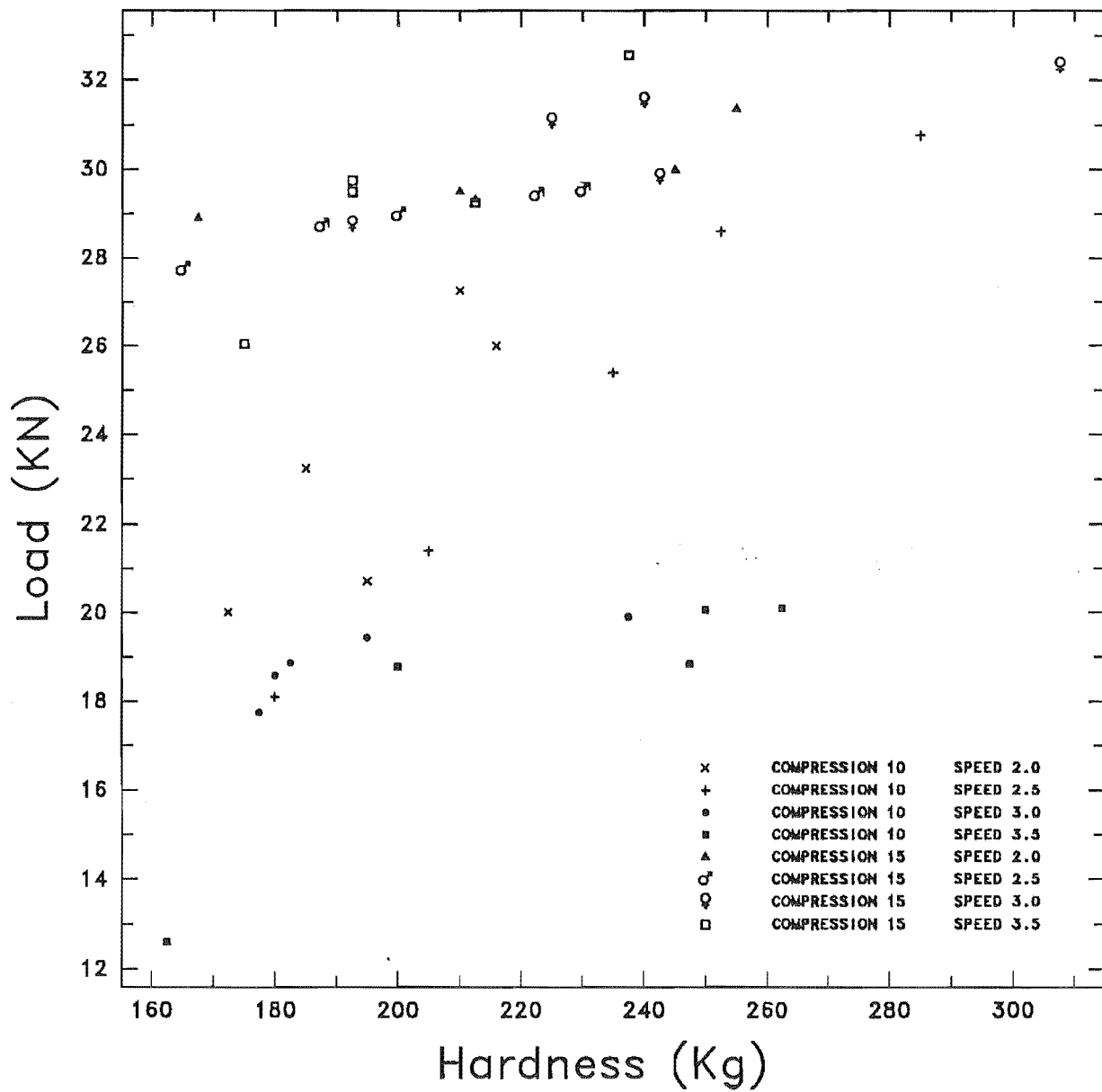


Figure 7.3.7 (B) Effect of Hardness on Torque

1. The hardness values are mean values of each timber board after compression rolling.
2. The torque values are mean values of each timber board.
3. The thickness of timber board is 25mm.
4. Moisture content is 12 -14%.
5. The compression level is 10% or 15%.
6. The feed speed is from 2m/s to 3.5 m/s.

Figure 7.3.7(B) EFFECT OF HARDNESS ON TORQUE

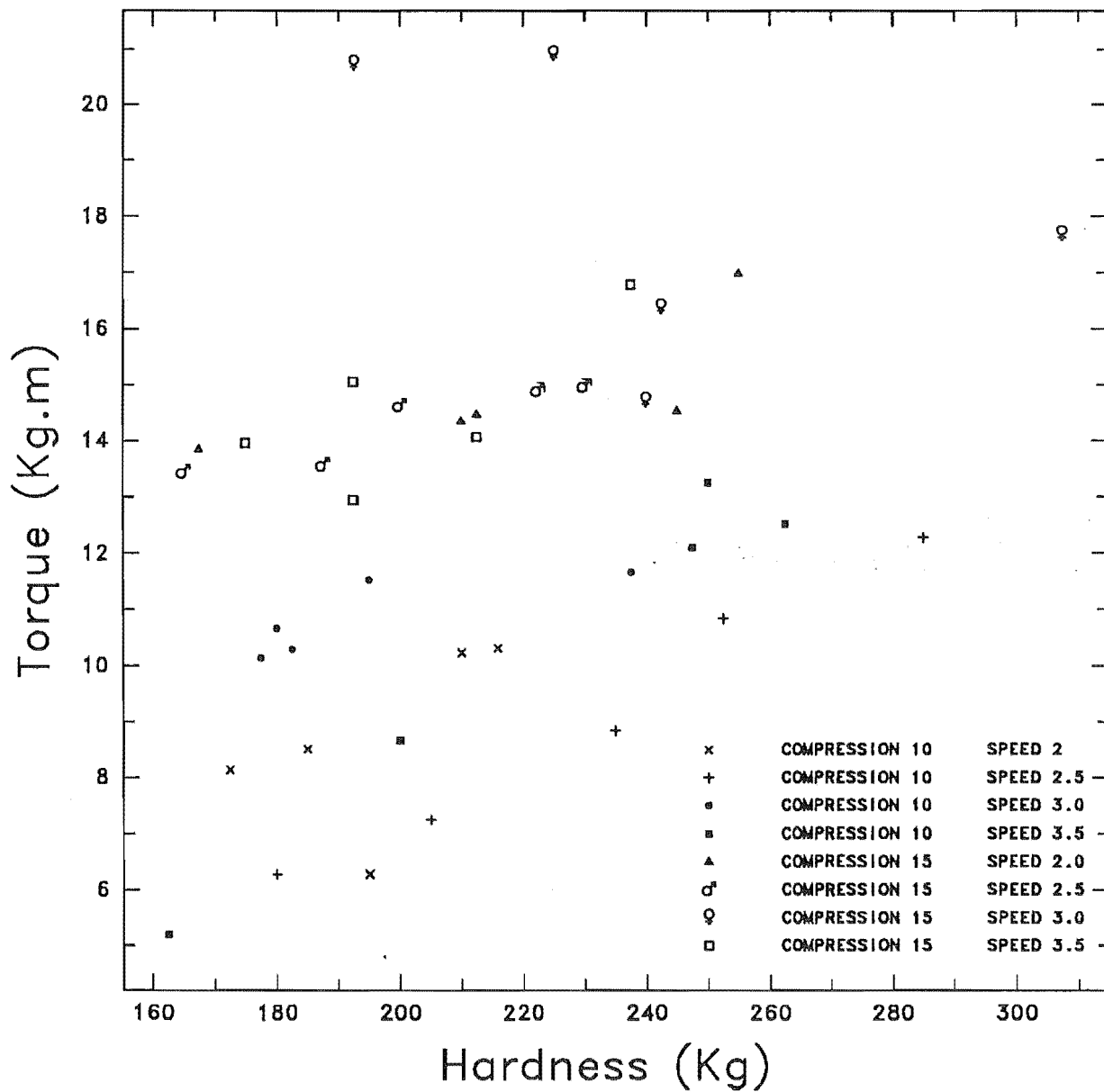


Figure 7.3.8 (A) (B) Distribution of Hardness Coefficient

1. The data are calculated from the second experiment.
2. The hardness values are mean values of six piece of timber boards under the same compression level and feed speed.
3. Each original hardness reading is from each the last section of each timber board before or after compression rolling.
4. The thickness of timber board is 33mm.
5. Moisture content is 11.5% - 14%.

Figure 7.3.8 (A) DISTRIBUTION OF HARDNESS COEFFICIENT

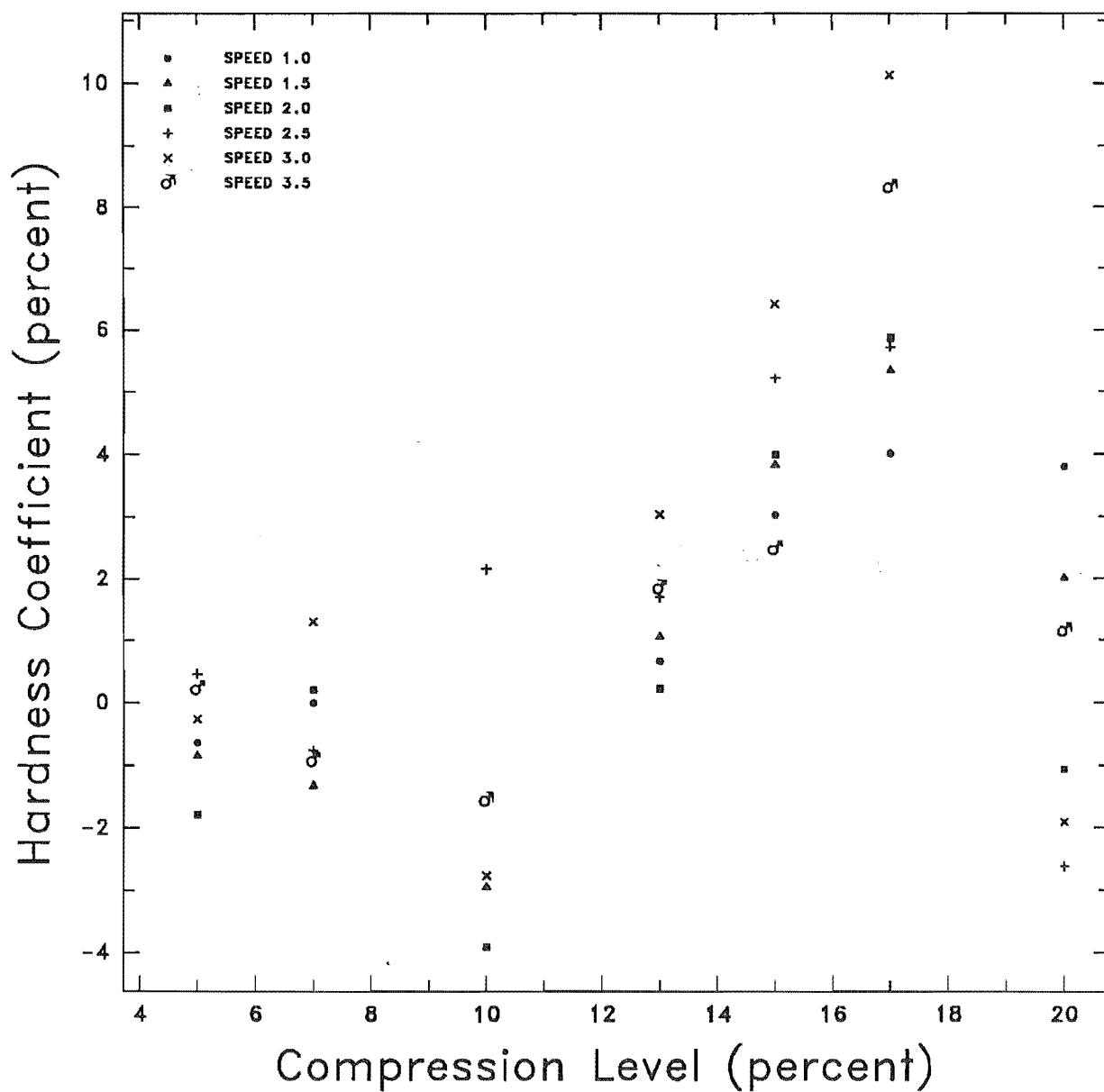
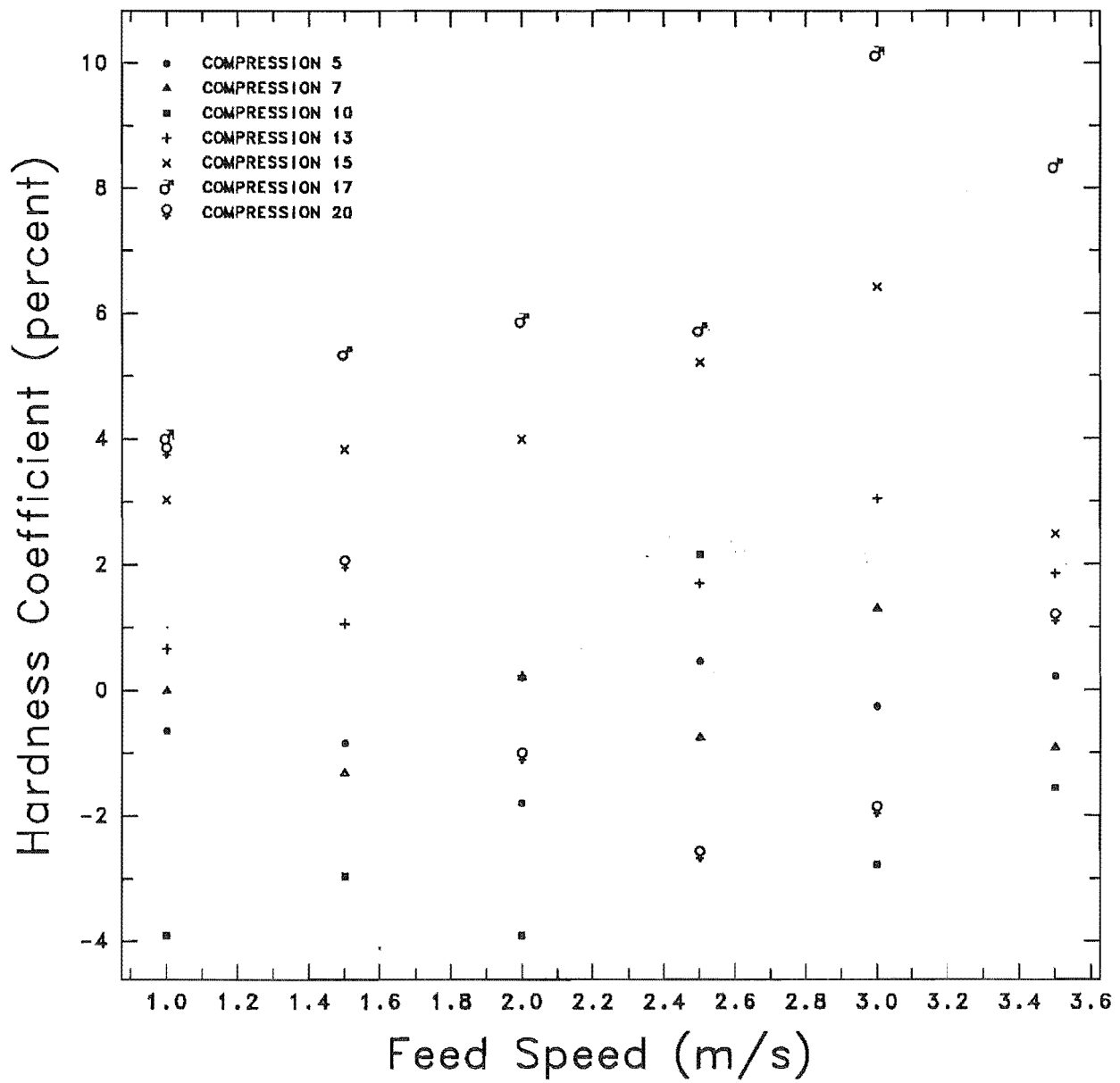


Figure 7.3.8(B) DISTRIBUTION OF HARDNESS COEFFICIENT



CHAPTER EIGHT:

DISCUSSION AND CONCLUSION

8.1 THE EVALUATION AND COMPARISON OF THE RESULTS

This experiment and data analysis concentrate on the physical and mechanical properties of timber boards during compression rolling.

The analysis results indicate: The experiment data is approached to the mathematical model. It is estimated by R squared (coefficient of determination). The value of R squared is from 0 to 1 (Maxwell, 1983). The more R squared approaches to 1, the more the experiment data close to the theoretical model. Referring to Table A.4.1 and Table A.4.2 of Appendix 4, R squared is 0.804 for first group experiments and 0.953 for second experiments. The theoretical model of compression rolling of timber board is similar to the results of data analysis. Correlation analysis of the results of experiments indicates: The regression model based on the equation (3.40) is highly correlated. It means these variables exhibit a strong linear relationship. Thus, the equation (3.40) can be considered to represent correctly the inter-relationship of mechanical properties of timber board during compression rolling.

The mechanical properties of the timber board displayed during compression rolling are discussed as follows:

Figure 7.3.1 indicates the relationship between hardness and load. The compression load increases while the hardness of timber increases. The range of the load values is quite large because the range of hardness of the timber is large. Comparing the effect of feed speed on the load during rolling, the effect produced by the mechanical properties of the timber itself is much noticeable. Thus, the mechanical properties of the timber is principal factor while considering and calculating the load.

Figure 7.3.2 indicates the same result: The torque increases while the hardness of timber increases. It is likely that the torque is linear with the hardness of the timber at the speed 2.5m/s and 10% compression level.

Figure 7.3.3 displays the same relationship between hardness and load as Figure 7.3.1 and expresses another fact: The range of compression load decreases because the hardness of timber decreases.

Figure 7.3.4 indicates the same relationship between hardness and torque as Figure 7.3.2. In the same way. the range of torque decreases since the range of hardness of the timber decreases.

Figure 7.3.5 expresses roughly the effect of compression level on the load. The load increases while compression level increases. Because the effect of the

hardness of the timber, it is hardly to get exact graph to express the relationship between compression level and the load. Figure 7.3.5 (A) is produced under the range of hardness values from 184Kg to 243.5Kg. In Figure 7.3.5 (B), it is likely that the torque is linear with the compression level.

Figure 7.3 6 (A) and (B) indicate a tendency: The load and torque slightly decrease while the feed speed increase. It can be explained as the effect of elastic recovery rate. This phenomenon happens when the elastic recovery rate of the timber is slower than feed speed (refer to Figure 3.6).

Figure 7.3.7 (A) is scatter diagram which is produced by load values in different hardness of timber. This scatter diagram expresses the distribution of hardness and load under the different compression level and different feed speed. From Figure 7.3.7 (A), we can observe this tendency: The load increases while hardness of timber increases.

The scatter diagram Figure 7.3.7 (B) presents the same tendency: The torque increases while hardness of timber increases.

Figure 7.3.8 (A) displays the hardness change with different compression level. The change is indicated and estimated by the hardness coefficient which has been defined in Chapter Seven. The coefficient represents either the percent of decrease of hardness if the value is negative or the percent of increase of hardness if the

value is positive. From Figure 7.3.8 (A), it is quite easy to observe that the hardness of the timber after compression obviously increases when the compression level is within 13% - 17%. The hardness of timber after rolling does not obviously change when the compression level is 5%, 7%, 10% and 20%. It can be explained as follows:

1. The densification and plastic deformation do not obviously occur on the surface of the timber board since lower compression level, so there is not obvious change on the hardness of the timber after compression rolling.
2. The hardness of the timber increases since the densification and slight plastic deformation occur on the surface of the timber board while the compression level increases to 13%.
3. The hardness of the timber slightly decreases (comparing with the increased hardness values) since the splits and resin expellation occur on the surface of the timber board while the compression level further increases up to 20%

The resin is concentrated and expelled on the surface of timber board under the condition of high compression level (20%) and high speed (over 3000mm/s). The expelled resin can be found under the following conditions:

1. Medium compression level and highest speed
(compression=17%, speed =3.5m/s).
2. High compression level and whole range of speeds
(compression=20%, speed=1m/s-3.5m/s).

It indicates: The properties of timber boards are affected by both compression level and feed speed of the timber board. Being accompanied by resin expellation, the local split and damaged resin pocket can be found.

8.2 CONCLUSION

1. The more accurate measurement of the parameters and the experiment data acquisition are realized by using the computer.
2. During compression rolling, the measuring results of the mechanical properties of the timber boards are in accord with theoretical analysis. The compression level, the feed speed and the properties of the timber board and compression load have the relationship as follows:

$$L = 1 * dh^j * v^m * H^n \quad (3.39)$$

3. The compression level is an important factor during compression rolling procedure. The surface of the timber boards and properties are not obviously changed if the compression level is less than 10% (moisture content 11.5 - 14%, thickness of timber 25 mm or 33 mm), but are changed in a small degree when the compression level increases from 10% to 17%.

There is some macroscopic damage -- splitting and resin condensation on the surface of timber boards when the compression level is more than 17%.

4. Through these experiments, the creep behaviour of timber boards is found. At a certain critical speed, when feed speed increases the load slightly decreases under the same compression level (Figure 7.3.6 (A) and (B)). It indicates: The recovery of the timber boards during compression rolling is a function of time. The load decreases when the feed speed is greater than the rate of recovery of the timber boards during compression rolling.
5. The hardness on the surface of the timber board is increased to some degree when the compression level is over 13%, but under the 20% compression level, the hardness values tend to decrease as a result of surface damage of the timber board. The change of hardness during compression rolling indicates: The improvement of surface quality in the timber boards - surface densification or increase of hardness can be realized by compression rolling at a suitable compression level. It is necessary for some usages, such as for floor and for some furniture.

8.3 THE PROSPECTIVE RESEARCH FIELD OF COMPRESSION ROLLING

8.3.1 FROM CLEAR WOOD TO COMMERCIAL GRADE TIMBER BOARD

Up to now, traditional testing method, such as ASTM - Designation: D143-83, is still used in experiments on the test of properties of wood. That is, the strength properties of wood are determined by testing the small specimens of clear defect-free wood. Consequently, the clear defect-free wood is used in almost all of the experiments on improving the properties of wood. But in practice, there are considerable differences between the clear defect-free wood and timber which contains natural growth characteristics such as knots. These differences have been found by a number of scientists and researchers (Bohannon, 1966, Barrett, 1974 and Buchanan, 1983).

Any material can exhibit behaviour somewhere between the two extremes of perfectly brittle and perfectly ductile behaviour. However, the timber as a natural material with macroscopic flaws (knots, slope of grain, compression wood and splits, etc) more approaches to brittle material than clear defect-free wood. This phenomenon is verified by comparing the failure mode in bending between clear wood and timber.

Straight-grained wood is stronger in tension than in compression, so failure in bending occurs in the compression zone where small visible wrinkles develop prior to final failure. Timber, on the other hand, often

contains knots in the tension zone, making it much weaker in tension than in compression. This causes failures to occur in the tension zone with a brittle fracture before any ductile compression yielding develops (Madsen and Buchanan 1986).

Since brittle fracture behaviour governs changes in the strength of the timber, it is necessary to understand the behaviour of compression rolling of large size timber board with macroscopic defects and effect of knots. Thus further research should be concentrated on compression rolling of large size commercial timber and test of mechanical properties by in-grade testing.

8.3.2 KNOT EFFECT AND STRENGTH BEHAVIOUR DURING COMPRESSION

In the application of commercial timber, it is necessary to consider the effect of knots. Since the strength of knots itself affects the strength of timber and most of the weakest links of timber are concentrated on the zone of knots, the change of strength and form of knots during compression rolling should be investigated in further research.

8.3.3 STUDIES ON THE POSSIBILITY OF IMPREGNATING TIMBER USING THE VACUUM OCCURRING DURING THE DECOMPRESSION PHASE.

It has been suggested that the vacuum presented in the timber during instantaneous and delayed recovery could be used to introduce solutions into the timber for different purposes (Gunzerodt, 1985).

This possibility is not investigated in the present study, but we believe that a improvement of intake and penetration can be achieved to a certain degree due to compression rolling-induced temporary pressure gradient, which can be great enough to produce sufficient transverse flow.

8.3.4 STUDIES ON POSSIBILITY OF APPLICATION IN PLYWOOD OR DECORATE VENEER

Previous researches on compression rolling of timber boards have more or less indicated that compression rolling effects are mainly concentrated on the surfaces of timber boards. The process of compression rolling of the timber board can be considered as a surface treatment process. Thus, the effect of compression on thin timber board is greater than that on thick timber board. According to this fact, it would be possible to apply the process of compression rolling into plywood production technology to decrease the drying time and to increase the surface quality of plywood.

Figure 8.1 shows this process, further investigation and studies need to be done to verify this conjecture.

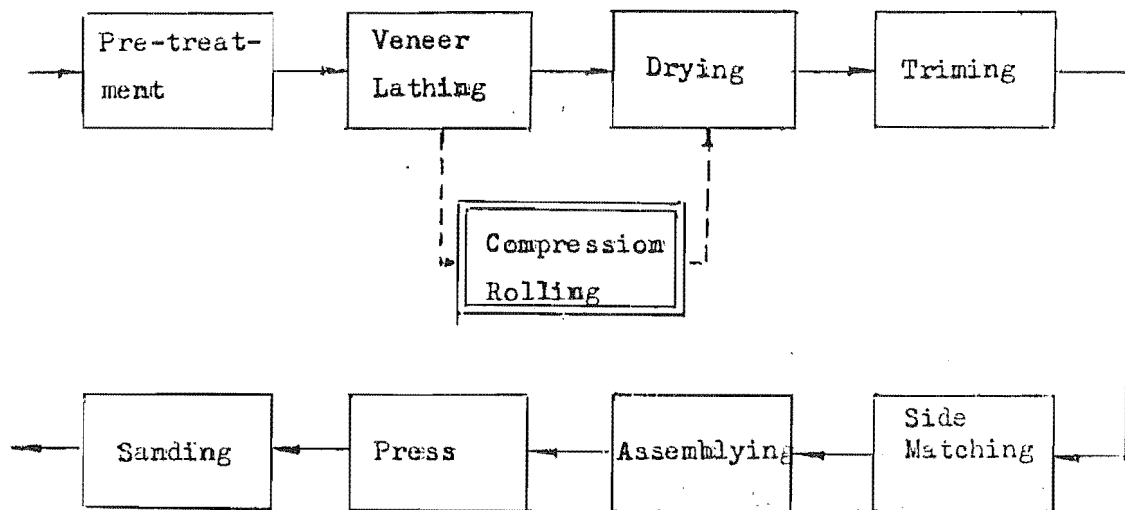


Figure 8.1 Proposed Flowsheet in Production of the Plywood

ACKNOWLEDGMENT

My thanks are in the first place directed to my supervisors Dr. K. Whybrew, Dr.J.C.F. Walker and Dr. R.J. Astley, who demonstrated a great degree of patience and understanding in the task of guiding me and encouraging me through this research.

I wish to express my thanks to Mr. H.J. Anink, Mr. O. Bolt, Mr. G.R. Johnson and Mr. C.S. Amies from the Department of Mechanical Engineering, who have given me very valuable advice and help on installation and application of the instrumentation and the computer.

I also wish to extend my sincere thanks to the late Mr. P.D. O'Hagan and Mr. H.A. Mobbs, who have given me a lot of instructions and assistance for testing the properties of wood.

In addition to the valuable contribution of the Department of Mechanical Engineering, I would like to thank Mr. P. Fuller from the Forestry Department, who has given me generous technical assistance and moral support through the research.

Finally, my special thanks belong to Dr. Diana Neutze who frequently gives me the necessary moral support and spiritual encouragement through the final research period.

APPENDIX

APPENDIX 1 PRINCIPLE OF THE RESISTANCE-TYPE STRAIN

GAUGE

The electrical resistance-type strain gauges used for measuring the torques and the loads in the research are thin metal-foil grids that are adhesively bonded to the surface of the load beams and the torque arms. When the load beams and the torque arms are loaded, the strains develop and are transmitted to the foil grid. The resistance of the foil grid changes in proportion to the load-induced strain. The principle can be explained as follows:

The resistance R of a uniform metallic conductor can be expressed as,

$$R = (\rho \times l)/A \quad (A.1.1)$$

where ρ is the specific resistance of the metal

l is the length of the conductor

A is the cross-sectional area of the conductor

Differentiating Equation (A.1.1) and dividing by the resistance R gives:

$$dR/R = d\rho/\rho + dl/l - dA/A \quad (A.1.2)$$

The term dA represents the change in cross-sectional area of the conductor resulting from the

applied load. For the case of a uniaxial stress state, recall that,

$$\epsilon_a = dl/l \quad (A.1.3)$$

$$\epsilon_t = -\tau \times \epsilon_a = -\tau \times dl/l \quad (A.1.4)$$

where ϵ_a is the axial strain in the conductor.

ϵ_t is the transverse strain.

τ is Poisson's ratio of the metal used for the conductor.

If the diameter of the conductor before application of the axial strain is d_0 , the diameter of the conductor after strain is expressed:

$$d_f = d_0 \times (1 - \tau \times dl/l) \quad (A.1.5)$$

From Equation (A.1.5), it is clear that,

$$dA/A = -2\tau \times dl/l + \tau^2 \times (dl/l)^2 \quad (A.1.6)$$

Neglecting the higher-order term yields,

$$dA/A \approx -2\tau \times dl/l \quad (A.1.7)$$

Substituting Equation (A.1.7) into Equation (A.1.2) and simplifying yields,

$$dR/R \approx d\ell/\ell + dl/l \times (1+2\tau) \quad (A.1.8)$$

which can be written as,

$$S_A = (dR/R)/\epsilon_a = (d\ell/\ell)/\epsilon_a + (1+2\tau) \quad (A.1.9)$$

The quantity S_A is defined as the sensitivity of the metal used for a conductor.

Finally, the electrical resistance-type strain gauge exhibits a resistance change $\Delta R/R$, that is related to the strain ϵ in the direction of the grid lines by the

expression,

$$\Delta R/R = GF \times \epsilon \quad (A.1.10)$$

where GF is the gauge factor

The gauge factor GF is always less than the sensitivity of the metallic alloy S_A because the grid configuration of the gauge is less responsive to strain than a straight uniform conductor.

The output $\Delta R/R$ of the strain gauge is converted into a voltage signal with a Wheatstone bridge.

APPENDIX 2: THE SELECTION AND INSTALLATION OF THE STRAIN GAUGES

A.2.1 THE CONSIDERATION OF SELECTION

To choose the type of strain gauges used for measuring the torque and the load and its installation method the following factors are considered:

1. The material and geometry of the torque arms and load beams should be considered.
2. The temperature and humidity environment should be considered.
3. The gauge length and width should be small so that the measurement approximates strain at a point.
4. The inertia of the gauge must be minimal to permit the recording of high-frequency dynamic strains.

5. The gauge factor, gauge resistance and the measured strain range also should be considered.
6. The response or output of the strain gauge should be linear over the entire strain range of the gauge.
7. The calibration constant for the strain gauge should be stable with respect to both temperature and time.
8. The measuring accuracy of the strain gauge should be considered.
9. The strain gauge should be economical.

The electric resistance-type strain gauges KFC-5-C1-11 are selected according to the criteria above-mentioned.

A.2.2 SPECIFICATION

The strain gauges used for measuring the torque and the load are KYOWA type KFC-5-C1-11. The code for the strain gauges, extracted from the manufacturer catalogue, is given in Table A.2.1.

The specifications of KFC-5-C1-11 type strain gauge is as follows:

Gauge Resistance	$120.0 \pm 0.3 \Omega$
Gauge Factor	$2.11 \pm 1\%$
Adoptable Thermal Expansion	$10.8 \text{ PPM}/^{\circ}\text{C}$
Gauge Length	5 mm
Gauge Factor Change with	$0.015\% /^{\circ}\text{C}$

TABLE A.2.1

KYOWA Strain Gage Coding System		
Gage Resistance in ohms (but no indication for 120 ohms)	Gage Pattern	Thermal Expansion Coefficient of SELCOM gage compatible material
Gage Length in millimeters	Lead Wire Provision, figures indicate lead wire length in centimeters, but no indica- tion is given for gage lead only.	3-Lead-Wire No indication for 2-lead-wire
Resistive Material & Base Material Classification		
KFC-5-350-C1-11-L30-3		
<p>KFC : Foil Phester Gage</p> <p>KFR : Foil Strain Gage (General)</p> <p>KFD : Foil Polyimide Gage</p> <p>KC : Phester Gage</p> <p>K : Paper Gage</p> <p>KP : Polyester Gage</p> <p>KFL : Foil Strain Gage (for low temperature)</p> <p>KFM : Foil Strain Gage (for high temperature)</p> <p>KFA : High Temperature Foil Strain Gage</p> <p>KH : High Temperature Gage</p> <p>KFE : High Elongation Foil Gage</p> <p>KLM : Ultra High Elongation Gage</p> <p>KL : High Elongation Gage</p> <p>KFW : Water-proofed Gage</p> <p>KFN : Non-inductive Gage</p> <p>KBN : Non-magneto-resistive Gage</p> <p>KFS : Shielded Gage</p> <p>KM : Embedment Gage</p> <p>KFF : Bending Strain Gage</p> <p>KSP : General-purpose Semiconductor Gage</p> <p>KSN : Self-temperature Compensating Semiconductor Gage</p> <p>KSPH : High Output Semiconductor Gage</p> <p>KSPL : Ultra High Linearity Semiconductor Gage</p> <p>KSPC : Sensitivity Compensated Semiconductor Gage</p>	<p>A1 : Uni-axial</p> <p>A4 : Uni-axial</p> <p>A9 : Uni-axial</p> <p>B2 : Biaxial, 90° crossed</p> <p>B4 : Triaxial, 45°/90° crossed</p> <p>C1 : Uni-axial</p> <p>C9 : Uni-axial (non-inductive)</p> <p>C11 : for uni-axial bending strain</p> <p>C12 : for uni-axial bending strain</p> <p>D1 : Biaxial, 90°</p> <p>D2 : Biaxial, 90°</p> <p>D3 : Triaxial, 45°/90°</p> <p>D4 : Triaxial, 60°</p> <p>D6 : 4-axial, 30°/90°</p> <p>D9 : Uni-axial, 5-element</p> <p>D16 : Biaxial, 90° crossed</p> <p>D17 : Triaxial, 45°/90° crossed</p> <p>D19 : Uni-axial, 5-element</p> <p>D20 : Biaxial, 90° (non-inductive type)</p> <p>D21 : Biaxial, 90°</p> <p>D22 : Triaxial, 45°/90°</p> <p>D25 : Triaxial, 45°/90°</p> <p>E3 : Uni-axial, leads both ends</p> <p>E4 : Uni-axial</p> <p>E5 : Uni-axial, leads both ends (without backing)</p> <p>F2 : Uni-axial, 2-element</p> <p>F3 : Biaxial, 90°</p> <p>G3 : Uni-axial, 2-element, Active & Dummy</p> <p>G4 : Uni-axial</p> <p>H1 : Uni-axial</p> <p>H2 : Uni-axial, 3 lead wire</p> <p>J1 : Uni-axial</p>	<p>5 : for wood ($5.0 \times 10^{-4}/^{\circ}\text{C}$) 2.8ppm/$^{\circ}\text{F}$</p> <p>11: for construction steel ($10.8 \times 10^{-4}/^{\circ}\text{C}$) 6ppm/$^{\circ}\text{F}$</p> <p>16: for stainless steel ($16.2 \times 10^{-4}/^{\circ}\text{C}$) 9ppm/$^{\circ}\text{F}$</p> <p>23: for aluminum alloy ($23.4 \times 10^{-4}/^{\circ}\text{C}$) 13ppm/$^{\circ}\text{F}$</p> <p>27: for magnesium ($27.0 \times 10^{-4}/^{\circ}\text{C}$) 15ppm/$^{\circ}\text{F}$</p>

A.2.3 INSTALLATION

The following procedures for bonding the strain gauge are adopted:

1. The surfaces of the torque arms and the load beams in the areas where the strain gauges are to be positioned must be carefully cleaned to remove rust.
2. The areas are sanded to obtain a smooth but not highly polished surface.
3. Following this, the area is thoroughly cleaned with trichloroethylene and LOCTITE Quick Clean 703 to eliminate all traces of oil and grease.
4. The surface area is smeared the LOCTITE affinity solution to give them the proper chemical affinity for the adhesive.
5. The gauge location is marked on the surface area with very light scribe line.
6. The strain gauge is positioned by using a rigid transparent tape in the manner illustrated in Figure A.2.1.
7. A layer of cyanoacrylate (LOCTITE PRISM 401 General Purpose Instant Adhesive) is smeared on the surface area.
8. The position and orientation of the gauge are maintained by the tape while the gauge is pressed on to the surface area by squeezing out the excess

adhesive.

9. When the gauge is installed, the adhesive is then exposed to pressure for a suitable length of time to ensure a complete cure.

10. The gauge leads are joined to the lead wires by

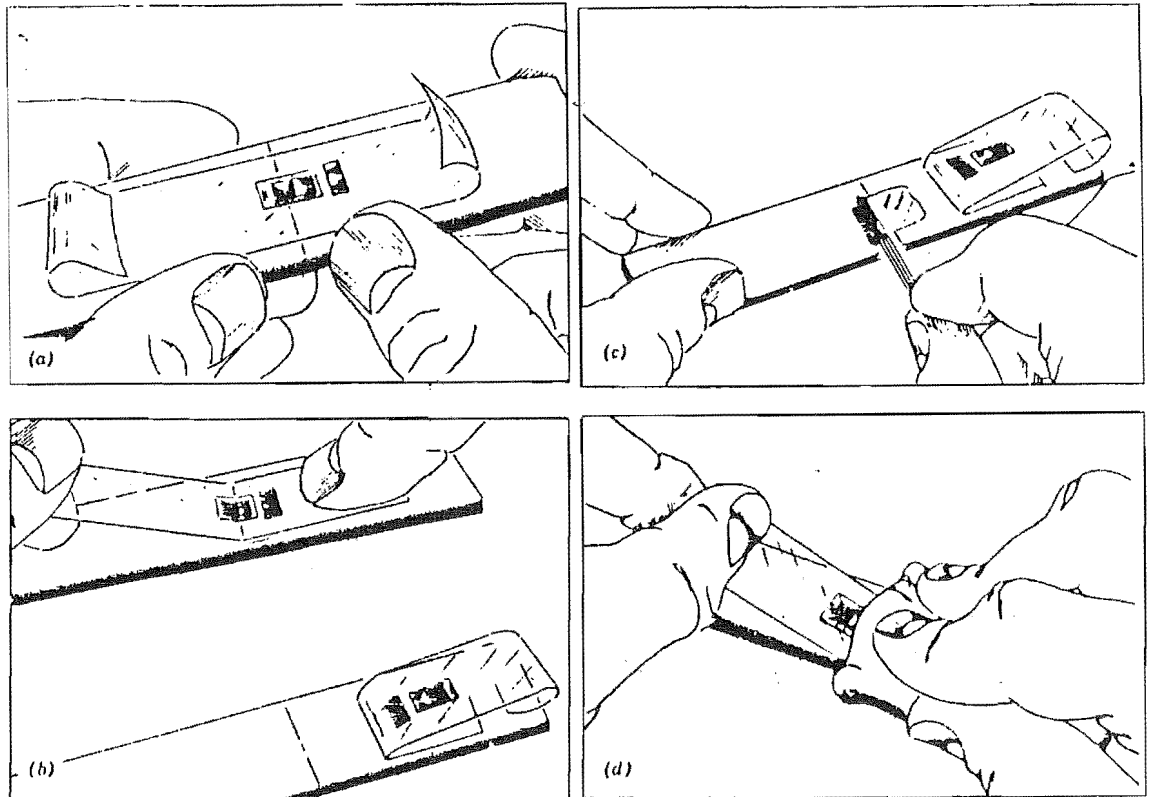


Figure A.2.1 Tape method for installing the electrical resistance strain gauge on the surface area

soldering.

11. After the adhesive is completely cured, the gauge is waterproofed with a light overcoating of EXPANDITE Silaflex RTV Fast Curing Silicone Sealant.

12. Finally, the lead wires are attached to the terminal blocks in the Wheatstone bridge.

APPENDIX 3: REFERENCE ON HYDRAULIC SYSTEM

1. In hydraulic system, the hydraulic oil is supplied by the VPT 3333 Hydrostatic Transmission Primary Unit to drive the hydraulic motors.

The specifications are as follows:

PRIMARY UNIT:

Displacement	0.033 l/rev
Maximum delivery/1000 rpm	33 l/min
Maximum speed	3000 r.p.m.
Maximum operating pressure	30 MPa
Maximum power input(3000rpm)	22 kw
Control trunnion operating torque	10 Nm / 10 MPa
Maximum pump case pressure	0.3 MPa

CHARGE PUMP

Displacement	0.031 l/rev
delivery / 1000 rpm	31 l/min
Operating Pressure	0.4 MPa

2. Char-Lynn 2000 Series low speed, high torque hydraulic motors are used for driving both compression rollers and feed rollers.

The specifications are as follows:

Displacement		14.9 cu.in./rev
Dimension of the shaft		1.25"
Flow (GPM)	Continuous	20
	Peak	25
Speed	Continuous	300
(RPM)	Peak	365
Torque	Continuous	3400
(lb.in.)	Peak	4250
Pressure	Continuous	1600
(p.s.i.)	Peak	2000

TABLE A.4.J

RESULTS OF THE DATA ANALYSIS OF
EXPERIMENT 1

REGRESSION CONDITION IS:

First Independent Variable is: Ln (dh)
 Second Independent Variable is: Ln (H)
 Third Independent Variable is: Ln (V)
 Dependent Variable is: Ln (L)

Regression Output:

Constant	-0.42573715
Std Err of Y Est	0.105767424
R Squared	0.803593080
No. of Observations	40
Degrees of Freedom	36

X Coefficient(s)	0.834493949	0.561540907	-0.30095897
Std Err of Coef.	0.082665881	0.109038442	0.080294016

REGRESSION CONDITION IS:

First Independent Variable is: Ln (dh)
 Second Independent Variable is: Ln (V)
 Third Independent Variable is: Ln (H)
 Dependent Variable is: Ln (T)

Regression Output:

Constant	-2.88741195
Std Err of Y Est	0.168401210
R Squared	0.739436613
No. of Observations	40
Degrees of Freedom	36

X Coefficient(s)	1.149198127	0.183344739	0.730205661
Std Err of Coef.	0.131619300	0.127842855	0.173609272

TABLE A.4.1 (2)

REGRESSION CONDITION IS:

First Independent Variable is: Ln (dh)
 Second Independent Variable is: Ln (H)
 Dependent Variable is: Ln (L)
 Speed is Constant: 1000mm/s

Regression Output:

Constant	0.500174484
Std Err of Y Est	0.087019477
R Squared	0.769830280
No. of Observations	10
Degrees of Freedom	7
X Coefficient(s)	0.506929859 0.413958973
Std Err of Coef.	0.147280871 0.230201828

REGRESSION CONDITION IS:

First Independent Variable is: Ln (dh)
 Second Independent Variable is: Ln (H)
 Dependent Variable is: Ln (T)
 Speed is Constant: 1000mm/s

Regression Output:

Constant	-1.82486607
Std Err of Y Est	0.145478652
R Squared	0.842215158
No. of Observations	10
Degrees of Freedom	7
X Coefficient(s)	1.215157964 0.542062749
Std Err of Coef.	0.246223295 0.384850065

TABLE A.4.1 (3)

REGRESSION CONDITION IS:

First Independent Variable is: Ln (dh)
 Second Independent Variable is: Ln (H)
 Dependent Variable is: Ln (L)
 Speed is Constant: 1500mm/s

Regression Output:

Constant	-1.96296145
Std Err of Y Est	0.084758710
R Squared	0.806403665
No. of Observations	10
Degrees of Freedom	7
X Coefficient(s)	0.693011168 0.832681156
Std Err of Coef.	0.146611270 0.189370820

REGRESSION CONDITION IS:

First Independent Variable is: Ln (dh)
 Second Independent Variable is: Ln (H)
 Dependent Variable is: Ln (T)
 Speed is Constant: 1500mm/s

Regression Output:

Constant	-5.27163381
Std Err of Y Est	0.100204739
R Squared	0.921363394
No. of Observations	10
Degrees of Freedom	7
X Coefficient(s)	1.556111543 1.109023486
Std Err of Coef.	0.173329019 0.223880869

TABLE A.4.1 (4)

REGRESSION CONDITION IS:

First Independent Variable is: Ln (dh)
 Second Independent Variable is: Ln (H)
 Dependent Variable is: Ln (L)
 Speed is Constant: 2000mm/s

Regression Output:

Constant	0.500174484
Std Err of Y Est	0.087019477
R Squared	0.769830280
No. of Observations	10
Degrees of Freedom	7
X Coefficient(s)	0.506939859 0.413958973
Std Err of Coef.	0.147280871 0.230201828

REGRESSION CONDITION IS:

First Independent Variable is: Ln (dh)
 Second Independent Variable is: Ln (H)
 Dependent Variable is: Torque - Ln (T)
 Speed is Constant: 2000mm/s

Regression Output:

Constant	-1.82486807
Std Err of Y Est	0.145478652
R Squared	0.842215158
No. of Observations	10
Degrees of Freedom	7
X Coefficient(s)	1.215157964 0.542062749
Std Err of Coef.	0.246223295 0.384850065

TABLE A.4.1 (5)

REGRESSION CONDITION IS:

First Independent Variable is: Ln (dh)
 Second Independent Variable is: Ln (H)
 Dependent Variable is: Load -- Ln (L)
 Speed is Constant: 2500mm/s

Regression Output:

Constant	-1.96296145
Std Err of Y Est	0.084758710
R Squared	0.806403665
No. of Observations	10
Degrees of Freedom	7
X Coefficient(s)	0.693011168 0.832681156
Std Err of Coef.	0.146611270 0.189370820

REGRESSION CONDITION IS:

First Independent Variable is: Ln (dh)
 Second Independent Variable is: Ln (H)
 Dependent Variable is: Torque -- Ln (T)
 Speed is Constant: 2500mm/s

Regression Output:

Constant	-5.27163381
Std Err of Y Est	0.100204739
R Squared	0.921363394
No. of Observations	10
Degrees of Freedom	7
X Coefficient(s)	1.556111543 1.109023486
Std Err of Coef.	0.173329019 0.223880869

TABLE A.4.1 (b)

REGRESSION CONDITION IS:

First Independent Variable is: Ln (dh)
 Second Independent Variable is: Ln (H)
 Dependent Variable is: Load -- Ln (L)
 Speed is Constant: 3000mm/s

Regression Output:

Constant	0.631618792
Std Err of Y Est	0.027415773
R Squared	0.991284867
No. of Observations	10
Degrees of Freedom	7
X Coefficient(s)	1.063812778 0.253150717
Std Err of Coef.	0.054851502 0.066041971

REGRESSION CONDITION IS:

First Independent Variable is: Ln (dh)
 Second Independent Variable is: Ln (H)
 Dependent Variable is: Torque -- Ln (T)
 Speed is Constant: 3000mm/s

Regression Output:

Constant	1.827683599
Std Err of Y Est	0.123205019
R Squared	0.856611135
No. of Observations	10
Degrees of Freedom	7
X Coefficient(s)	1.303570255 -0.12171972
Std Err of Coef.	0.246499719 0.296789087

TABLE A.4.1 (7)

REGRESSION CONDITION IS:

First Independent Variable is: Ln (dh)
 Second Independent Variable is: Ln (H)
 Dependent Variable is: Load -- Ln (L)
 Speed is Constant: 3500mm/s

Regression Output:

Constant	-2.80965674
Std Err of Y Est	0.072281647
R Squared	0.954324111
No. of Observations	10
Degrees of Freedom	7
X Coefficient(s)	1.421253272 0.812864652
Std Err of Coef.	0.118560458 0.155519408

REGRESSION CONDITION IS:

First Independent Variable is: Ln (dh)
 Second Independent Variable is: Ln (H)
 Dependent Variable is: Torque -- Ln (T)
 Speed is Constant: 3500mm/s

Regression Output:

Constant	-7.48535117
Std Err of Y Est	0.125277555
R Squared	0.893791367
No. of Observations	10
Degrees of Freedom	7
X Coefficient(s)	1.339419120 1.582112149
Std Err of Coef.	0.205487353 0.269544095

TABLE A.4.2

RESULTS OF THE DATA ANALYSIS OF
EXPERIMENT (2)

RESULT OF ANALYSIS OF RELATIONSHIP BETWEEN
LOAD AND TORQUE:

Independent Variable is: Load (KN)
Dependent Variable is: Torque (Kg.M)

TREATMENT CONDITION:

Moisture Content: 11.5% - 14.5%
Range of Speed: 1 - 3.5 m/s
Compression Level: 5% - 20%
Average Hardness: 215.20

RESULTS:

Constant	-9.7791205
Std Err of Y Est	1.42975046
R Squared	0.94511072
No. of Observations	42
Degrees of Freedom	40
X Coefficient(s)	0.88393964
Std Err of Coef.	0.03368177

TABLE A.4.2 (2)

THE VARIABLES OF REGRESSION ANALYSIS ARE:

First Independent Variable is: Compression Ln(dh)
 Second Independent Variable is: Hardness Ln(H)
 Third Independent Variable is: Speed: Ln(V)
 Dependent Variable: Load Ln(L)

RESULTS:

Constant	1.78816947
Std Err of Y Est	0.05893787
R Squared	0.95298285
No. of Observations	42
Degrees of Freedom	38
X Coefficient(s)	0.53778510 0.00387661 0.09579261
Std Err of Coef.	0.01963786 0.11063699 0.02157127

THE VARIABLES OF REGRESSION ANALYSIS ARE:

First Independent Variable is: Compression Ln(dh)
 Second Independent Variable is: Hardness Ln(H)
 Third Independent Variable is: Speed: Ln(V)
 Dependent Variable: Torque Ln(T)

RESULTS:

Constant	-0.7072305
Std Err of Y Est	0.10925801
R Squared	0.95438543
No. of Observations	42
Degrees of Freedom	38
X Coefficient(s)	0.98644630 -0.0826631 0.30946333
Std Err of Coef.	0.03640434 0.20509696 0.03998845

TABLE A.4.2 (3)

THE VARIABLES OF REGRESSION ANALYSIS ARE:

First Independent Variable is: Compression Ln(dh)
 Second Independent Variable is: Hardness Ln(H)
 Dependent Variable: Load Ln(L)
 Speed: 1000 mm/s

RESULTS:

Constant	1.58374659
Std Err of Y Est	0.07771292
R Squared	0.94715325
No. of Observations	7
Degrees of Freedom	4
X Coefficient(s)	0.55456638 0.16105772
Std Err of Coef.	0.08948693 0.50859200

THE VARIABLES OF REGRESSION ANALYSIS ARE:

First Independent Variable is: Compression Ln(dh)
 Second Independent Variable is: Hardness Ln(H)
 Dependent Variable: Torque Ln(T)
 Speed: 1000 mm/s

RESULTS:

Constant	2.15068658
Std Err of Y Est	0.10276260
R Squared	0.97967902
No. of Observations	7
Degrees of Freedom	4
X Coefficient(s)	1.13347467 -0.2467295
Std Err of Coef.	0.11833195 0.67253039

TABLE A.4.2 (4)

THE VARIABLES OF REGRESSION ANALYSIS ARE:

First Independent Variable is: Compression Ln(dh)
 Second Independent Variable is: Hardness Ln(H)
 Dependent Variable: Load Ln(L)
 Speed: 1500 mm/s

RESULTS:

Constant	1.17477760
Std Err of Y Est	0.04948198
R Squared	0.98051015
No. of Observations	7
Degrees of Freedom	4

X Coefficient(s)	0.57060521	0.23777677
Std Err of Coef.	0.04037939	0.18231866

THE VARIABLES OF REGRESSION ANALYSIS ARE:

First Independent Variable is: Compression Ln(dh)
 Second Independent Variable is: Hardness Ln(H)
 Dependent Variable: Torque Ln(T)
 Speed: 1500 mm/s

RESULTS:

Regression Output:

Constant	-1.9662341
Std Err of Y Est	0.07963412
R Squared	0.98645492
No. of Observations	7
Degrees of Freedom	4

X Coefficient(s)	1.10319009	0.53966228
Std Err of Coef.	0.06498480	0.29341559

TABLE A.4.2 (5)

THE VARIABLES OF REGRESSION ANALYSIS ARE:

First Independent Variable is: Compression Ln(dh)
 Second Independent Variable is: Hardness Ln(H)
 Dependent Variable: Load Ln(L)
 Speed: 2000 mm/s

RESULTS:

Constant	5.06606697
Std Err of Y Est	0.04956418
R Squared	0.97744662
No. of Observations	7
Degrees of Freedom	4
X Coefficient(s)	0.52517590 -0.4713130
Std Err of Coef.	0.04050347 0.29552239

THE VARIABLES OF REGRESSION ANALYSIS ARE:

First Independent Variable is: Compression Ln(dh)
 Second Independent Variable is: Hardness Ln(H)
 Dependent Variable: Torque Ln(T)
 Speed: 2000 mm/s

RESULTS:

Constant	3.82211329
Std Err of Y Est	0.12805071
R Squared	0.95586066
No. of Observations	7
Degrees of Freedom	4
X Coefficient(s)	0.96660332 -0.4925672
Std Err of Coef.	0.10464206 0.76349195

TABLE A.4.2 6)

THE VARIABLES OF REGRESSION ANALYSIS ARE:

First Independent Variable is: Compression $\ln(dh)$
 Second Independent Variable is: Hardness $\ln(H)$
 Dependent Variable: Load $\ln(L)$
 Speed: 2500 mm/s

RESULTS:

Constant	-0.4171347
Std Err of Y Est	0.04311431
R Squared	0.98328201
No. of Observations	7
Degrees of Freedom	4

X Coefficient(s)	0.51380479	0.55976415
Std Err of Coef.	0.03648056	0.26221786

THE VARIABLES OF REGRESSION ANALYSIS ARE:

First Independent Variable is: Compression $\ln(dh)$
 Second Independent Variable is: Hardness $\ln(H)$
 Dependent Variable: Torque $\ln(T)$
 Speed: 2500 mm/s

RESULTS:

Constant	1.27462653
Std Err of Y Est	0.11015749
R Squared	0.96335350
No. of Observations	7
Degrees of Freedom	4

X Coefficient(s)	0.92128192	0.01361498
Std Err of Coef.	0.09320820	0.66996924

TABLE A.4.2 (7)

THE VARIABLES OF REGRESSION ANALYSIS ARE:

First Independent Variable is: Compression Ln(dh)
 Second Independent Variable is: Hardness Ln(H)
 Dependent Variable: Load Ln(L)
 Speed: 3000 mm/s

RESULTS:

Constant	6.26990981
Std Err of Y Est	0.03442374
R Squared	0.98926857
No. of Observations	7
Degrees of Freedom	4
X Coefficient(s)	0.61648116 -0.7015380
Std Err of Coef.	0.03816189 0.21305920

THE VARIABLES OF REGRESSION ANALYSIS ARE:

First Independent Variable is: Compression Ln(dh)
 Second Independent Variable is: Hardness Ln(H)
 Dependent Variable: Torque Ln(T)
 Speed: 3000 mm/s

RESULTS:

Constant	3.97854526
Std Err of Y Est	0.10335582
R Squared	0.96400868
No. of Observations	7
Degrees of Freedom	4
X Coefficient(s)	0.92820673 -0.4738024
Std Err of Coef.	0.11457946 0.63970110

TABLE A.4.2 (8)

THE VARIABLES OF REGRESSION ANALYSIS ARE:

First Independent Variable is: Compression Ln(dh)
 Second Independent Variable is: Hardness Ln(H)
 Dependent Variable: Load Ln(L)
 Speed: 3500 mm/s

RESULTS:

Constant	2.68363657
Std Err of Y Est	0.09429193
R Squared	0.92094689
No. of Observations	7
Degrees of Freedom	4
X Coefficient(s)	0.52449916 -0.0169903
Std Err of Coef.	0.08202465 0.64120805

THE VARIABLES OF REGRESSION ANALYSIS ARE:

First Independent Variable is: Compression Ln(dh)
 Second Independent Variable is: Hardness Ln(H)
 Dependent Variable: Torque Ln(T)
 Speed: 3500 mm/s

RESULTS:

Constant	0.31814958
Std Err of Y Est	0.12860782
R Squared	0.94743166
No. of Observations	7
Degrees of Freedom	4
X Coefficient(s)	0.90038747 0.21869340
Std Err of Coef.	0.11187607 0.87456439

REFERENCES

- Bamber, R. K. and Burley, J. (1983)
The Wood Properties of Radiata Pine
Slough: Commonwealth Agricultural Bureaux
- Banks, W.B. (1973)
Preservative Penetration of Spruce
Timber Trades Journal, June
- Barrett, J.D. (1974)
Effect of Size on Tension Perpendicular-to grain
Strength of Douglas-fir.
Wood and Fiber, 6(2), pp126-143
- Bauch, J. and Liese, W. (1970)
Biological Investigations for the Improvement of
the Permeability of Softwoods
Holzforschung 24(6), 199-205
- Becker, Hans and Wilke, Thomas (1878)
Calculation of the power and moments required in
cold rolling compression of metal powers taking
into account the surface conditions of the
compression rolls
Neue Huette Vol.23 (8)

Bendtsen, B.A. and Galligan, W.L.

Mean and tolerance limit stresses and stress modeling for compression perpendicular to grain in hardwood and softwood species. U.S.D.A. Forest Service Forest Products Laboratory.

Bendtsen, B.A., Galligan, W.L. (1979)

Modelling the Stress-Compression Relationship in Wood in Compression Perpendicular to Grain
Forest Product Journal 29(2) 42-48

Berni, C.A. and Christensen, F.J. (1979)

Influence of dynamic transverse compression and redrying conditions on internal checking in 45mm thick treated Radiata Pine.

19th Forest Products Research Conference,
C.S.I.R.O., Highett, Australia

Betts, J. A. (1970)

Signal Processing, Modulation and Noise
London, English Universities Press

Bodig, Jozsef and Jayne, Benjamin A. (1982)

Mechanics of Wood and Wood Composites
Van Nostrand Reinhold Company

Bohannon, B. (1966)

Effect of Size on Bending Strength of Wood Members
United States Forest Service, Research Paper FPL
56, 30p

Bowden, F.P. and Tabor, D. (1964)

The Friction and Lubrication of Solids Part II
Oxford University Press

Buchanan, A.H. (1983)

Effect of Member Size on Bending and Tension
Strength of Wood.

Proceedings, Wood Engineering Meeting,
International Union of Forestry Research
Organizations S5.02 Madison, WI

Cech, M.Y. (1971)

Dynamic transverse compression treatment to improve
drying behaviour of yellow birch.

Forest Products Journal, Vol.21, No.2

Cech, M.Y. and Goulet, M. (1968)

Transverse compression treatment of wood to improve
its drying behaviour.

Forest Products Journal, Vol.18, No.5, 90-91

Cech, M.Y. and Huffman, D.R. (1970)

Dynamic transverse compression treatment of spruce
to improve intake of preservative.

Forest Products Journal, Vol.20, No.3, 47-52

Cech, M.Y. and Huffman, D.R. (1972)

Dynamic compression results in greatly increased
creosote retention spruce heartwood.

Forest Products Journal, Vol.22, No.4, 21-25

- Cech, M.Y. and Pfaff F. (1977)
Dynamic transverse compression.
Kiln operators manual for eastern Canada
- Cech, M.Y. and Pfaff, F. (1975)
Kiln-Drying of 1-inch Red Oak.
Forest Products Journal, Vol.25, No.8, 30-37
- Cech, M.Y., Pfaff, F. and Huffman, D.R. (1974)
CCA-Retention and Disproportioning in White Spruce.
Forest Products Journal, Vol.24, No.7, 26-32
- Chu, E. (1984)
Finite strain evaluation in metal forming: A user's
manual,
Department of mechanical Engineering, Mac Master
University, Hamilton, Ontario
- Cooper, P.A. (1973)
Effects of species, precompression and seasoning on
heartwood preservative treatability of six western
conifers.
Forest Products Journal, Vol.23, No.7
- Dally, J.W., Riley, W.F., McConnell, K.G. (1984)
Instrumentation for Engineering Measurements
John Wiley & Sons, Inc.
- Doyle, J. (1980)
The hardness of wood.
Ph. D. Thesis, University of Canterbury,
Christchurch, New Zealand

Finkel, Jules (1975)

Computer-Aided Experimentation: Interfacing to
Minicomputers.

A Wiley-Interscience Publication

Fung, Y.C. (1965)

Foundations of Solid Mechanics

Englewood Cliffs, N.J., Prentice-Hall

Grozdzits, G. and Chauret, G. (1981)

Influence of wood-structure on seasoning and
gluing: Application of wood anatomy in research and
development.

Forest Products Journal, Vol.31, No.2

Gunzerodt, H. et. al. (1986)

Compression Rolling and Hot-water Soaking: Effects
on the drying and treatability of *Nothofagus fusca*
Heartwood.

New Zealand Journal of Forestry Science 16(2) 223-
36

Gunzerodt, H. et. al. (1988)

Compression Rolling of Sitka spruce and Douglas-fir
Forest Products Journal Vol.38(2) 16-18

Gunzerodt, H. et. al. (1984)

Compression rolling of New Zealand red beech
(*Nothofagus fusca*).

Proceedings of the Pacific Timber Engineering
Conference, Auckland, New Zealand
Volume II Timber design theory

- Haslett, A.N. and Kininmonth, J.A. (1986)
Pretreatments to hasten the drying of *Nothofagus fusca*.
New Zealand Journal of Forestry Science 16(2)
- Hoadley, R.B. (1968)
Strain analysis of wood by means of moire patterns.
Forest Products Journal, Vol.18, No.5
- Hult, Jain (1974)
Mechanics of Visco-Elastic Media and Bodies
Symposium, Gothenburg, Sweden September 2-6,
Berlin: Springer 1975
- Ivanov, Yu. M. (1986)
Forced Highly Elastic Deformations of Wood in
Compression Perpendicular to Grain
Khimiya Drevesiny (1986) No.5 91-96 Forest
Products Abstracts Vol.10 No.2 298
- Johns, K. and Madsen, B. (1982)
Duration of Load Effects in Lumber. Part I: A
Fracture Mechanics Approach
1982 National Research Council of Canada
- Johnson, K.L. and Tabor, D (1968)
Rolling Friction
Conference on Lubrication and Wear: Fundamentals
and Application to Design
The Institution of Mechanical Engineers
Proceedings 1967-68 Vol.182 Part 3A 168-72

- Johnston, J.S. and St.Laurent, A. St (1978)
Compression slicing of wood.
Forest Products Journal, Vol.28, No.7
- Jones, Larry D.and Chin, A. Foster (1983)
Electronic Instruments and Measurements
New York: Wiley, c1983 498p
- Kallmann, F., Cote, W.A. Jr. (1968)
Principles of Wood Science and Technology
Springer-Verlag, Berlin-Heidelberg New York
- Kininmonth, J.A. (1971)
Permeability and Fine Structure of Certain
Hardwoods and Effects on Drying: I. Transverse
Permeability of Wook to Micro-Filtered Water
Holzforschung,25, Heft 4
- Kirbach, E. et.al. (1976)
On the Fractional Stress Relaxation of Coniferous
Wood Tissues
Wood and Fiber (1976) 8(2) 74-84
- Knuffel, W.E. (1985)
The effect of CCA preservative treatment on the
compression strength of South African Pine
structural timber
Nat. Timber Res. Inst., CSIR, Pretoria, South
Africa.
Holzforschung und Holzverwertung 37 (5) 96-99
- Koch, Peter (1971)
Wood machining Abstracts 1970 and 1971

- Kou, Benjamin C. (1980)
Digital Control Systems
University of Illinois, Urbana. Holt, Rinehart and
Winston, INC.
- Kundson and Schniewind (1971)
Effect of Organic Solvents on Wood Steel Friction
Wood Science Vol.5 No.2 153-60
- Kunesh, R.H. (1968)
Strength and Elastic Properties of Wood in
Transverse Compression
Forest Products Journal Vol.18 No.1
- Lemoine, T.J., et. al. (1970)
Wood Variables Affecting the Friction Coefficient
of Spruce pine on Steel
Wood Science 2(3), 144-148
- Madsen, B. (1976)
In-grade Testing Degree of Damage Due to Proof
Loading of Lumber in Bending.
Structural Research Series Report No.17
I.S.S.N. 0318-3378, Vancouver, British Columbia.
- Madsen, B. (1989)
Size Effects in Lumber. Are They Important?
Proceedings of the second pacific timber
engineering conference
University of Auckland New Zealand 28-31 August
1989 Vol.1 269-72

- Madsen, B. and Buchanan, A.H. (1986)
Size effects in timber explained by a modified
weakest link theory
Canadian Journal of Civil Engineering Vol.13(2)
218-232
- Madsen, B. and Nielsen, P.C. (1976)
In-grade Testing Size Investigation on Lumber
Subjected to Bending.
Structural Research Series Report No.15
I.S.S.N. 0318-3378, Vancouver, British Columbia
- Maxwell, E.A. (1983)
Introduction to Statistical Thinking
Englewood Cliffs, N. J. Prentice-Hall
- Mckenzie, W. M. and Karpovour, H. (1968)
The Frictional Behaviour of Wood
Wood Science and Technology, Vol.2, 138-152
- McMillin, C. W. etc (1970)
Friction Coefficient of Spruce Pine on Steel -- A
Note on Lubricants
Wood Science Vol.3, 100-101
- McMillin, Charles W. etc. (1970)
Friction Coefficient of Oven-dry Spruce Pine on
Steel, As Related to Temperature and Wood
Properties
Wood and Fibre Vol.2(1)

Mekinzie, W.M. (1969)

Applying Grid Patterns to Wood Surfaces Using
Photosensitive Lacquers
Forest Products Journal Technical Note, Vol.19(2)

Mindess, S. (1976)

Effect of Constant Deformation Rate on the Strength
Perpendicular to the grain of Douglas-Fir
Wood Science 8(4) 262-266

Monroe, Alfred J. (1962)

Digital Processes for Sampled Data Systems
New York, Wiley

New Zealand Directory of Technology 1987-1988

Nicholas, D. D. (1973)

Wood Deterioration and Its Prevention by
Preservative Treatments Vol.II Preservatives and
Preservative Systems.
Syracuse Wood Science Series 5, Wilfried Cote,
Syracuse University Press

Nielsen, L.F. (1978)

Crack Propagation in Linear Viscoelastic Materials.
Bygningsstatistiske Meddelelser, 49 p.1 (In Danish,
extensive English summary)

Norton, Harry N. (1969)

Handbook of Transducers of Electronic Measuring
Systems
Prentice-Hall, Inc., Englewood Cliffs, N. J.

- Palka, L.C. (1973)
Predicting the Effect of Specific Gravity, Moisture
Content, Temperature and Strain Rate on the Elastic
Properties of Softwoods
Wood Science and Technology 7(2) 127-141
- Panshin, A.J. and Zeeuw, C. (1980)
Textbook of Wood Technology
McGraw-Hill Book Company
- Perrin, P. W. (1978)
Review of Incising and Its Effects on Strength and
Preservative Treatment of Wood.
Forest Products Journal Vol.28(9) 27-33
- Peters, C.C. et. at. (1968)
Effects of roller-bar compression and restraint in
slicing wood 1-inch
Forest Products Journal Vol.18(1)
- Popov, E.P. (1978)
Mechanics of Materials
SI version, 2nd edition, Englewood Cliffs, N.J.:
Prentice-Hall
- Sheingold, Daniel H. (1980)
Transducer Interfacing Handbook - A Guide to Analog
Signal Conditioning
Analog Devices, Inc. 1st ed. Norwood Mass.

- Sliker, A. (1975)
Young's Modulus of Wood As Affected By Strain Rate,
Grain Angle, and Stress Level.
Wood Science 7(3) 223-231
- Stamm, A. J. (1963)
Permeability of Woods to Fluids
Forest Products Journal Vol.13(11) 503-507
- Stamm, A.J. (1967)
Flow of Fluids in Wood
Wood Science and Technology Vol.1, 122-141
- Stanley, W.D. et. at. (1984)
Digital Signal Processing
2nd ed. Reston, Va.: Reston Pub. Co.
- Steel, Robert G.D. and Torrie, James H.(1960)
Principles and Procedures of Statistics--A
Biometrical Approach
New York: McGraw-Hill Book Company Inc. 1960
- Sutton, W.R.J. (1984)
New Zealand Experience with Radiata Pine Vancouver,
B.C.: University of British Columbia, The H.R.
MacMillan lectureship in forestry, 1984
- Sydenham, Peter H. (1980)
Transducers in Measurement and Control
3rd ed. Bristol: Hilger c1985

- Tarkow, H. and Seborg, Raymond (1968)
Surface Densification of Wood
Forest Products Journal 18(9)
- Tesoro, F.O. and Choong, E.T. (1976)
Relationship of Longitudinal Permeability to
Treatability of Wood
Holzforschung, Vol.30, Heft 3, 91-96
- Trenard, Y. and Gueneau, P. (1984)
On the Penetration Pathways of liquid gallium in
Fafus sylvatica
Wood and Fiber Science, Vol.16(3)
- Ugolev, B. (1976)
General Laws of Deformation and Rheological
Properties of Hardwood
Wood Science Technology 10(3), 169-181
- Varga, O.H. (1966)
Stress-Strain Behavior of Elastic Materials:
Selected Problems of Large Deformations.
N.Y. Interscience
- Wingate-Hill, R. and Cunningham, R. (1984)
Removal of moisture from green sapwood by
compression.
Journal of the Institute of Wood Science 10(2) 66-
75

- Wingate-Hill, R. and Cunningham, R.B. (1986)
Confined and Unconfined Radial Compression
Perpendicular to the Grain of Green Sapwood from
Pinus Radiata and Eucalyptus Regnans
New Zealand Journal of Forestry Science 16(2)
- Wusatowski, Z. (1969)
Fundamentals of Rolling
RERGAMON PRESS
- Yee, Cheong Heok (1983)
Roll Forming of Metals
Report No.346 School of Engineering University of
Auckland